

STRETCH BEND TESTING OF
HIGH STRENGTH LOW ALLOY SHEET STEELS

STRETCH BEND TESTING OF
HIGH STRENGTH LOW ALLOY SHEET STEELS

By

ANIL K. BANSAL, B.Sc. (MECH. ENGG.) HONS., M.TECH.

A Thesis

Submitted to the School of Graduate Studies
in Partial Fulfilment of the Requirements
for the Degree

MASTER OF ENGINEERING

McMaster University

JANUARY 1977

© ANIL K. BANSAL 1977

TO
LYNDA DARCHUK

ACKNOWLEDGEMENTS

I wish to express my deep sense of gratitude to Dr. J.L. Duncan for his invaluable guidance and suggestions at every stage of this work.

I am also indebted to Dr. G. Glover, Senior Research Officer, BHP Research Laboratory, Australia. He was a postdoctoral fellow in the Department of Metallurgy. Without his keen interest and fruitful suggestions, the project would have not reached to the present stage. The work presented in this thesis is a part of the joint work done with Dr. Glover, and much of the description of the experimental work presented here is based on the Metalworking Report #93 written by Dr. Glover and myself. His contribution is greatly appreciated.

Thanks are also due to Ms. Bharatha for the typing of this thesis.

MASTER OF ENGINEERING
(PRODUCTION ENGINEERING)

McMASTER UNIVERSITY
HAMILTON, ONTARIO

TITLE: STRETCH BEND TESTING OF HIGH STRENGTH LOW ALLOY SHEET STEELS.

AUTHOR: ANIL K. BANSAL, B.Sc. (Mech. Engg.) Hons.,
Kurukshetra University, India

M.Tech. (Design of Production Machines),
Indian Institute of Technology, Delhi, India

SUPERVISOR: PROFESSOR J.L. DUNCAN

NUMBER OF PAGES: 134

A B S T R A C T

The stretch bend test has been used to investigate the formability of a series of high strength, low-alloy sheet steels with yield strengths in the range 35 to 90 ksi, varying compositions and inclusion shapes.

The results of the stretch bend tests have been compared with those of tensile, hole expansion and punch stretching tests on the same steels to obtain an indication of the sensitivity of the test to steel quality. In addition some stretch bend tests have been carried out to investigate the influence of varying the lubrication, specimen width and specimen span in the test.

The results show that the stretch bend is somewhat insensitive to the presence of elongated inclusions at the lower strength levels and inclusion contents but this sensitivity does increase with increasing test span and should be adequate at the larger spans. Local strains at fracture in both tensile and stretch bend tests give a more reliable indication of the presence elongated inclusions. Of the bulk formability measurements the hole expansion limit exhibits the greatest sensitivity to steel quality.

TABLE OF CONTENTS

	PAGE
LIST OF FIGURES	xi
LIST OF TABLES	xvii
CHAPTER I	LITERATURE SURVEY
1.1	Review of HSLA Sheet Steels 1
1.2	General aspects of Formability 5
1.2.1	Limitations of FLD 6
1.3	Effect of Microstructure on Ductility 7
1.3.1	Plastic Instability 7
1.3.2	Criterion for Ductile Fracture 7
1.3.3	Ductile Fracture Cavity Nucleation 8
1.3.4	Ductile Fracture Cavity Growth 10
1.3.5	Ductile Fracture Void Coalescence and Failure 12
1.4	Effects of second Phase Particles on Fracture 14
	Strain
1.5	Effect of Sulphides, Oxides and Carbides 15
1.6	Inclusion Distribution 21
1.7	Sulphide Modifiers 21
1.8	Review of Mechanical Tests for Assessing Sheet 25
	Material Formability
CHAPTER II	AIM OF THE PRESENT INVESTIGATION 29
CHAPTER III	MATERIALS TESTED
3.1	Materials 31
3.2	Metallography 31

	PAGE
3.3 Results & Discussion	36
CHAPTER IV MECHANICAL TESTS	
EXPERIMENTAL TECHNIQUES	41
4.1 Tensile Test	41
4.2 Notched Tensile Test	44
4.3 Stretch Bend Test	44
4.4 Hole Expansion Test	47
4.5 Punch Stretching Test	48
CHAPTER V RESULTS & DISCUSSION	
5.1 Strain Measurement	52
5.2 Shearing	52
5.3 Tensile Tests	55
5.3.1 Tensile Properties of the HSLA Sheet Steels	55
5.3.2 Variation of n , E_T , R of A , E_L with Yield Strength and Inclusion Characteristics	59
5.3.3 Dependence of E_T and E_L on Drawability Index	63
5.3.4 Plot of Ratio of Trans. / Long. Properties with Y.S. and Inclusion Characteristics	63
5.3.5 Fracture Characteristics of Steel D	68
5.4. Notched Tensile Test	68
5.4.1 Variation of E_{TN} and the Ratio of Trans. / Long. E_{TN} with Y.S. and Inclusion Characteristics	68
5.5 Stretch Bend Test	
5.5.1 Punch Load--Punch Travel Plots	68
5.5.2 Stretch Bend Formability of the HSLA Sheet Steels	71

	PAGE
5.5.3 Correlation of Punch Travel at Maxm. Load, Local Strain Ratio, % Reduction in Width with r Value	74
5.5.4 Fracture Characteristics of Stretch Bend Test	80
5.5.5 Discussion on the Stretch Bend Formability of the HSIA Sheet Steel Results	83
5.6 Correlation of SB Results with Tensile and Notched Tensile Formability Parameters	87
5.7 Local Strain Measurement at Fracture in Stretch Bend Test	88
5.7.1 Variation of Local Fracture Strain Measurement from Stretch Bend Test with Y.S. and Inclusion Charac- teristics	88
5.7.2 Change in Strain Distribution with Y.S. for Specimens deformed to 0.80 in.	94
5.7.3 Change in Strain Distribution with Punch Radius for Steel E Deformed to 0.80 in.	97
5.7.4 Discussion on the Local Fracture Strain results in Stretch Bend Test as a Formability Parameters	97
5.8 Hole Expansion Test	99
5.8.1 Hole Expansion Limit--Yield Strength Plot	99
5.8.2 Discussion on Hole Expansion Test and Stretch Bend Test	101
5.8.3 Correlation between Hole Expansion Test and Tension Test	105

	PAGE
5.8.4 Correlation between Hole Expansion & Notched Tensile Test	105
5.9 Punch Stretching Test	105
5.9.1 Cup Height--Yield Strength Plot	105
5.9.2 Discussion--Punch Stretching & Stretch Bend Tests	107
5.9.3 Discussion on the Relative Assessment of Punch Stretching, Hole Expansion and Stretch Bend Tests	107
CHAPTER VI INFLUENCE OF TESTING CONDITION IN STRETCH BENDING	
6.1 Effect of Lubrication on:	110
6.1.1 Punch Deflection for Different Bend Radii	110
6.1.2 Reduction of Width	
6.2 Effect of Specimen Width on:	118
6.2.1 Punch Deflection for Different Bend Ratio	118
6.2.2 Width Strains	118
6.3 Development of Strains during Stretch Bend Process & the Effect of Specimen Thickness	123
6.4 Effect of Specimen Span	123
CHAPTER VII CONCLUSIONS	127
REFERENCES	130

LIST OF FIGURES

<u>Figure</u>		<u>PAGE</u>
1	Schematic illustration of the forming limit diagram in the region of biaxial stretching.	4
2	Theoretical model of Void Growth (18).	9
3	Comparison of predicted Void Growth rates for sulphides (decohesion) and carbide (cracking with $c_0 = 0.5$), strain intensification factor $k = 2$ (18).	11
4	Effect of Second Phase Particles on ϵ_T (11).	13
5	Effect of sulphide volume fraction on total ductility during longitudinal and transverse testing (12).	16
6	Effect of carbide volume fraction on the strain required to crack carbides and initiate voids (12).	17
7	Void Growth as a function of strain (18).	19
8 (a)	Type II Sulphide Network	
(b)	Type I Sulphide network	20
9	Effect of rare earth (cerium) additions on longitudinal and transverse shelf energy.	22
10	Comparison of inclusion shape control by zirconium and rare earth additions on the anisotropy of charpy shelf energy.	23
11	Typical inclusion structures of the experimental steels.	
	a) Rare earth modified sulphides in steel A Mag. X 1350	32
	b) Elongated sulphides in steel B Mag. X 440	
	c) Partly modified sulphides in steel C Mag. X 440	
	d) Rare earth modified sulphides in Steel D Mag. X 880	
	e) Rare earth modified sulphides in steel E Mag. X 440	
	f) Elongated sulphides on steel F Mag. X 440	
	g) Elongated sulphides in steel G Mag. X 440	

12	Typical matrix structures of the experimental steels. Polygonal ferrite-pearlite structure of a) Steel A Mag. X 640 2% Nital etchant b) Steel B Mag. X 240 2% Nital etchant c) Partly acicular structure of Steel C Mag. X 640 Nital etchant d) Bonded grains and carbides in Steel D Mag. X 640 2% Nital etchant Polygonal ferrite-pearlite structure of e) Steel E. Mag. X 640 2% Nital etchant f) Steel F. Mag. X 640 2% Nital etchant g) Steel G. Mag. X 320 2% Nital etchant	37
13	Dimensions of the notched tensile test piece.	42
14	A schematic diagram of the stretch bend test.	43
15	Specimen for Hole Expansion Test.	45
16	Die set for 1.00" O.D. holes.	46
17	Schematic diagram of the two halves of a sheared sheet illustrating the measurement of depth of blade penetration.	50
18	The dependence of the blade penetration depth (as a percentage of sheet thickness) upon yield strength and inclusion shape.	51
19	Engineering stress strain curves for Steels A, E, & G.	56
20	The dependence of the drawability index, r value, upon the range of strain over which it is measured.	57
21	The variation of some tensile formability parameters with yield strength and inclusion characteristics. a) The workhardening index, n b) The total elongation on 2 in., E_T c) The reduction of area, R and A d) The local elongation at fracture measured from 0.09 in. grid circles, E_L	60
22	The dependence of total elongation and local elongation in the tensile test on the drawability index. Results are grouped into bands for steels of similar yield strength.	61

		PAGE
23	The variation of transverse/longitudinal ratio with yield strength and inclusion characteristics. a) the total elongation b) the reduction of area c) the local elongation	62
24	Optical micrographs showing the delamination phenomenon encountered in steel D during tensile testing. a) general view of a section perpendicular to the fracture surface. Mag. 640 X 2% nital etchant. b) the association between carbide stringers and the advancing crack tip. Mag. 640 X, 2% nital etchant.	64
25	The variation of the notched tensile elongation and the ratio of the transverse/longitudinal notched tensile elongation with yield stress and inclusion characteristics.	65
26	Typical load vs punch travel curves for steel B in the stretch bend test.	66
27	The variation of punch travel at maximum load with bend ratio for the experimental steels. Curves for machined edge samples lie above those for the sheared edge samples of the same steel. Longitudinal, transverse and diagonal specimens are represented by open, closed and half open points respectively.	69
28	The variation with drawability index of, a) punch travel at maximum load b) the local strain ratio measured from .09 in. dia. electroetched grids of circles. c) the reduction of width from measurements made on specimens deformed both to maximum load and fracture, for specimens with machined edges.	73
29	Typical examples of fracture in the stretch bend test a) Normal edge cracking at the bend apex. b) Centre cracking at the bend apex. c) Edge cracking at the specimen/punch junction for large bend radii. d) Centre cracking at the apex of the punch for large	76

	bend radii. Note the deviation of the crack from the bend apex along the lines of shear towards the specimen edges.	
30	Strain distribution along the axis of the bend a) Edge cracking b) Centre cracking	78
31	The variation of punch travel in sheared edge specimens yield strength and inclusion characteristics for bend ratios of : a) 1, b) 3 and c) 5.	82
32	The correlation between punch travel and the formability parameters from the tensile test: a) work hardening index, n b) reduction of area, R of A c) local elongation at fracture, E_L d) total elongation, E_T e) the elongation of notched tensile specimens, E_{TN} . Punch travel measurements have been taken from the smoothed curves of Fig. 14 at a bend ratio of 4.5.	85
33	The variation of the local fracture strains measured from stretch-bent specimens with yield strength and inclusion characteristics. a) Local elongation at fracture measured from 0.9 in. dia. grid circles, E_B . b) reduction of specimen width at the apex of the bend at fracture, R of W c) reduction of thickness at fracture R of T	89
34	Effect of yield stress on strain distribution.	93
35	Effect of Punch radii on strain distribution.	95
36	The variation with yield strength and inclusion characteristics of a) the local elongation at fracture, E_B b) the reduction of width at fracture, R of W c) the reduction of thickness at fracture, R of T in the stretch bent samples.	96
37	The variation of the hole expansion limit, λ , with yield strength and inclusion characteristics.	98

		PAGE
38	A hole expansion test piece illustrating the mode of failure. Steel E.	100
39	The correlation between the hole expansion limit and a) the tensile reduction of area, R of A b) the elongation of notched tensile specimens, E_{TN}	102
40	Correlation between fracture strain in hole expansion test and a) Notched elongation % b) Red. of area % c) Total elongation % d) Local elongation %	103
41	The variation of the cup height obtained in hemispherical punch stretching with yield strength for the experimental steels.	104
42	An example of failure in hemispherical punch stretching.	106
43	FLD for the experimental steels..	108
44	A comparison of the punch travel-bend relationship for normally lubricated specimens of steel F and specimens tested without any lubrication whatever.	111
45	A comparison of the strain distributions obtained perpendicular to the axis of the bend for a) normal lubricated tests b) dry tests for steel F.	112
46	Typical failures for specimens tested without lubrication a) failure at the clamping jaws b) failure in a tensile mode half way between bend apex and the clamping jaws Note the restricted width strain over the punch radius and the excessive width strain in the arm of the stretch bent specimen.	114
47	The variation of width strain in the stretch bend test with punch radius for dry & lubricated conditions.	116
48	The influence of specimen width on the punch travel-bend ratio relationship.	117

<u>Figure</u>		<u>PAGE</u>
49	The influence of specimen width on the width reduction at fracture at the apex of the bend for tests with 0.5 in. and 0.125 in. punch radii.	119
50	Strain development during stretch bending a) outside the bend b) inside the bend	120
51	Effect of specimen thickness on the strain distribution during stretch bending. a) Outside the bend b) Inside the bend	121
52	The influence of specimen span on the punch travel-bend ratio relationship for steel F. Note the increased separation of the curves for longitudinal and transverse specimens in the tests at the larger span.	124

LIST OF TABLES

<u>TABLE</u>		<u>PAGE</u>
1.	Composition of the Hot Rolled Steels	30
2.	Number of inclusions / mm ² in different length ranges	35
3.	Tensile properties of the HSLA sheet steels	53-54
4.	Maximum punch load & maximum punch travel for transverse sheared edge specimens	67
5.	Position of crack initiation	79
6.	Effect of specimen width on width strain--Machined edge specimen, Steel E	122

CHAPTER I

LITERATURE SURVEY1.1 REVIEW OF HSLA SHEET STEELS

High Strength Low Alloy (HSLA) steels are a relatively new group of alloys, similar in some respects to hot rolled, low carbon steels, but having higher strengths as a result of composition and processing variations. The family of HSLA steel is usually characterized by

- i) grain refinement strengthening by hot strip mill controlled rolling and cooling.
- ii) strengthening from vanadium, columbium or titanium precipitation.
- iii) some solid solution strengthening.
- iv) low carbon contents to promote weldability and formability and
- v) additives such as zirconium or rare earth elements to control inclusion shape.

Major developments of HSLA steels have been stimulated by the demand for

- i) higher yield strength ($> 350 \text{ N/mm}^2$) for greater load bearing capacity or lighter sections.
- ii) a high degree of weldability.
- iii) high resistance to brittle failure and low energy ductile fracture, as well as low transition temp.

- iv) good cold forming, particularly by bending, as well as ductility and fracture resistance in the through thickness direction.
- v) lower costs using hot rolled rather than heat treated sections, plus higher ingot yields.

These stringent requirements have been met as knowledge increased about the inter-relationship between the microstructure and mechanical properties. A regression analysis on typical steels of this kind yielded the following relationship for cold forming applications (1)

- i) Flow stress at $\epsilon = 0.2$ (σ_f) MPa

$$\begin{aligned} \sigma_f = & [16 + 0.27 (\% \text{ pearlite}) + 2.9 (\% \text{ Mn}) \\ & + 9.0 (\% \text{ Si}) + 60 (\% \text{ P}) + 11 (\% \text{ Sn}) \\ & + 244 (\% N_f) + 0.97 d^{-1/2}] \\ & \times 1.57 \text{ (90\% explained)} \end{aligned}$$

where N_f = free nitrogen not combined as a stable nitride.

d = grain size.

- ii) work hardening rate at $\epsilon = 0.2$

$$\begin{aligned} \frac{d\sigma}{d\epsilon} = & [25 + 0.09 (\% \text{ pearlite}) + 7.2 (\% \text{ Si}) \\ & + 30 (\% \text{ P}) + 9.9 (\% \text{ Sn}) + 89 (\% N_f) \\ & + 1.0 d^{-1/2}] \times 1.57 \text{ (55\% explained)} \end{aligned}$$

- iii) maximum uniform strain (ϵ^*)

$$\begin{aligned} \epsilon^* = & 0.27 - 0.016 (\% \text{ pearlite}) - 0.015 (\% \text{ Mn}) \\ & - 0.040 (\% \text{ Si}) - 0.043 (\% \text{ Sn}) \\ & - 1.1 (\% N_f) \text{ (60\% explained)} \end{aligned}$$

- iv) total strain at fracture (ϵ_T)

$$\begin{aligned}\epsilon_T = & 1.3 - 0.020 (\% \text{ pearlite}) + 0.30 (\% \text{ Mn}) \\ & + 0.20 (\% \text{ Si}) - 3.4 (\% \text{ S}) \\ & - 4.4 (\% \text{ P}) + 0.29 (\% \text{ Sn}) \\ & + 0.015 d^{-1/2} \text{ (65\% explained)}\end{aligned}$$

v) fracture stress σ_{fr} (MPa)

$$\begin{aligned}\sigma_{fr} = & [32 - 0.22 (\% \text{ pearlite}) + 16 (\% \text{ Mn}) \\ & + 18 (\% \text{ Si}) - 170 (\% \text{ S}) \\ & - 47 (\% \text{ P}) + 16 (\% \text{ Cr}) \\ & + 430 (\% N_f) + 2.9 d^{-1/2}] \\ & \times 1.57 \text{ (73\% explained)}\end{aligned}$$

The above table indicates that while there is reasonable prediction of mechanical properties, there is still considerable scope for refinement and in particular it is noticed that the initial yield strength is not predicted. This is very sensitive to small variations in structure and processing.

The search for improved HSLA steels will continue with perhaps more ductility and attempts are being made to take advantage of every possible increase in strength, and toughness. In a future of scarce raw materials and energy supplies, it would both be uneconomical and irresponsible to employ materials other than those offering a maximum potential. HSLA steels may meet this challenge by offering an optimum balance of properties per unit cost.

HSLA steels find their major applications in Pressure vessels, Pipe line, & transportation industries. Major applications in transportation industry includes chasis members, body frames, door strengthening bars, wheel centres and bumper parts. It has been estimated recently that weight

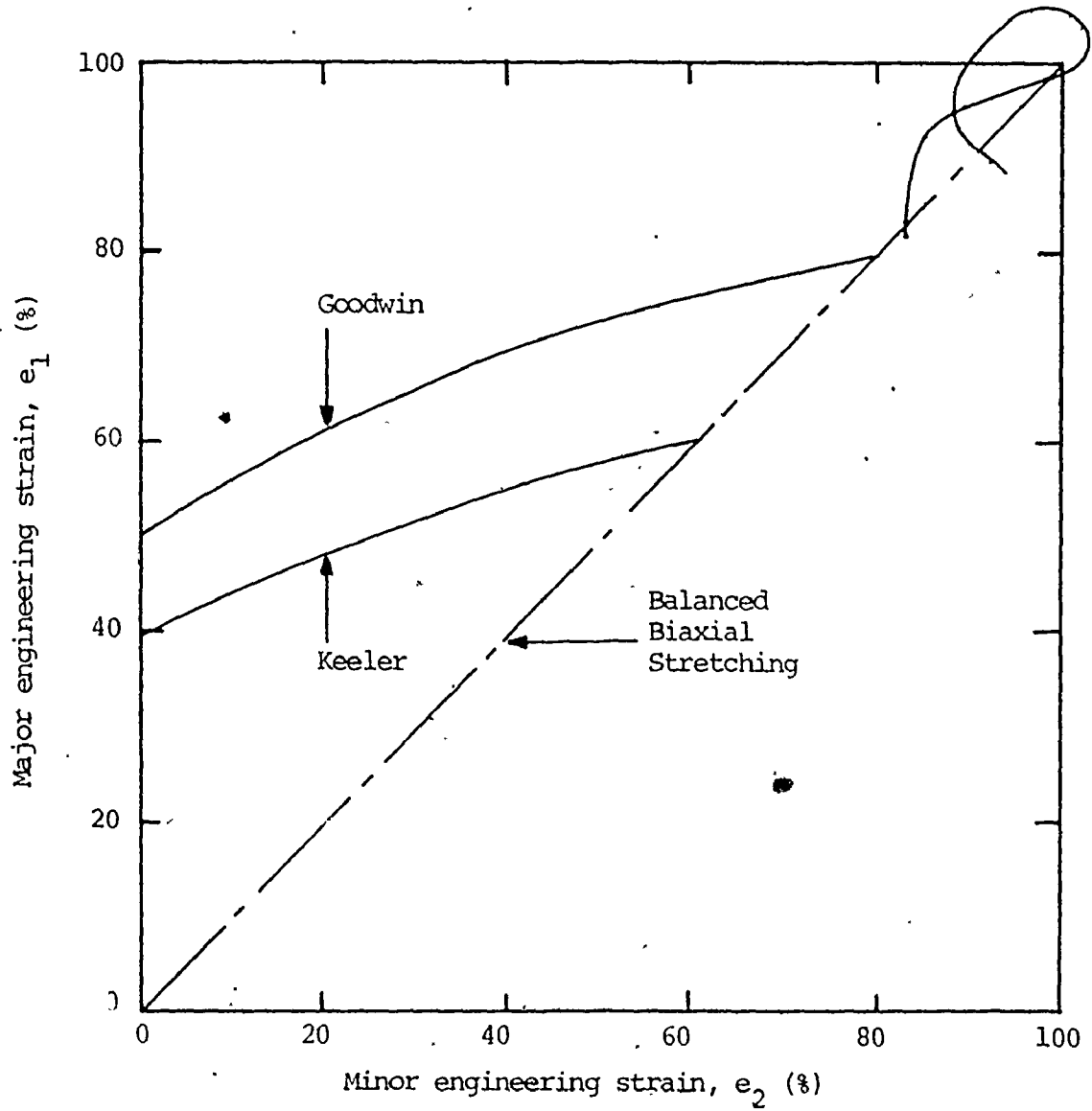


Fig. 1 Schematic illustration of the forming limit diagram in the region of biaxial stretching.

savings of 22.5 - 62.5 % can be achieved in bumper parts, body frames and chasis members by using HSLA steels and by 1978 (2) 200 kg of HSLA steel will be used in every motor car compared to 20 kg used presently.

1.2 GENERAL ASPECTS OF FORMABILITY

Strain analysis of sheet steels formed into various parts illustrates that steel deforms in three basic modes, STRETCH, DRAW, and PLANE STRAIN. The deformation mode is defined by the minor surface strain, which is positive for stretch, negative for draw, and zero for plane strain deformation. The major principal strain is always positive. The degree of sheet steel thinning before necking depends on the deformation mode.

Literature published by Keeler and by Goodwin showed curves which describe the local strain occurring in sheet metal at the onset of failure under any combinations of strains. Keeler examined the limit strain close to the site of fracture and Goodwin computed principal fracture strains at the fracture site. The difference between the Keeler and Goodwin curves suggest that some very localised process preceeds fracture. Strain values lying below the curve represent safe conditions i.e., no failure, strains lying on the curve show failure by the onset of necking and points above the curve indicates more advanced or severe failure. Such a curve is known as Forming Limit Curve (FLC) or Forming Limit Diagram (FLD) shown schematically in Fig. 1.

The study of formability is aimed at facilitating the prediction of material behavior in press forming operations from known material properties under various conditions of stress and strain using "Fracture" and "Instability" criteria and / or reliable testing.

FLD have been found very useful in the following applications (3)

- i) solving splitting problems during forming.
- ii) determining the effectiveness of remedial actions taken to eliminate forming problems.
- iii) anticipating forming problems showing how close strains are to the fracture.
- iv) establishing steel grades required for new parts.
- v) evaluation of the press performance of new steels.

An analytical technique for obtaining the Keeler Forming Limit diagram has been proposed by Sowerby and Duncan (4 , 5) based on a hypothesis by Marcinik (6). He proposed that inhomogenities exist in any material and these could be modelled analytically by imposing a local thickness variation in the sheet and studying the strain development in the parent sheet and the localized groove. Minh et al (7) proposed material inhomogenities as the source of variation in the useful strain levels of the identical formed parts.

1.2.1 LIMITATIONS OF FLD

The FLD does not provide the information on the material ability to distribute strain during forming. Sheet metals with the ability to distribute strains during forming are more suitable for making parts of complex contours. Therefore, both the FLD and the material ability to distribute strain are important considerations in sheet formability. The use of FLD's is also limited when the sheet thickness and contours are such as to promote considerable outer fibre stretch (8).

1.3 EFFECT OF MICROSTRUCTURE ON DUCTILITY

Ductility is the ability of a material to undergo extensive plastic deformation, limited by either fracture processes or by plastic instability. An example of an instability controlled ductility is the elongation in the uniaxial tensile test. An example of fracture controlled ductility is the reduction of area in the same test.

1.3.1 PLASTIC INSTABILITY

Plastic instability depends strongly on the work hardening characteristics of a material. In steels which exhibit low strain rate dependence of flow stress, uniaxial tensile instability occurs at a low strain when the work hardening rate is insufficient to maintain the rate of decrease of the cross-sectional area. Higher strength steels, (ie. steels with elevated yield and flow stresses) show reduced elongation values although this is not entirely due to the low strain hardening.

However, the onset of plastic instability has proved to be of limited significance in many cold forming processes, (eg. cold bending), while reduced elongation values are not harmful in microalloyed steel applications. In fact, because of the limited potential for changing the work hardening characteristics of ferrite steels, elongation values at a given strength level are very similar for all steels.

1.3.2 CRITERION FOR DUCTILE FRACTURE

The various criteria which have been proposed to explain the fracture of metals generally allow the derivation of fracture strains under the known conditions of loading from known constitutive behavior of materials. Criteria like "Maximum Tensile Stress", "Maximum Shear Stress", "Maximum Tensile Work", "Maximum Volume Strain" etc. have been advanced to explain

the fracture behaviour of various materials. Most of these provide a simplified end condition for fracture without taking into consideration the gradual increase of internal damage during deformation of ductile materials. Cockcroft (9) in his maximum tensile work criterion related material damage to the plastic work done by the maximum tensile stress. This however, lacked any real microstructural explanation of the process of damage as experimentally observed by many investigators.

The most realistic fracture criteria for ductile metals was proposed by McClintock (10). The process involves cavity nucleation, growth and coalescence in the final catastrophic stage of fracture.

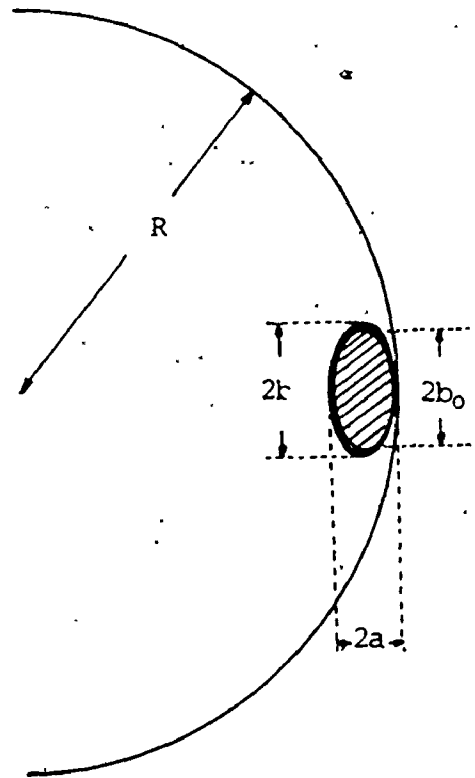
1.3.3 DUCTILE FRACTURE CAVITY NUCLEATION

There are many methods (10, 12, 41, 42) of cavity nucleation, in the cold forming operations, however, it usually occurs by decohesion of the interface between matrix and the second phase particles or by cracking of second phase particles. In general, cavities nucleated on nonmetallic inclusions form by interface decohesion while those nucleated at cementite particles are formed by particle cracking (11). Experiments by Gladman et al. (12) suggest that particle decohesion in non-metallic inclusions can occur at negligibly small strains. Cementite-particle cracking is a stress dependent phenomenon, and the stresses needed to crack the carbide particles may not be developed until the aggregate has undergone quite large strains.

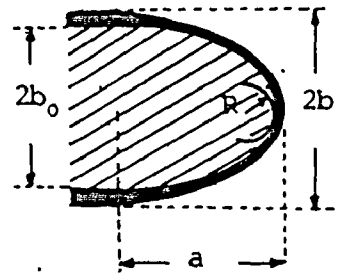
Recent work (12) has shown that carbide morphology is a major factor in controlling the onset of particle cracking. The stress dependence of particle cracking is given by the following equation (12)

$$\tau_c = \tau_0 + k_c (\sqrt{c} / p)$$

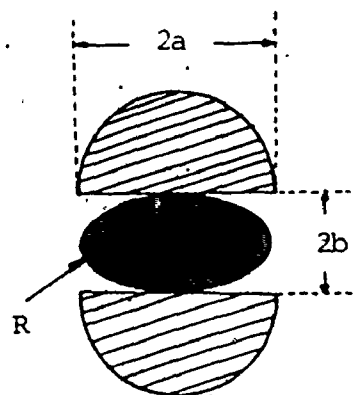
a. Decohesion (Prolate Spheroid)



b. Decohesion (Oblate Spheroid)



c. Particle Cracking



Tensile
Axis

- ▨ Particle
- Void

Fig. 2 Theoretical model for void growth.

where c = the carbide thickness
 p = pile up length and
 τ_0 and k_c = constants.

The critical shear stress can be translated into an applied tensile stress and, through the true stress/ true strain curve, to a nucleation strain. This is a simplified model of carbide cracking since it implies that carbide cracking is totally dependent on the resolved shear stress and stress intensification at the head of a pile up. While this has been confirmed by considerable evidence, other aspects of particle cracking, such as fibre loading, may also have some effect on elongated or plate like carbide particles.

These aspects of carbide cracking are dependent on the stress system. Stress triaxiality could dramatically change strain to cavity nucleation. Nevertheless, for a given stress system, carbide refinement might increase strain to carbide fracture ie. the cavity nucleation strain, but there is little evidence supporting this.

1.3.4 DUCTILE FRACTURE CAVITY GROWTH (12)

The basic theory of cavity growth proposed by Henry and Plateau is that strain intensification occurs in a manner analogous to stress intensification near notches or cavities. Strain intensification is therefore controlled by the frontal radius of curvature of the cavity Fig. 2 (12)

$$d\epsilon = db/b \left(1 + k a^2/b^2 \right)$$

Integration of this equation provides a description of the development of the cavity with strain.

$$\epsilon = \epsilon_0 + \ln \left[(b^2 + k a^2) / (L^2 + k a^2) \right] / 2 \quad (1)$$

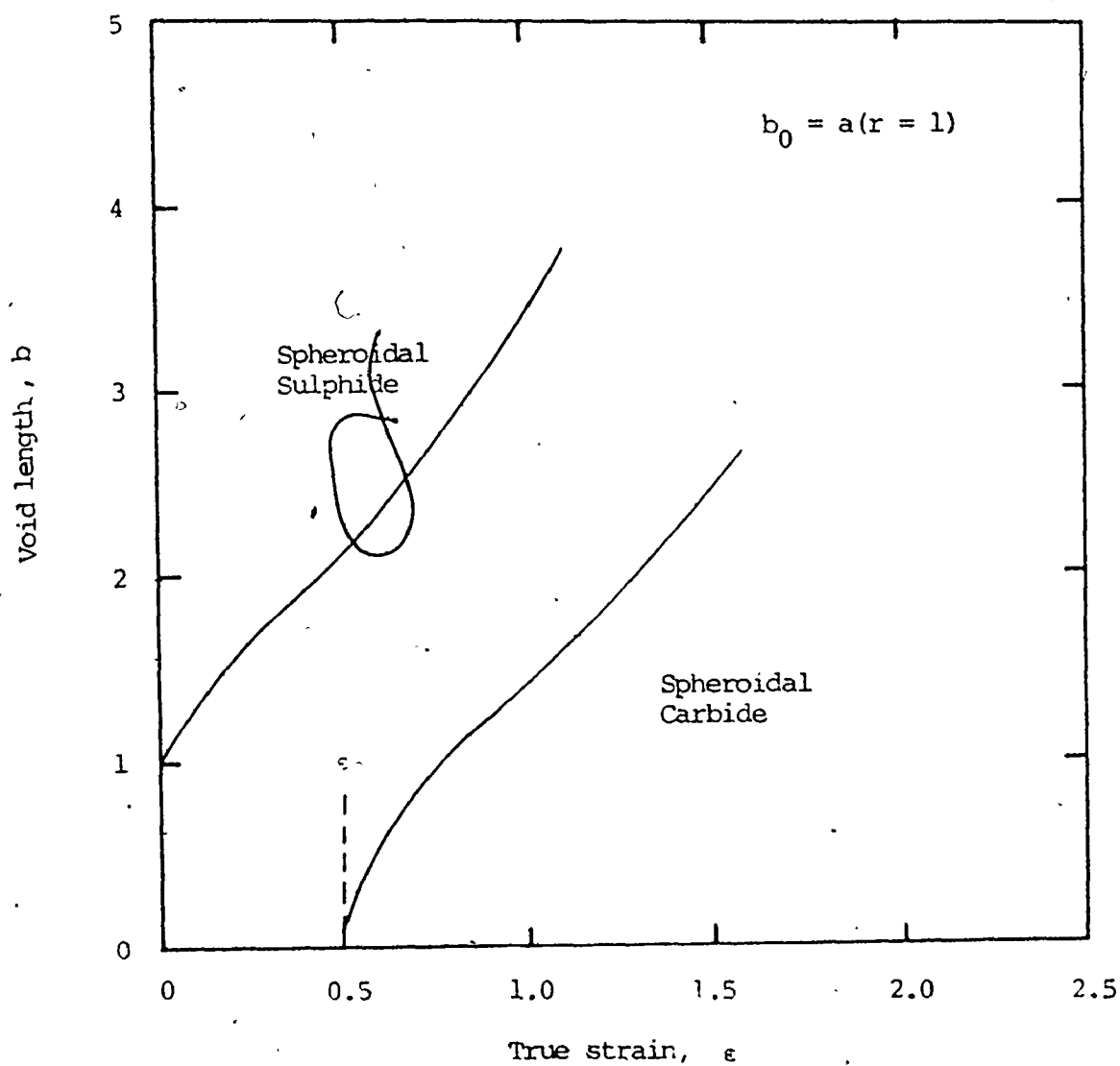


Fig. 3 Comparison of predicted void-growth rates for sulphide (decohesion) and carbide (cracking with $\epsilon_0 = 0.5$), strain intensification factor, $k = 2$.

where the constant of integration, ϵ_0 = the strain at which cavity nucleation occurs.

L = the initial length of the cavity, ie. b_0 in the case of particle decohesion and, o in the case of particle cracking.
 k = strain intensification factor.

It is assumed that all inclusions behave similarly with respect to void formation. The comparison of cavity development formed by inclusion decohesion and carbide cracking is shown in Fig. 3.

1.3.5 DUCTILE FRACTURE VOID COALESCENCE AND FAILURE (12)

There is no precise description of the critical distribution of cavities required for cavity coalescence. Most theories however, imply a critical ratio of hole size to hole spacing. A modification of Henry and Plateau's model for hole spacing, however, allowed the development of a relatively simple model of ductile fracture, in which the resulting equation implies a critical volume fraction of holes (11). Theoretical treatments of more complex stress and strain conditions also indicate a critical volume fraction of holes of less than 10% (13).

Thus, the factors which encourage the early development of the critical volume fraction of holes are those which reduce fracture strain including a high volume fraction of inclusions and an unfavourable shape. Unfavourable shapes promote strain intensification, (eg. lenticular particles where the strain is applied parallel to the short axis--Fig. 2b).

Particle size does not have any effect on ductility in many cases, as supported by the work of Edelson and Baldwin (14). However, this is not

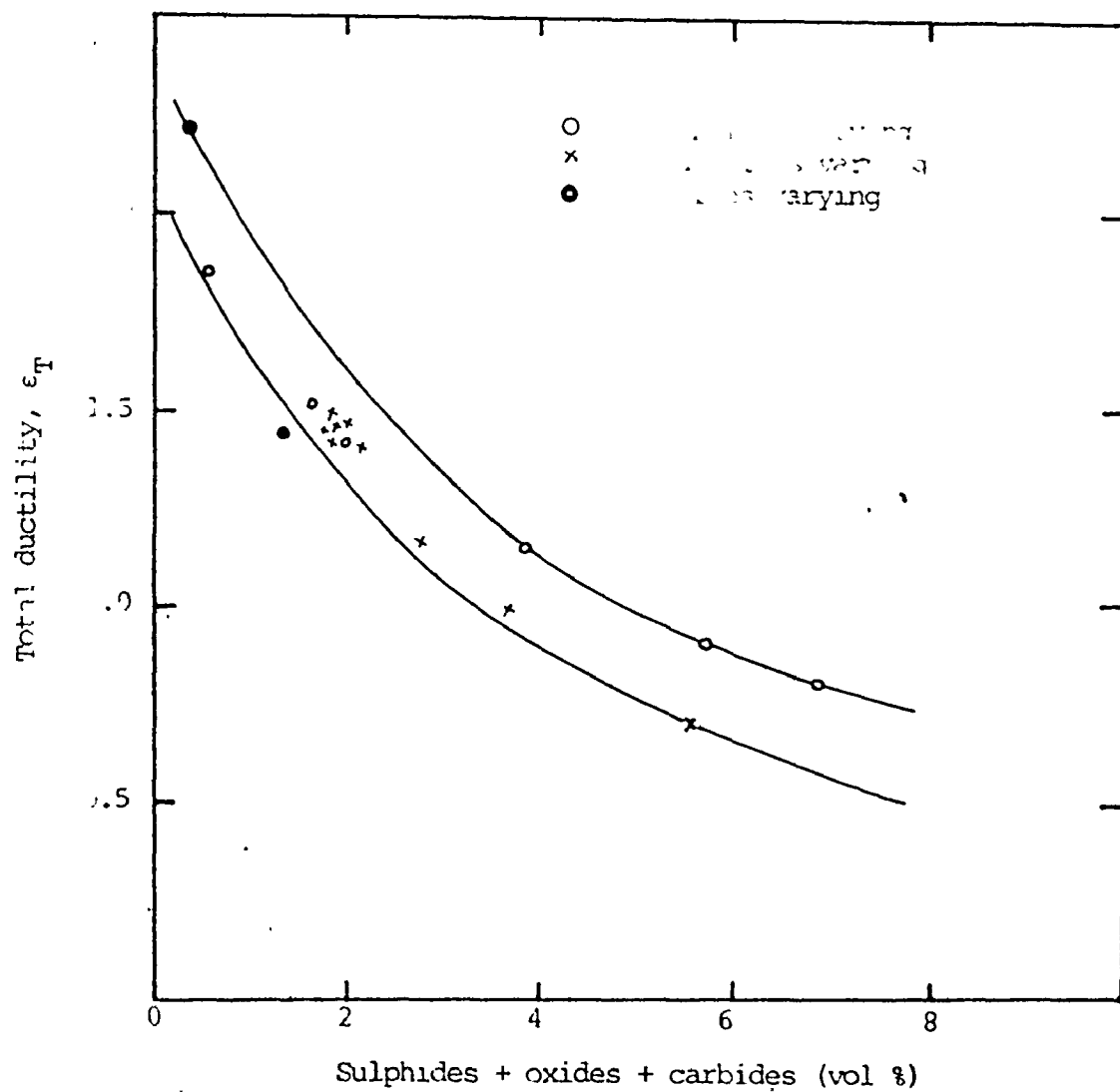


Fig. 4 Effect of second-phase particles on ϵ_T .

true for cementite particles and stress dependent cracking, since void nucleation strain depends on the critical stress. Thus, carbide dispersion could dramatically affect the strain at which the critical stress level was attained due to the stress-strain relationship.

1.4 EFFECTS OF SECOND PHASE PARTICLES ON FRACTURE STRAIN

The theory outlined above leads to the formation of two ductile fracture equations (12). The first relates to nonmetallic inclusions in steel where cavitation occurs by decohesion of the interface at negligible strains. The strain to fracture, ϵ_T is given by

$$\epsilon_T = \ln \left[\left(\phi^2 / f_0^2 + k(r^2) / 1 + k / r^2 \right) \right] / 2 \quad (2)$$

where ϕ = the critical volume fraction of holes (approximately 0.05)

f_0 = the initial volume fraction of inclusions

k = a strain intensification constant of about 2, and

r = the length-width ratio of the inclusion where straining was in the length direction.

This equation indicates that increasing the volume fraction of inclusions reduces the strain to fracture. The shape factor, r , exerts a major effect on the denominator of the logarithmic term when $\phi \gg f_0$. An increase in the length-to-width ratio of the inclusion will improve ductility in the longitudinal direction. A decrease in the inclusion length-to-width ratio to a value less than unity will reduce longitudinal ductility.

The theory is based on inclusions occurring as oblate or prolate spheroids where the rotational axis is coincident with the tensile axis. The theories (10, 16, 41) only estimate highly elongated inclusions where the tensile axis is normal to the longitudinal axis. For the transverse tensile test, highly elongated inclusions would be undesirable and would

reduce the strain to fracture.

The second equation relates to carbide cracking as follows

$$\epsilon_T = \epsilon_0 + \ln \left[\left(4\phi^2 r^2 / 9kf_0^2 \right) + 1 \right] / 2 \quad (3)$$

where ϵ_0 = the void nucleation strain.

This is a highly idealized system implying that all carbides crack at a strain of ϵ_0 , and all are of similar shape and orientation. This is obviously not the case for cementite in microalloyed steels. The major effects of carbides on ductility are probably caused by their influence on the void nucleation strain, ϵ_0 . In addition, the orientation of pearlite cementite is generally random and would not therefore give a specific value of r .

In summary, carbides have a major influence on ductile fracture through their effect on volume fraction and ϵ_0 (11).

1.5 EFFECT OF SULFIDES, OXIDES and CARBIDES

The effect of second phase particles, such as manganese sulfides, oxide inclusions, or carbides, is to decrease the total ductility. However, the effect is not linear but is an exponential decrease with increasing volume fraction of second phase particles Fig. 4. This change is predicted by a theoretical analysis of the effect of second phase particles on the ductile fracture process. (10).

Irrespective of the precise mechanism of void coalescence, however, total ductility depends on the shape of the particle which create the voids. Increasing the length-width ratio of the second phase particles gives a higher tensile ductility when the long axis of inclusions is parallel to the tensile axis, compared with plate like inclusions tested parallel to

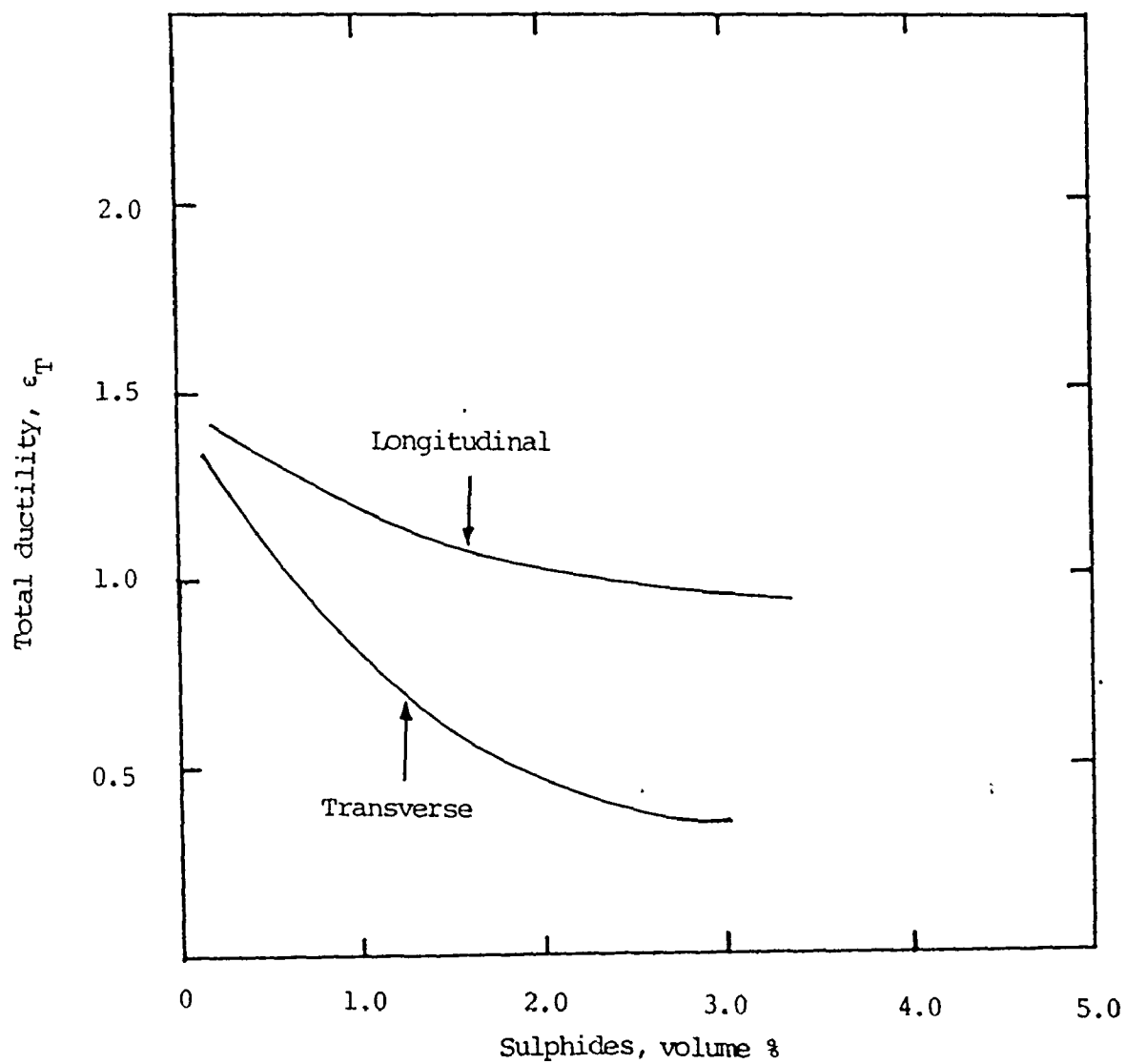


Fig. 5 Effect of sulphide volume fraction on total ductility during longitudinal and transverse testing.

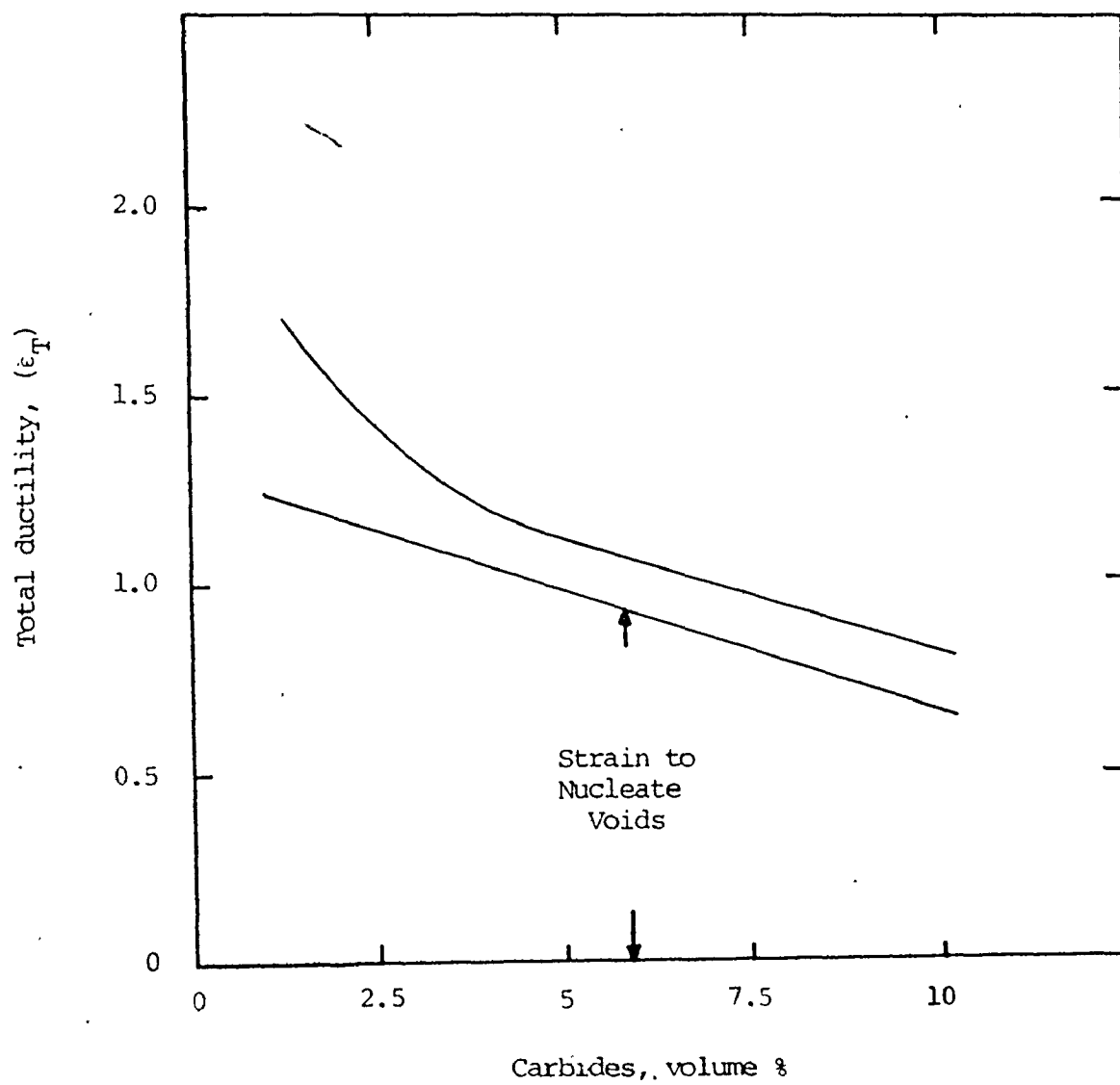


Fig. 6 Effect of carbide volume fraction on the strain required to crack carbides and initiate voids.

their minor axis. This produces ductility anisotropy in which ductility is much lower for a given volume fraction of second phase particles in transverse than in longitudinal tests, Fig. 5. This anisotropy effects the longitudinal bendability of flat-rolled products (15) and lamellar tearing during welding.

Although carbides appear to affect total ductility in a manner similar to non metallic inclusions, there is a significant difference since carbides do not crack or lose coherence at low strains. Consequently steel with carbides can undergo significant deformation prior to void nucleation (16). In fact, carbide cracking depends on stress (17).

Thus, the strain needed to nucleate voids decreases as the volume fraction of carbide increases Fig. 6. This occurs because the strain required to achieve the stress level for cracking decreases with carbide volume fraction. Carbide cracking and void nucleation can therefore occur at smaller strains with increasing flow stress and work hardening rate. This explains why lamellar pearlite has a much lower total ductility than spheroidized pearlite. (18).

In terms of void growth, a high work hardening rate can be beneficial, as it inhibits void growth by developing high flow stresses in the regions of strain concentration around the void and also by confining the spread of plastic zone. Because of less uniformly distributed carbides, spheroidized ferrite-pearlite structures have lower total ductilities for a given carbide volume fraction than do spheroidized martensite structure (18). This is similar to the lamellar tearing phenomenon and points to the detrimental effect of localized segregates of second phase particles.

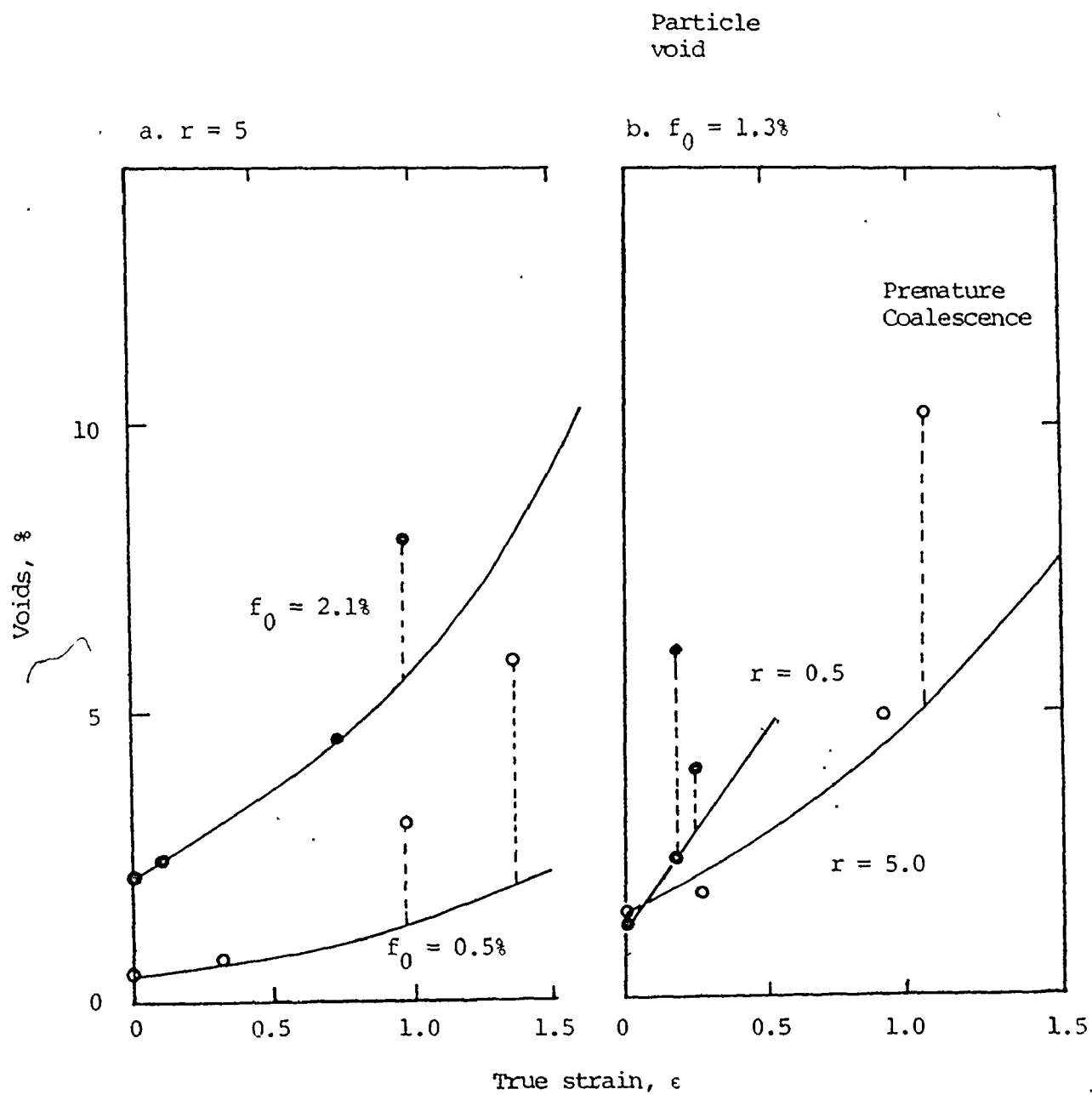
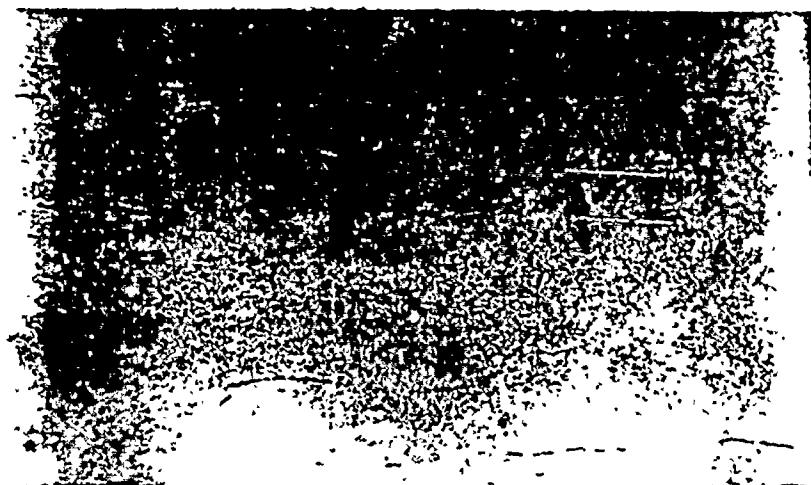
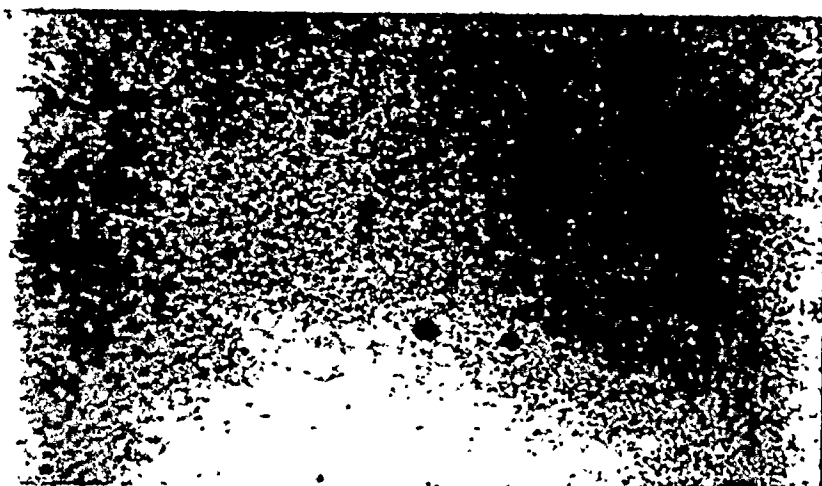


Fig. 7 Void Growth as a Function of strain where f_0 is the initial-volume fraction of inclusions and r is the length-width ratio of inclusions. Full lines show Henry and Plateau Model.



a) Type II Sulphide Net work



b) Type I Sulphide Net work

Fig. 8

1.6 INCLUSION DISTRIBUTION

The model of ductile fracture is based on the assumption that the distribution of inclusions is uniform. Localized clusters of inclusions, however can lead to the premature onset of void coalescence (11), which causes increased cavity development as shown by the deviations between theoretical and observed cavity volumes in Fig. 7. The formation of Type II (Fig. 8a) inclusions are particularly detrimental, resulting in local concentrations of sulfide particles (12, 40) as opposed to Type I (Fig. 8b) sulfides. The local concentration of sulfides can also be influenced by macro-segregation.

1.7 SULFIDE MODIFIERS

A recent method of combating the property anisotropy problem in HSLA steels has been the modification of sulfides and oxides by the addition of calcium (19), zirconium (19-21) or rare earths (18,19). This modification, which is most effective for sulfides is caused by the decrease in inclusion plasticity by altering their constitution (18). Thus they remain as rounded globules rather than deform into elongated ribbons or planar arrays in rolled products.

Control over inclusion shape is achieved by the addition of: CALCIUM which globularizes alumina type oxides by forming calcium aluminates and causes the sulfides (mainly calcium sulfide) to associate with the oxides. Due to its high vapour pressure, low solubility in steel, and great reactivity, calcium is considered difficult to control (19). Recent developments have overcome these problems to a large extent.

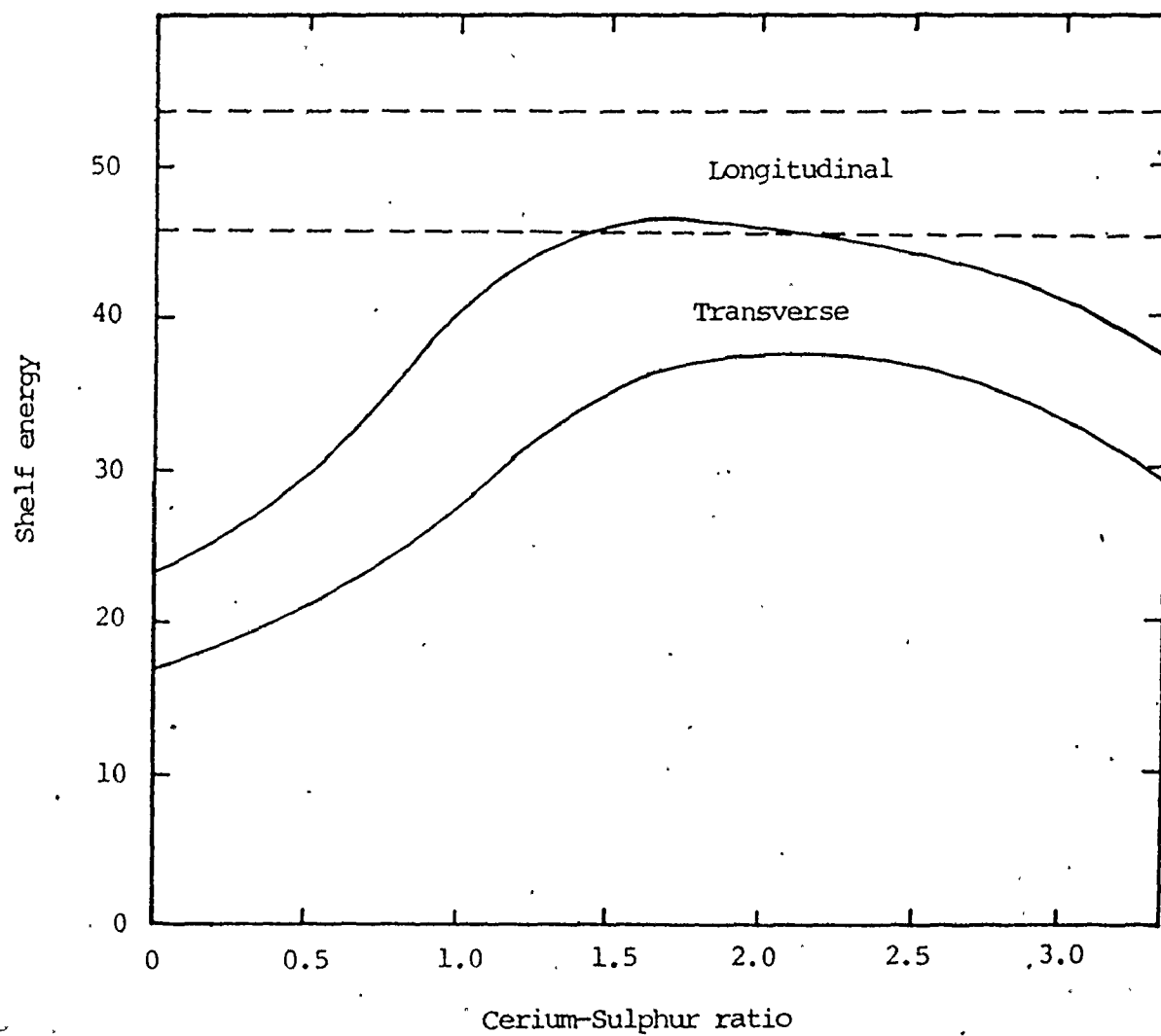


Fig. 9 Effect of rare-earth (cerium) additions on longitudinal and transverse Charpy shelf energy.

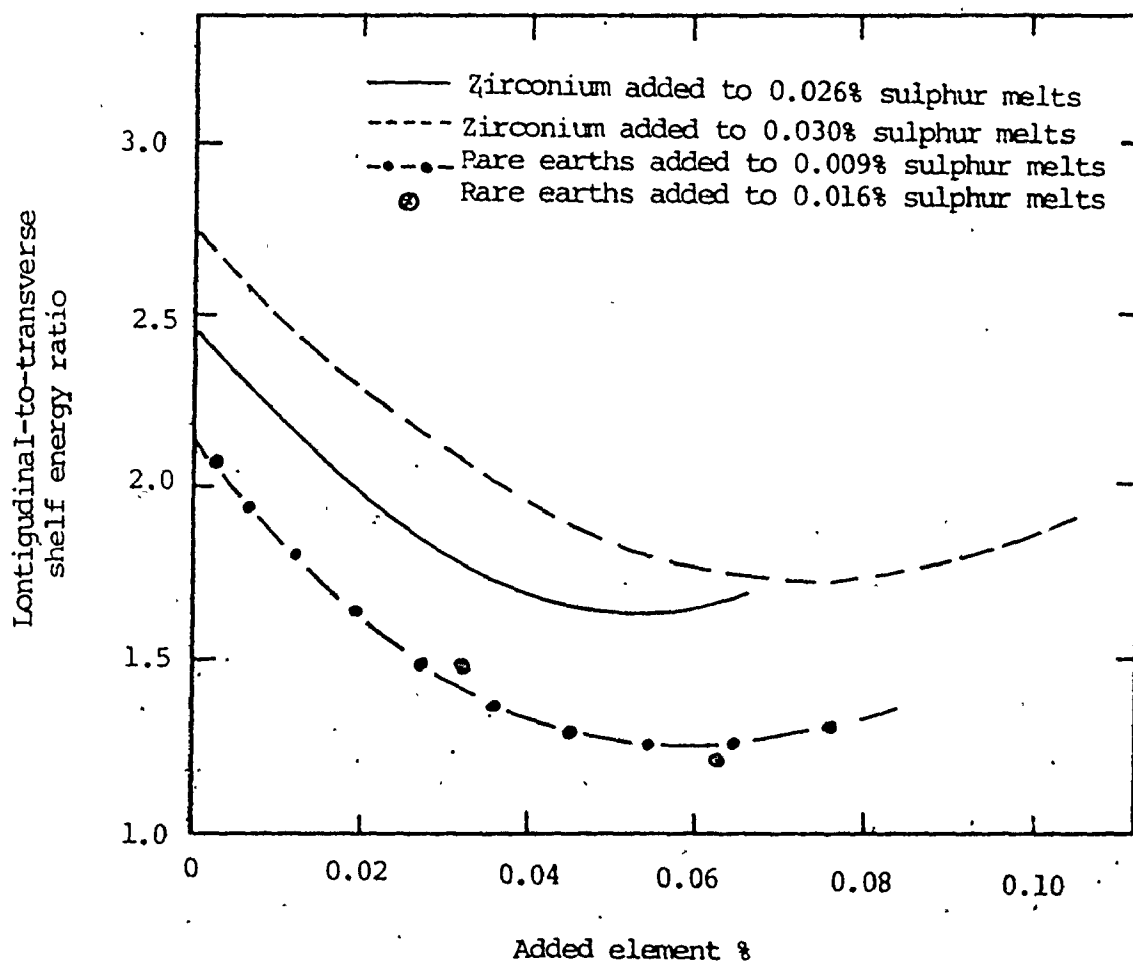


Fig. 10 Comparison of inclusion-shape control by zirconium and rare-earth additions on the anisotropy of Charpy shelf energy.

ZIRCONIUM

Zirconium must be added in amounts depending on the sulphur, nitrogen, and oxygen contents of the steel (15, 19-21). Zirconium can dissolve in manganese sulfide and thus decrease its plasticity. Sufficient zirconium is added so that manganese sulfide is replaced by a non deformable zirconium sulfide. Zirconium cannot be used as a sulfide modifier in steels whose properties are enhanced by high nitrogen contents, such as vanadium steels.

RARE EARTHS

Rare earths, which form a virtually non-deformable sulfide or oxy-sulfide. Because of their high affinity for oxygen and sulfur, the amount of rare earths must be sufficient to account for both these elements. Depending on the method of addition, recoveries can be erratic (18, 19). Under certain conditions, rare earth additions may lead to desulphurization reaction in steel. Little evidence exists suggesting that rare earths can replace manganese in manganese sulfides (20, 21). While rare earths are expensive, an optimum sulphur level of app. 0.010% in steel will lead to minimum costs. Appropriate addition techniques can overcome a tendency for gross segregation of rare earth inclusions.

The major effects of sulfide-modifying additions are to increase the transverse and through thickness ductility and charpy-shelf energy to levels comparable to those obtained in the long. direction, and to minimize the anisotropy of these properties. The optimum rare earth/sulphur ratio for minimum anisotropy is about 2.0 Fig. 9 (18). Rare earth additions seem to be more effective than zirconium additions Fig. 10 (18).

Above the optimum addition of either rare earth or zirconium, the charpy shelf energy values tend to decrease. This is apparently caused by zirconium forming embrittling zirconium carbide $Zr_4C_2S_2$ and rare earths forming a carbide or intermetallic compound.

Good formability therefore requires a low-carbon content, low and uniform dispersion of equiaxed nonmetallic inclusions, low sulphur contents and shape control of inclusions. It was recently suggested that non-metallic inclusions are the prime cause of limited formability of Hot Rolled HSLA Steels (22). It is possible, however, to design steels for optimum formability.

1.8 REVIEW OF MECHANICAL TESTS FOR ASSESSING SHEET MATERIAL FORMABILITY

In commercial operations a number of tests have been used by steel-makers and steel users to assess the formability of sheet steel for quality control purposes. None of these tests have gained wide acceptance on the basis of sensitivity, reproducibility, convenience etc. Some are used more widely than others, although this is usually because they have become established in steel specifications (e.g. tensile elongation and simple bendability) and does not necessarily indicate that they have particularly great sensitivity in determining steel quality. The more important of the tests currently used are briefly reviewed below.

The tensile test is universally used commercially to determine whether steels meet quoted strength specification limits. A natural consequence of this has been to use a parameter from this test, usually the total elongation at failure E_T , for formability specification. However, it has been shown that E_T does not always correlate well with press formability

and bendability (23-28) , presumably because it is largely governed by geometric instability rather than non-metallic inclusion content or shape. As pointed out above geometric instability does not seem to be a major factor limiting the formability of high strength steels, at least when these contain significant quantities of elongated inclusions.

If inclusions are important in failure during commercial forming then one would expect a correlation between commercial formability and the true strain at fracture or the reduction of area (R of A) in the tensile test. Published data is limited but supports a correlation between R of A and formability (24, 29) and also ductile fracture toughness (30). Unfortunately, this parameter is not easy to measure precisely in sheet materials because of the complex shape of the fracture surface and the difficulty of measuring thicknesses accurately for thin gauge materials. In consequence it has not been widely used for commercial quality control although its wider use is anticipated once a standard method of measurement has been established.

The simple bend test has been requested in steel specifications for many years as a supplement to the tensile elongation in the assessment of formability. The test is semi-quantitative and is usually only used on a pass-fail basis. It is difficult to adapt it to the quantitative measurement of relative formability although reasonable success has been achieved by the rather tedious and time consuming measurement of crack length at a given bend angle (28, 31, 32). For the more highly ductile or thinner gauge materials 180⁰ bending is achieved even over sharp bend radii and consequently the test cannot be used to rate the formability of these materials (25).

In the Hutchinson bend test (33) the bend specimen is prepared with sheared edges and is bent with the shear burr facing towards the outside of the bend. This is a rather more severe test than the simple bend test (with machined edges) since the sheared edge contains nucleating microcracks (25, 32). During the bending cracks grow from these microcracks at the specimen edges towards the centre. Quantitative results can be obtained, as with in the case of the simple bend test, by measuring these cracks at a given bend angle (21). The test is subject to the same limitations as the simple bend test.

Recently Japanese workers have shown that the elongation of notched tensile specimens shows an excellent correlation with bendability and press formability for hot rolled sheet steels (23, 27, 28) although the relation is poorer for cold rolled sheet. In comparison to the deformation mode in tensile tests the plane strain deformation created in the notched specimen is closer to that generally found in bending and press forming operations. Also the triaxial state of stress at the root of the notch probably assists in opening up cracks along inclusions and so amplifies the effect of elongated inclusions in the microstructure. A slight drawback to the use of this test in quality control work is the need to prepare accurately notched specimens.

The degree of expansion of a sheared circular hole during punch stretching has also been used as a measure of the quality of hot rolled HSLA sheet steel and has been shown to predict the effects of sulphide shape control (25). The hole expanding limit (34, 35) based on the initial and final diameters of the hole is generally used as a measure

of formability. The test is simple and easy to perform. However, it requires the construction of a hole blanking die and in addition the results obtained do not enable a comparison of longitudinal and transverse ductilities.

More recently, a stretch-bend test has been developed (36) which requires very simple specimen preparation, is easy to perform and analyse and appears to distinguish readily between steels of different quality. In the test a strip of material is clamped rigidly at the ends and stretch-bend over a radiused punch. The deflection of the punch at failure is normally used as the measure of formability of the test sample. A comparison of deflections for longitudinal and transverse specimens may give an indication of the presence of elongated inclusions or banded microstructures.

This test was first developed at Dofasco Research Laboratories using a rig of simple design incorporating a mechanical hold down (36). Subsequently other rigs have been built (37, 38). Uko (37) designed a sophisticated rig incorporating a hydraulic hold down for the specimen and allowing use of a variety of punch radii and two specimen spans. Some testing was carried out on HSLA pipeline steels using this rig and specimens with machined edges (39).

CHAPTER II

AIM OF THE PRESENT INVESTIGATION

The aim of the present work was to investigate the performance of the stretch bend test in characterising the formability of a number of HSLA sheet steels having a variety of strength levels, microstructures and inclusion contents and to compare the results obtained from stretch bend tests with those obtained from hole expansion and simple punch stretching tests using the same steels.

TABLE 1 Compositions of the Hot Rolled Steels

Steel	C	Mn	Si	P	S	V	Cb	Mo	Al	N	Nom. Min. YS. (ksi)	S Con- trol	Sheet Thick- ness in
A	.08	1.20	.33	.011	.005	.136	<.005	-	.056	.022	80	Yes	.103
B	.09	1.12	.22	.005	.014	.12	-	-	.031	.019	80	No	.096
C	.08	1.04	-	.003	.016	-	.073	-	.049	-	80	Yes	.100
D	.04	1.70	.11	.005	.009	-	.07	.28	.03	-	80	Yes	.106
E	.08	.46	-	.002	.010	.02	.007	-	.04	-	50	Yes	.095
F	.08	.46	-	.002	.010	.02	.007	-	.04	-	50	No	.085
G	.04				.038						30	No	.097

Composition in wt%

CHAPTER III

MATERIALS TESTED3.1 MATERIALS

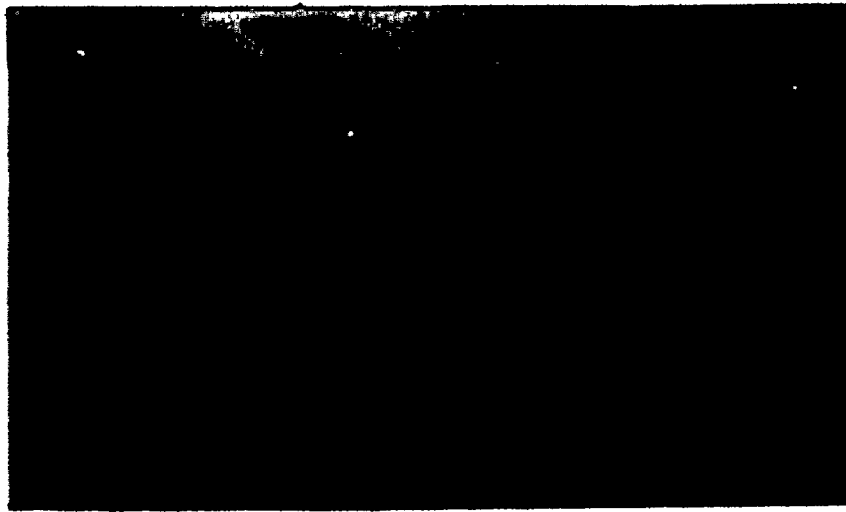
Seven commercially produced as-hot rolled sheet steels were used for the main part of the work. Their chemical composition, nominal yield strengths and sheet thickness are shown in TABLE 1.

All were low carbon aluminum killed steels. Steels A, B, C, E, and F had carbon levels of .08 - .09% and steel D a much lower content of .04%. Sulphur contents varied from .005% in steel A to .016% in steel C. Rare earth or zirconium additions were made to some steels to control sulphide inclusion shape as indicated in the table.

Steels A to D were nominally 80 ksi yield strength grades, steels E and F were 50 ksi grades and steel G was a conventional forming grade 'mild steel'. Of the 80 ksi steels A and B were Mn -V-N steels, one with (A) and one without (B) sulphide control. Steel C was a Mn - Cb steel and steel D a Mn - Mo -Cb steel. Sulphide modification additions had been made to both steels. The two 50 ksi steels were Cb - V types, again one with (E) and one without (F) sulfide control. Steel sheet thicknesses were in the range 0.085 - 0.103 in. for these steels.

3.2 METALLOGRAPHY

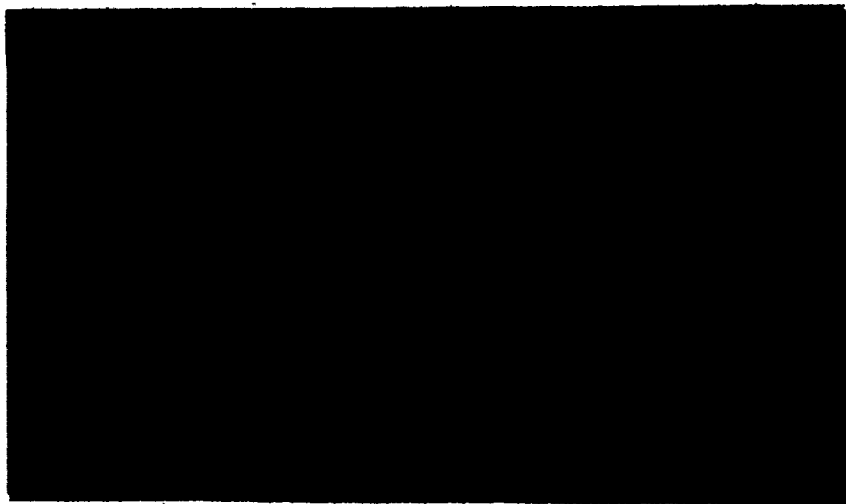
All the steels used were examined by optical microscopy on longitudinal sections perpendicular to the sheet surface. Inclusion



a) Steel A 1350X



b) Steel B 440X



c) Steel C 1360X

Fig. 11 Typical inclusion structures of the experimental steels.



d) Steel D light 2% Nital 800X



e) Steel E light 2% Nital 440X



f) Steel F light 2% Nital 440X



g) Steel G light 2% Nital 800X

TABLE 2
The Number of Inclusions / mm² in
Different Length Ranges

Steel	Inclusion Length Range μm			Mean Linear Intercept Grain size μm
	10-20	20-40	> 40	
A	4.6	2.0	0	4.75
B	60	49	38	5.95
C	46	21	11	4.05
D	2.5	0	0	2.80
E	3.4	0	0	7.75
F	48	40	36	6.30
G	74	63	53	11.10

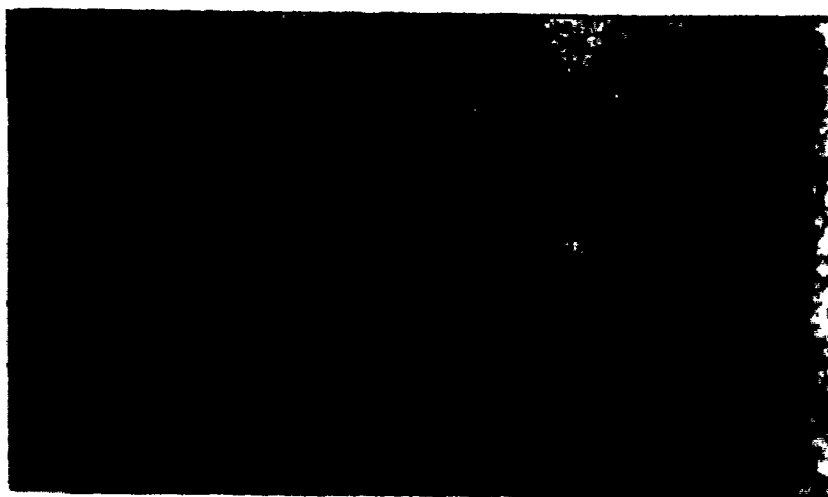
structures were examined in the unetched or lightly etched condition. Inclusion lengths were measured using a grid on the projection screen of an optical microscope at a magnification of about 650X. Measurements were made at a depth from the specimen surface of about one quarter the specimen thickness. The inclusions were categorised into different size ranges and the number of inclusions of a given size range per unit area of sample determined. These values were used for correlation with forming properties.

Grain sizes were measured at about the quarter thickness position in both longitudinal and through thickness directions. The two measurements did not differ greatly and an average value was calculated.

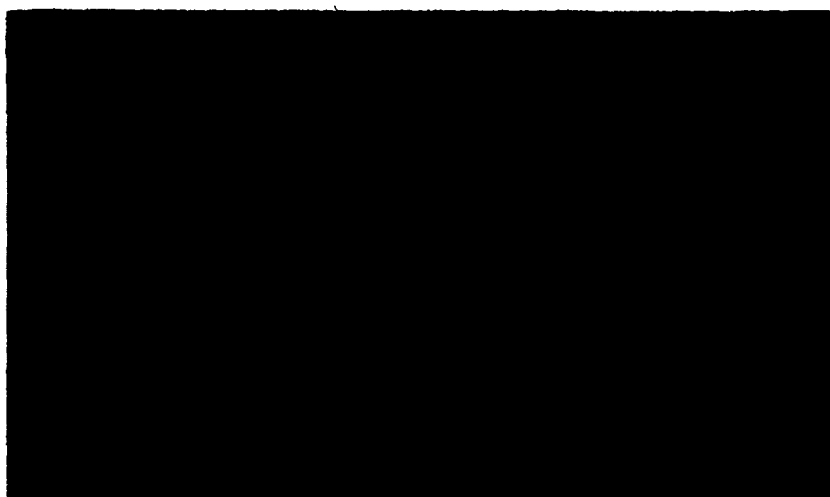
3.3 RESULTS AND DISCUSSION

The optical microscope examination of unetched or lightly etched samples revealed globular or blocky sulphides in steels A, D, and E, (Fig. 11 a, d, e) to which modifying additions had been made during steel making. The unmodified steels B, F, and G contained very thin highly elongated manganese sulphides (Fig. 11 b, f, g). Steel C was found to be partly modified and the sulphides exhibited a variety of shapes from globular through elliptical to thin elongated. (Fig. 11c).

The numbers of sulphides per unit area with lengths in the range 10-20 μm , 20-40 μm and over 40 μm are tabulated in TABLE 2. Steel G had the largest content of elongated inclusions closely followed by steels B and F. The modified steels A, D, and E had very low contents of inclusions greater than 10 μm . The elongated inclusion content of the partially modified steel, steel C, fell at levels intermediate between the fully modified



a) Steel A light 2% Nital 640X

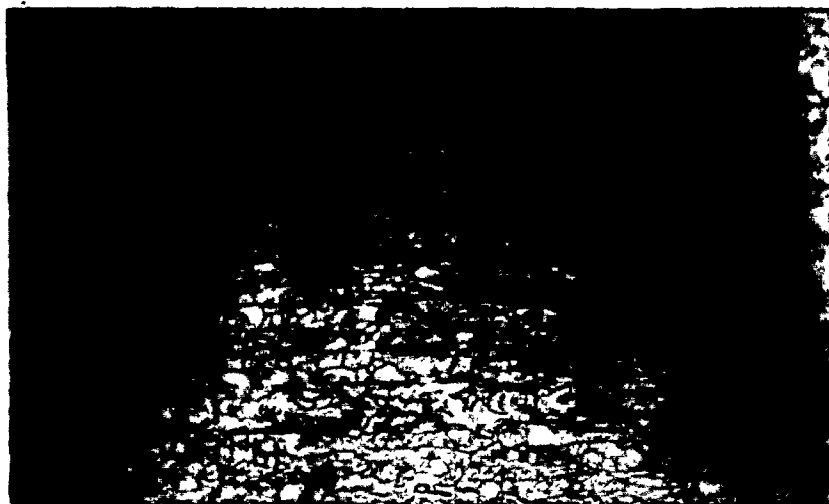


b) Steel B light 2% Nital 200X



c) Steel C light 2% Nital 640X

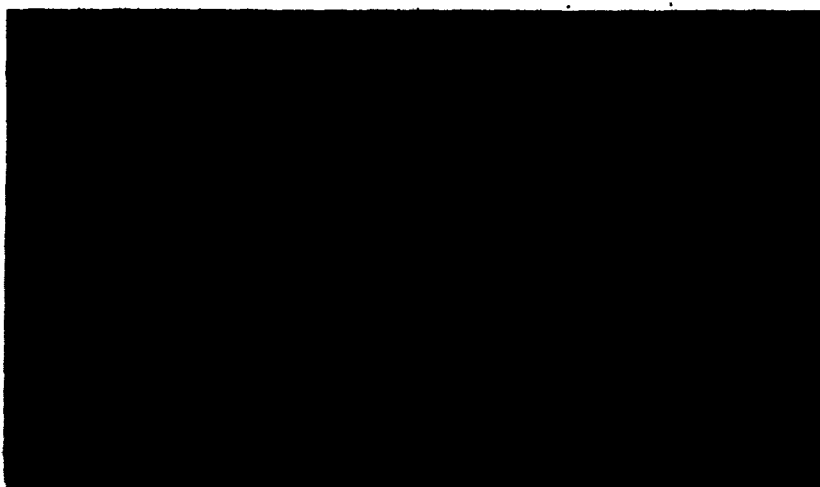
Fig. 12 Typical matrix structures of the experimental steels.



d) Steel D 2% Nital 640X



e) Steel E 2% Nital 640 X



f) Steel F 2% Nital 640X

Fig. 12 (contd)



g) Stéel G 2% Nital 320X

and unmodified steels as might be expected.

Most steels exhibited relatively uniform polygonal grain structures (Fig. 12). Steels D and particularly steel C had significant amounts of acicular structures towards the centre thickness of the sheets (Fig. 12d). Average linear intercept grain sizes shown in TABLE 2 varied from 2.8 μm in steel D to 11.1 μm in the drawing grade steel, steel G. Steels A, B, E, and F showed significant quantities of uniformly distributed fine lamellar or degenerate pearlite. In steels C and D pearlite was not evident and cementite was present as distinct particles. Steel G exhibited some pearlite but in much smaller amounts than the higher strength steels and most cementite was present as carbide films at grain boundaries. A prominent feature of steel D was the banded appearance of its grain structure in which carbide stringers could be distinguished (Fig. 12d).

CHAPTER IV

MECHANICAL TESTEXPERIMENTAL TECHNIQUES4.1 TENSILE TEST

Two tensile samples were tested for each steel in the longitudinal, transverse and diagonal directions to the rolling direction. Tensile testing was carried out on an Instron tensile machine at a crosshead speed of 0.1 in/minute. ASTM A370 type specimens were used with a 2 in. gauge length and 0.5 in. gauge width. A 1 in. gauge length extensometer was used to measure specimen extension during the test.

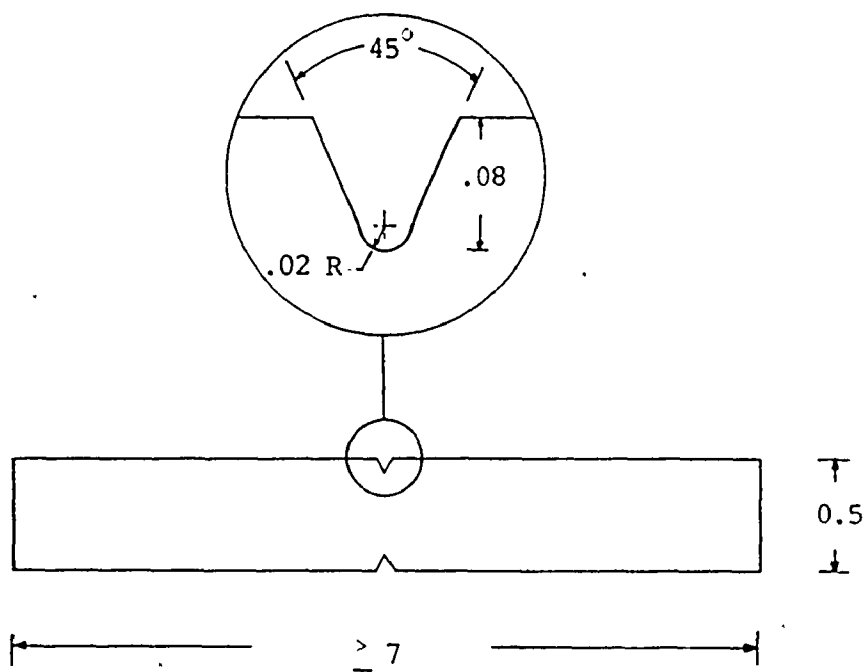
The drawability index, r value, was measured on all the hot rolled commercial steel specimens by recording length and width over a 1 in. gauge length in the centre of the specimen after 10 - 16% strain-prior to maximum load. Following these measurements specimens were reloaded and strained to failure so that total elongation and reductions of area at failure could be obtained.

Work hardening indices, n values, were measured on all steels by iterative fitting (48) of the stress vs strain curve to the equation

$$\sigma = k(\epsilon_0 + \epsilon)^n \quad (4)$$

where k and ϵ_0 are constants. Uniform elongations were estimated from the elongation of electrochemically etched grid marks, originally of about 0.25 in. length, away from the necked regions on fractured specimens.

Thickness and width at fracture were measured using a point



ALL DIMENSIONS ARE IN INCHES

Fig. 13 Dimensions of the NOTCHED TENSILE TEST
PIECE.

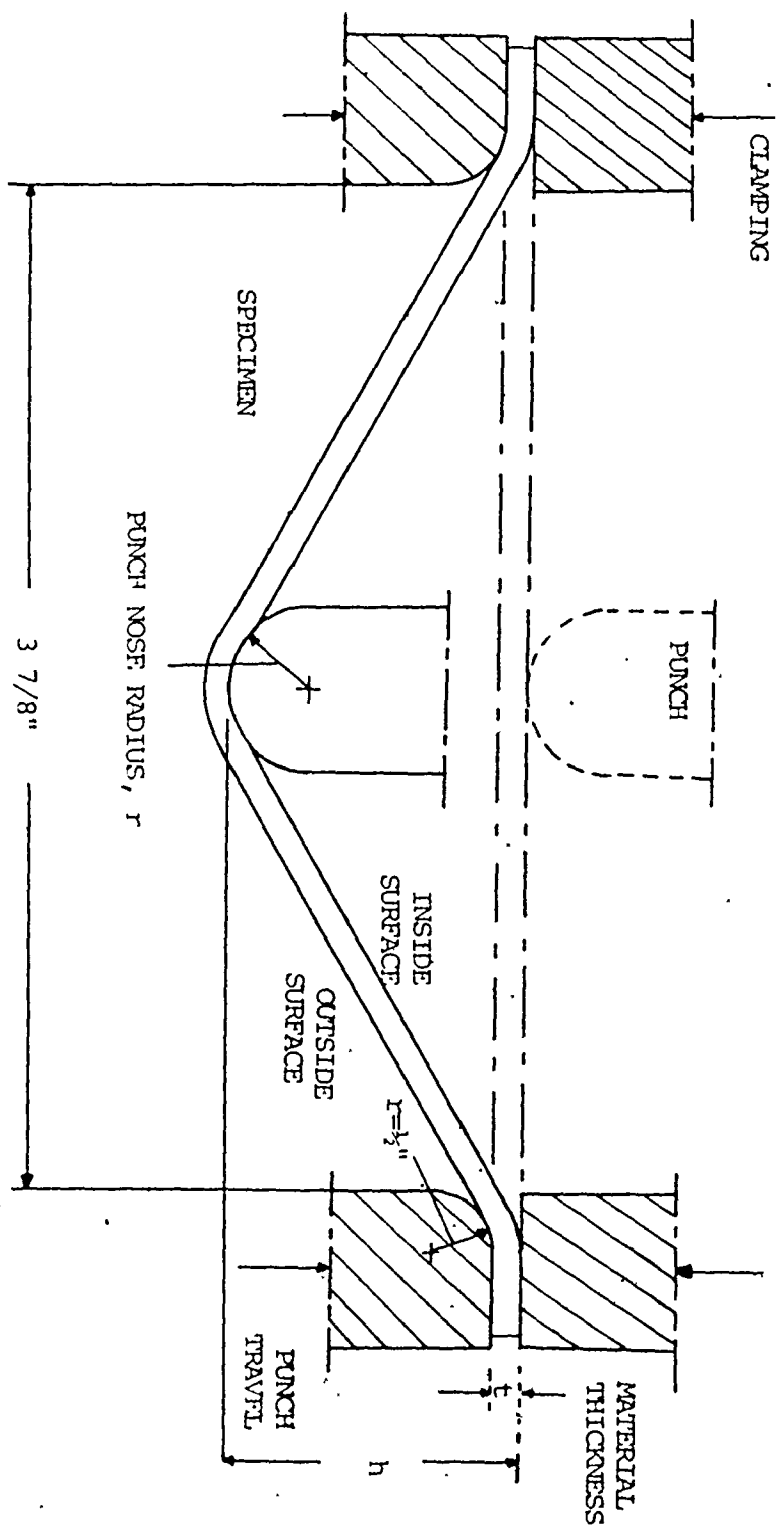


Fig. 14 A schematic drawing of the stretch-bend test

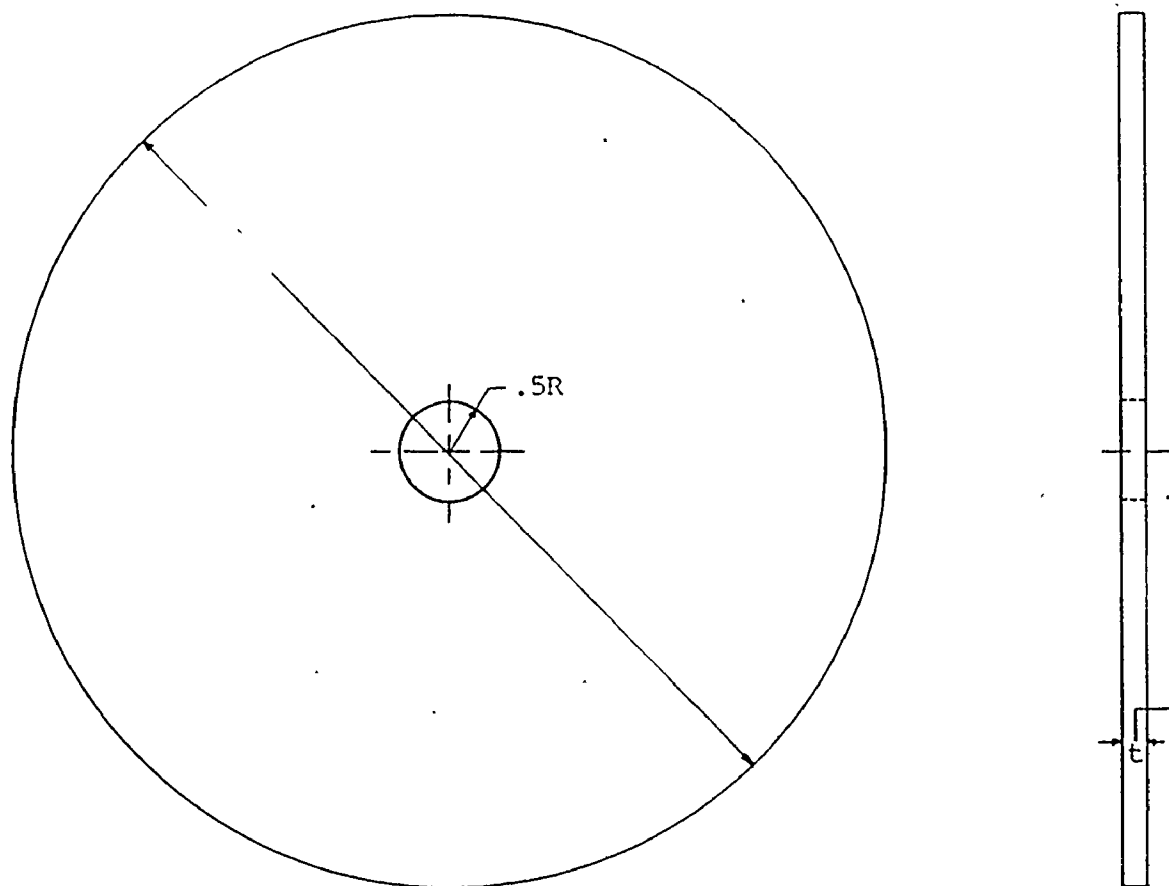
micrometer for calculations of reductions of area. Thickness varied markedly across the widths of the specimens at fracture and an average value was used in the calculation. In addition local surface elongations at fracture were measured from electromarked grid circles spanning the fracture. These measurements were made on circles at the centre width of the specimen which were approximately bisected by the fracture crack. It is not proposed that such measurements have any fundamental significance, due to the strain gradients in the local neck, however, they appear to have value in distinguishing the relative forming quality of different steels.

4.2 NOTCHED TENSILE TEST

Notched tensile tests were carried out on longitudinal and transverse samples of all the steels to supplement the formability parameters obtained from the tensile test. The specimen dimensions are shown in Fig. 13. Measurements of specimen elongation at fracture were taken during testing using a 1 in. extensometer placed symmetrically across the notch. Elongation measurements were also made on the fractured specimens from 1 in. scribed gauge marks. In addition, local strains at fracture in the centre of the specimen width were measured from a .09 in. scribed grid.

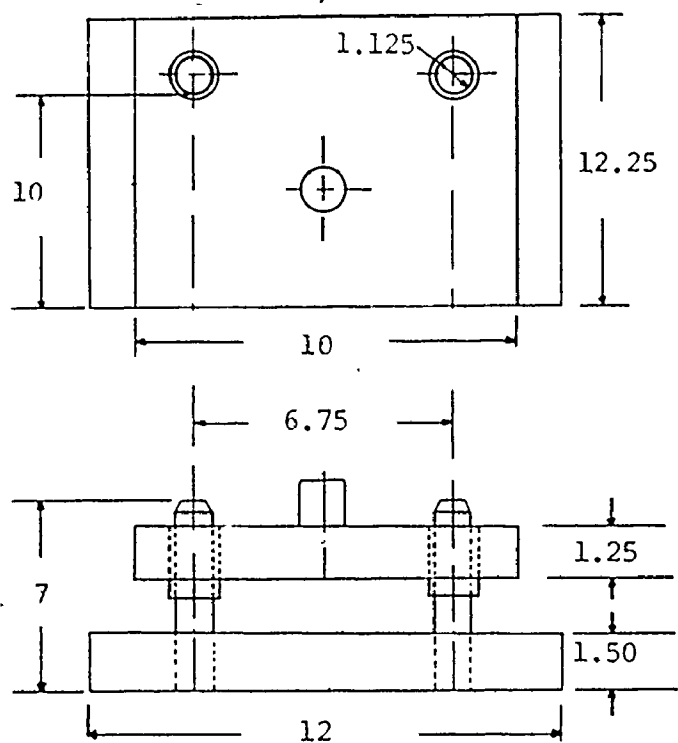
4.3 STRETCH BEND TEST

A schematic representation of the stretch bend test is shown in Fig. 14. A strip sample of the material to be tested is clamped firmly between jaws and bent in tension over a radiused punch. The formability of the specimen is usually measured from the punch travel at maximum load



ALL DIMENSIONS ARE IN INCHES
 t thickness of the specimen

Fig. 15 Specimen for Hole Expansion Test



NOT TO SCALE

ALL DIMENSIONS ARE IN INCHES

Fig. 16 Die set for punching 1 in. dia. holes.

or failure.

The stretch bend test equipment used in the present work has been described in detail by Uko (37). Samples 7 in. long and 2 in. wide were used for most of the work with a 3.375 in. span between the clamping jaws. Two sets of samples were prepared, one set with machined edges and one set with sheared edges.

Sheared edge specimens were prepared on a mechanical shear with a 0.020 in. clearance between the shear blades. The specimens were prepared so that the shear burrs were on the same surface of the sheet and were always tested with these burrs towards the outside of the bend.

All the hot rolled specimens were tested at three punch radii, .125, .25, and .50 in. Sheared edge specimens for some steels were also tested at .05 in. and .75 in. radius. In all tests a hydraulic clamping pressure of 1500 psi., equivalent to about 15 ton load on each of the clamped flanges, was used and this was effective in preventing any drawing-in from the flanges. In all but a few tests reported later, 0.004 in. thick polythene oiled on both surfaces with General Purpose Motor Master oil SAE-140, was used as lubricant between punch and specimen.

Punch speed for all tests was 0.4 in./min. Punch load and travel were autographically recorded during the test and, in addition, the maximum load value was read from a digital recorder.

4.4 HOLE EXPANSION TEST

The blanks for hole expansion tests were 9 in. dia. discs with 1 in. dia. central hole as shown in Fig. 15. The central holes were punched out in a subpress using commercially available punch & die set (Fig. 16) with .015 in. clearance.

The hole expansion tests were carried out by stretching these blanks over a 4 in. dia. hemispherical punch through a 4.25 in. dia. die plate, using a similar testing rig to that described by Paul-Chowdhury for simple punch stretching tests (43). Blanks were oriented such that the burr on the sheared hole faced away from the punch. The blanks were clamped in the flange region under 1500 psi pressure (i.e. about $30T$ on the flange). Oiled polythene lubrication was used between punch and specimen. The punch speed used was 4.4×10^{-3} in./sec and load and deflection were autographically recorded during the test. Crack propagation from the sheared edge was taken as the end point of the test and this point was evidenced by a sharp drop in load or sudden decrease in slope on the chart record.


The diameter of the hole at failure was measured in the longitudinal, diagonal and transverse directions and the average value calculated. The hole expansion limit λ_{av} was then calculated from

$$\lambda_{av} = \frac{d_{av} - d_0}{d_0}$$

where d_{av} and d_0 are the final and original hole sizes.

4.5 PUNCH STRETCH TEST

Punch stretching was carried out using the same equipment and the same testing conditions as those used for the hole expansion tests. Again autographic load vs. cup height curves were obtained during the test and failure of the cup was evidenced by a sudden drop in forming load. Two tests were carried out for each steel tested. The blanks for punch



stretching tests were 9 in. in dia. discs.

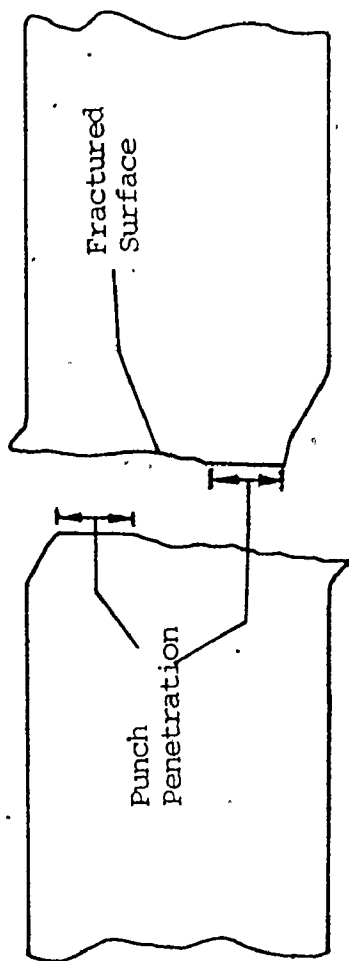


Fig. 17 Schematic diagram of the two halves of a sheared sheet illustrating the measurement of depth of blade penetration.

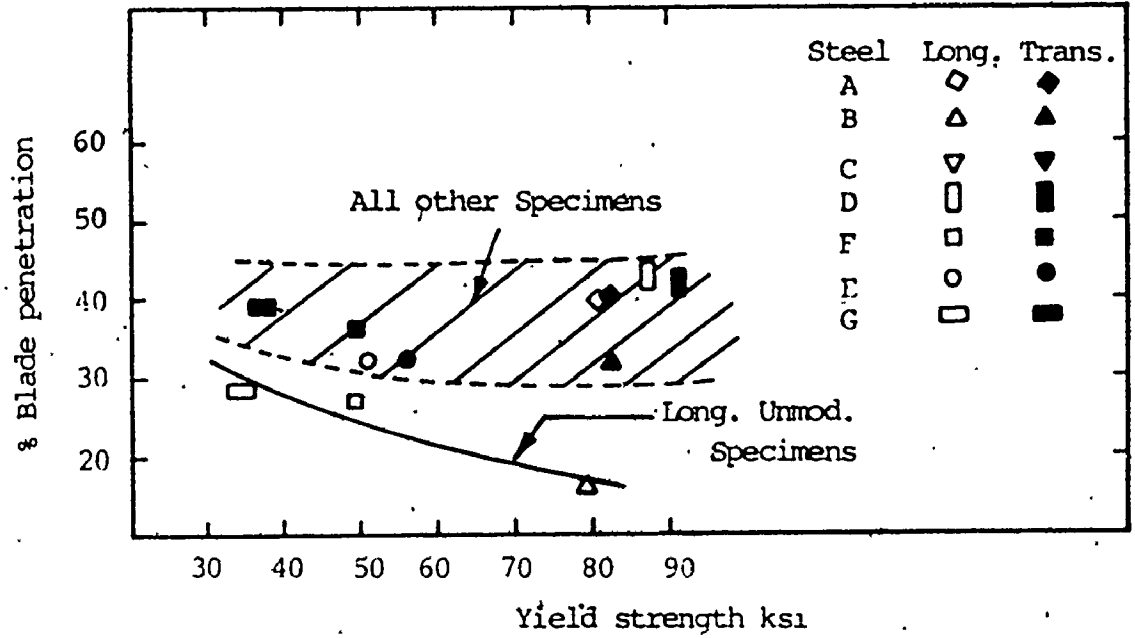


Fig. 18 The dependence of the blade penetration depth (as a percentage of sheet thickness) upon yield strength and inclusion shape.

NOTE DATA FOR 'STEEL C' NOT AVAILABLE

CHAPTER V

RESULTS AND DISCUSSION

5.1 STRAIN MEASUREMENT

To enable the measurement of local strains on tensile, stretch bend and punch stretch specimens grids of 0.09 in. dia. overlapping circles were electroetched onto the steel surface using commercially available equipment. The grid circles were measured using a tool makers microscope. The errors in strain measurements due to variations in circle diameter on the stencils and to measurement errors are estimated to be about $\pm 3\%$. This error could be significant for measurements of small strains.

5.2 SHEARING

During shearing the shear blades penetrate the surface of the sheet being sheared for a distance before the intervening material fractures (Fig. 17). The penetration depth might be expected to depend on microstructures since it should be sensitive to fracture characteristics. Since there was an interest in the influence of microstructure on the fracture characteristics in the present work it was pertinent to determine whether this dependence could be detected.

Measurements of the depth of blade penetration were made on the longitudinal and transverse sheared stretch bend specimens using the micrometer stage of an optical microscope. The results are shown in Fig. 18. The results for most of the samples measured fall in a broad band at punch penetrations between 30 and 45% exhibiting a small dependence only on yield

TABLE 3

TENSILE PROPERTIES OF THE HSLA STEELS

Steel	YS ksi	UTS ksi	YH %	E _T %	n	r	ϵ_0	R of A %	E _L %
A L	80.5	95.7	-	13.5	.137	.80	.0125	65.0	102
A T	82.0	95.9	-	14.1	.134	.91	.0155	60.5	100
A D	81.8	94.8	-	14.5	.143	.99	.0175	64.5	109
Average	81.6	95.6	-		.92				
B L	79.4	96.0	0.2	13.7	.153	.85	.005	61.0	97
B T	82.6	96.6	0.6	12.2	.141	.94	.004	50.5	83
B D	82.6	96.3	1.0	9.5	.142	.88	.004	63.5	99
Average	81.8	96.4	0.6		.89				
C L	74.9	83.7	1.3	14.7	.117	.61	0	72.0	100
C T	79.3	86.4	1.9	11.7	.109	.74	0	58.5	94
C D	76.1	82.5	2.4	11.5	.117	1.10	0	68.5	117
Average	77.4	84.8	1.9		.89				
D L	87.2	91.8	5.2	14.0	.142	.46	0	67.0	98
D T	91.7	93.4	7.1	15.5	.130	.59	0	64.0	102
D D	86.9	89.1	6.8	15.0	.132	1.20	0	72.0	128
Average	89.4	91.9	6.6		.93				
E L	51.2	63.2	1.90	29.5	.162	.90	0	69.5	127
E T	55.7	62.5	3.60	21.5	.150	.92	0	69.5	125
E D	54.6	62.0	3.50	22.2	.151	.99	0	69.5	128
Average	54.3	62.6	3.15		.95				
F L	49.2	63.4	0.2	23.0	.159	.71	.008	72.0	119
F T	49.4	63.2	-	26.0	.183	.86	.017	62.0	112
F D	48.3	62.1	-	26.5	.179	.98	.016	70.0	129
Average	49.1	63.0			.88				

No sulphide control
- Elongated inclusions

No sulphide control
- Elongated inclusions

TABLE 3 (Continued)

Steel	YS ksi	UTS ksi	YH %	E_u^* %	E_T %	n	r	ϵ_0	R of A %	E_L %
G L	34.8	48.4	-	29.7	42.0	.231	.86	.028	75.5	142
G T	36.5	48.5	-	25.7	38.5	.220	.84	.020	68.0	130
G D	34.8	47.5	-	28.5	41.0	.225	.98	.020	74.0	145
Average	35.7	48.2			40.0		.91			

No S control
- elongated inclusions

* Estimated from 1/4" gauge marks on area outside the neck after fracture.

YH Horizontal Yield estimation

E_L Local Elongation at Fracture

strength level. However, the results for longitudinal specimens of the unmodified steels B, F and G show much lower blade penetration distances before fracture than do the other specimens and this indicates a significant influence of elongated inclusions on blade penetration during shearing. , Pearce and Mazhar (15) have previously shown that blade penetration could be related in a general way to material ductility.

5.3 TENSILE TESTS

5.3.1 TENSILE PROPERTIES OF HSLA SHEET STEELS

The tensile results for these steels are shown in TABLE 3 where properties are given for the longitudinal, transverse and diagonal specimens. This table also includes the averaged properties calculated using the normal averaging formula,

$$\bar{C} = 1/4 (C_0 + 2C_{45} + C_{90}),$$

where \bar{C} is the average of the property C and C_0 , C_{45} and C_{90} the property at 0° , 45° and 90° to the rolling direction.

For each of the steels the strength levels were generally greatest in the transverse specimens and least in the longitudinal specimens. The highest yield strength level was found in steel D (89 ksi), steels A and B were of similar strength level (82 ksi) with steel C slightly lower (77 ksi). Of the nominally 50 ksi yield strength steels, steel E (54 ksi) was somewhat stronger than steel F (49 ksi).

The tensile curves of steels C, D and E showed sharp yield points and significant yield point elongations. This was particularly noticeable in the very fine grained steel D where yield elongations in the range 5 - 7% were obtained.. Steels A, B, F and G had been temper rolled during

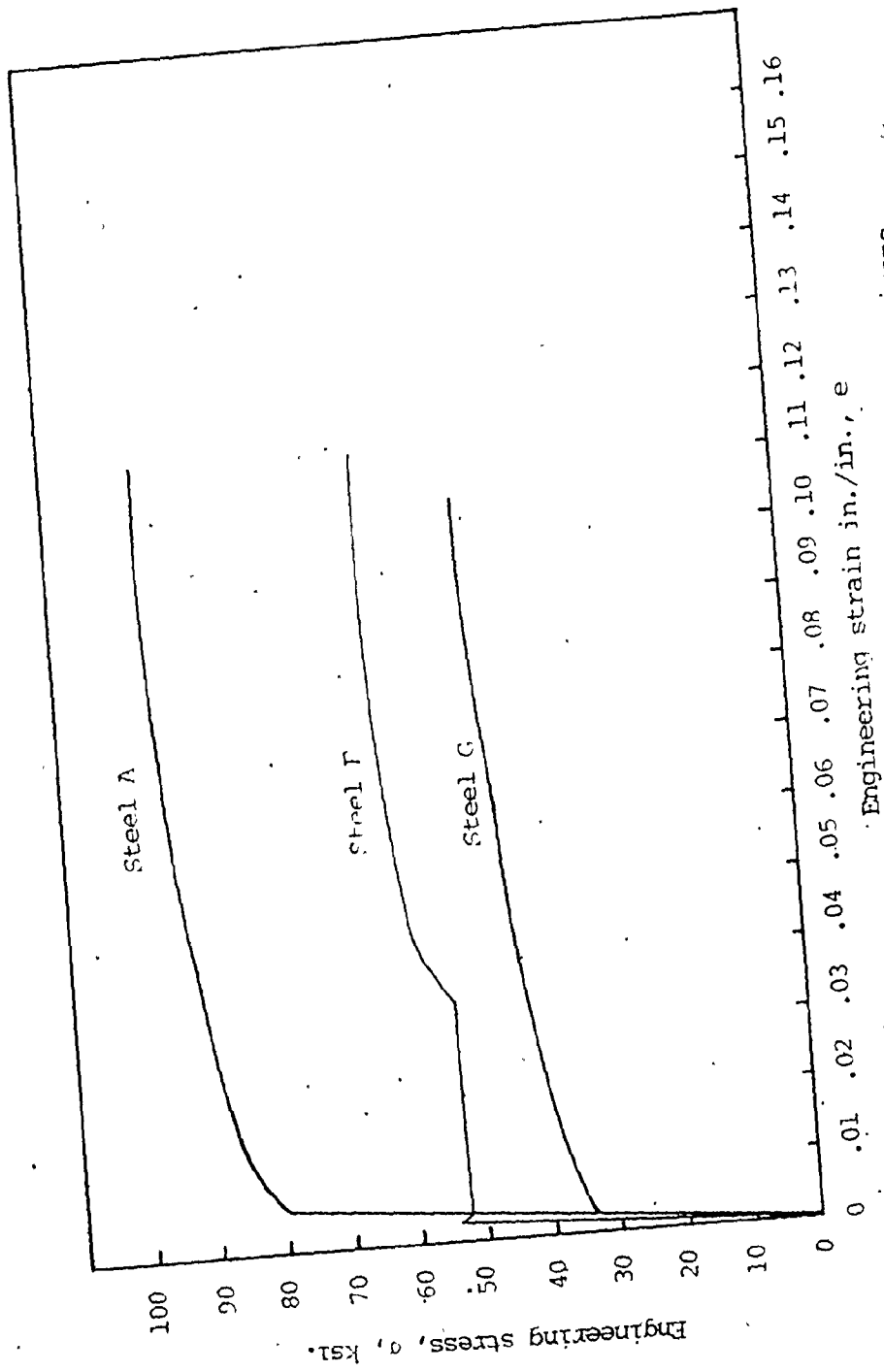
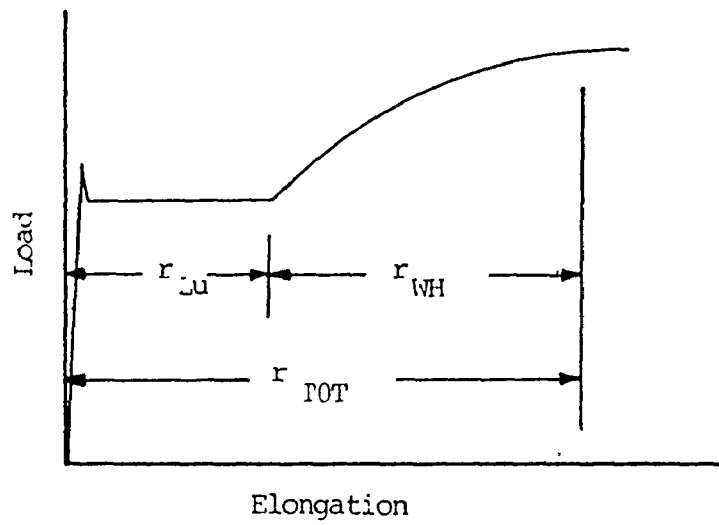


Fig. 19 Engineering stress-strain curves for transverse specimens



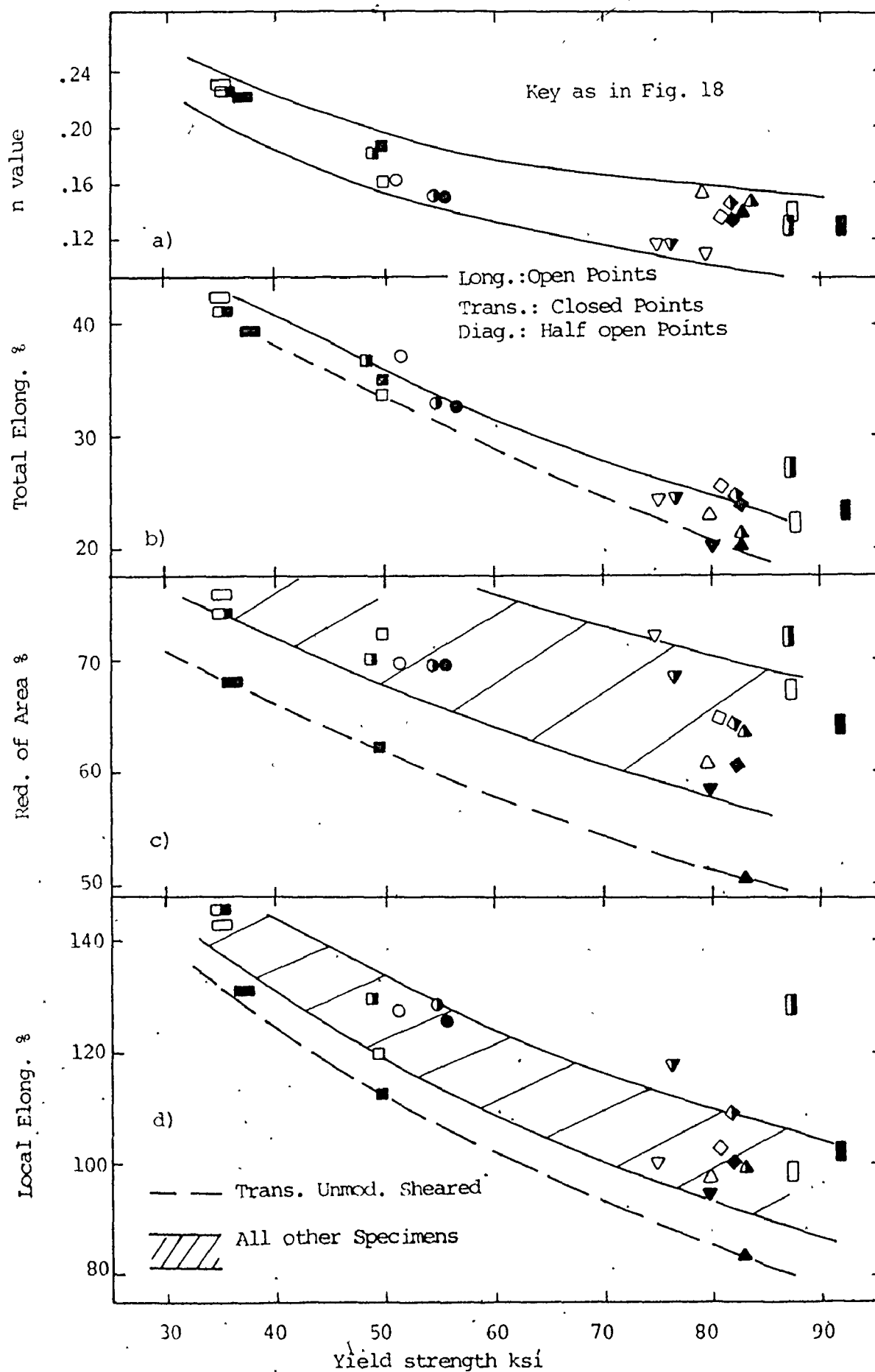
Specimen Orientation	r_{Lu}	r_{TOT}	r_{WH}
Long.	.45	.56	.64
Trans.	.55	.61	.68
Diag.	1.32	1.27	1.24

Fig. 20 The dependence of the drawability index, r value, upon the range of strain over which it is measured.

commercial processing to eliminate the yield point elongation. Rounded yield points were observed in these steels except for steel B which exhibited a small (0.2 - 1 %) yield horizontal suggesting insufficient temper rolling. Steels that had been temper rolled exhibited a positive value of ϵ_0 in equation 4 whereas in those that had not been temper rolled this value was generally zero. Previous work has shown that the value of ϵ_0 can be related to the strain applied during temper rolling (44). Engineering stress-strain curve for different strength levels are as shown in Fig. 19.

The r values of most of the steels fell in the range 0.8 to 1.0 with the higher values corresponding to diagonal specimens. However, the high manganese, high niobium steels, C and D, and particularly steel D, which also contained molybdenum, exhibited much lower values of r in longitudinal and transverse directions and higher values in diagonal directions than for other steels. This phenomena has been noted before in such steels and associated with transformation of heavily rolled unrecrystallized austenite (45).

It was considered possible that the unusual distribution of r values in steel D might be due to errors in measurements associated with the constraints to width strain imposed during the long Lüders elongation of this steel. Therefore, tensile tests were repeated for this steel and measurements for r values were made at the end of the Lüders region and then again at strains just prior to maximum load. The results are shown in Fig. 20, together with an inset illustrating the three strain ranges over which r was measured. It is clear that the measured r values are



influenced by the discontinuous deformation in the yield horizontal but in this steel the effect is not large. For consistency the r values used in subsequent discussion are those measured over the whole strain regime and given in TABLE 3.

5.3.2 VARIATION OF n , E_T , R OF A , E_L WITH YIELD STRENGTH AND INCLUSION

CHARACTERISTICS

The work hardening index n , total elongation E_T , reduction of area R of A , and local elongation at fracture E_L are shown in Fig. 21, as a function of yield strength level. All these parameters decreased with increasing yield strength level. In most steels the n values were larger in longitudinal than transverse specimens, however, the magnitude of this difference did not seem to be influenced by sulphide modifying additions and appears to be mainly due to the differences in yield strength level between longitudinal and transverse specimens. Steel C exhibited a generally lower n value than the other 80 ksi yield strength steels and this possibly reflects its higher overall inclusion content.

In contrast to the results for n values the results for E_T , R of A and E_L show a clear dependence on sulphide modification. The values for transverse specimens of the unmodified steels B, F & G fall to lower levels than the values for all other specimens. This is most noticeable in the E_L (Fig. 21d) and R of A (Fig. 21c) plots. The effect is relatively small in E_T (Fig. 21b) and indicates a relative insensitivity of this parameter to inclusion shape as mentioned previously. The results for the transverse specimen of the partly modified steel, steel C, fall towards the bottom of the general bands of results but above the bands of results for the

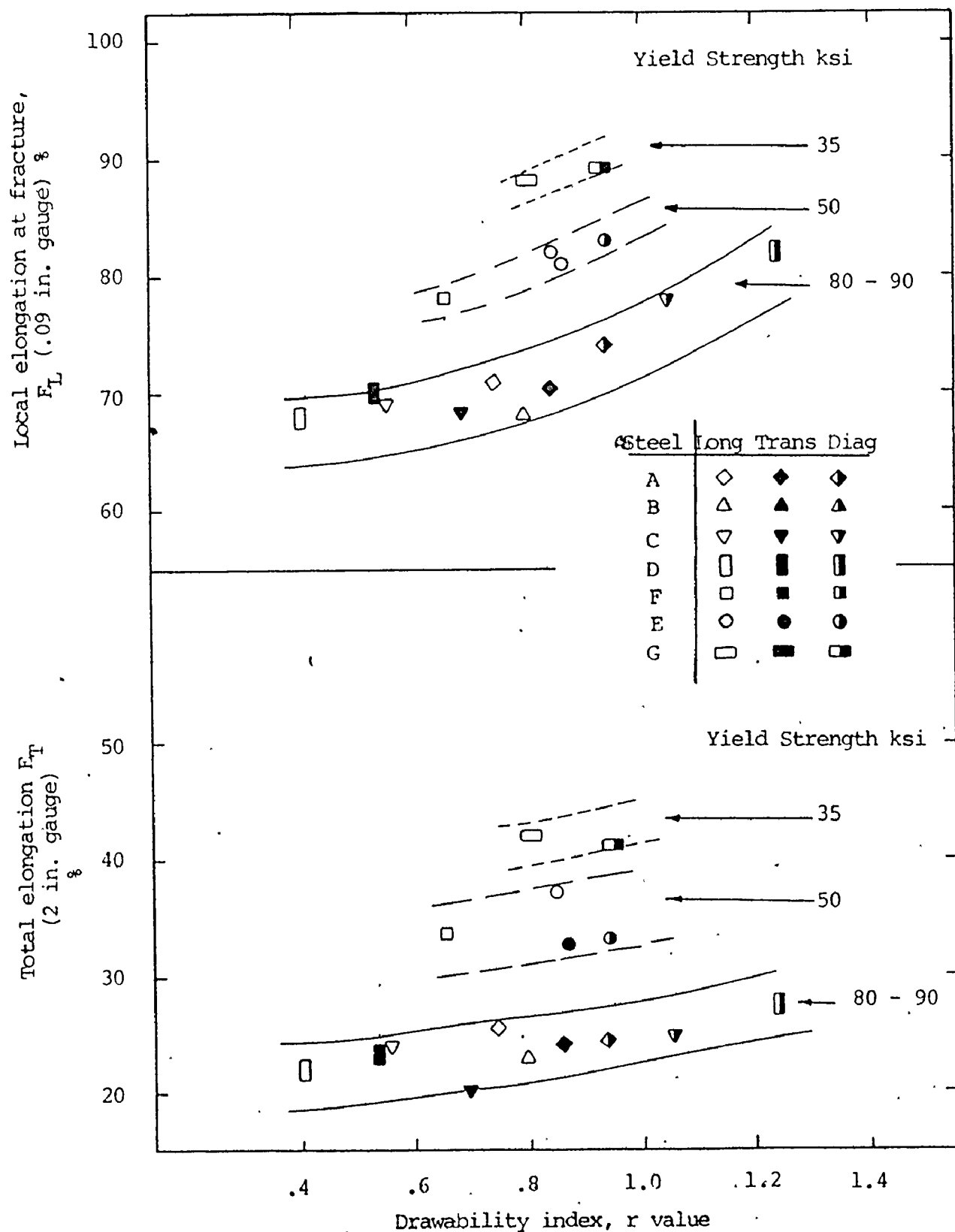


Fig. 22 The dependence of total elongation and local elongation in the tensile test on the drawability index. Results are grouped into bands for steels of similar yield strength.

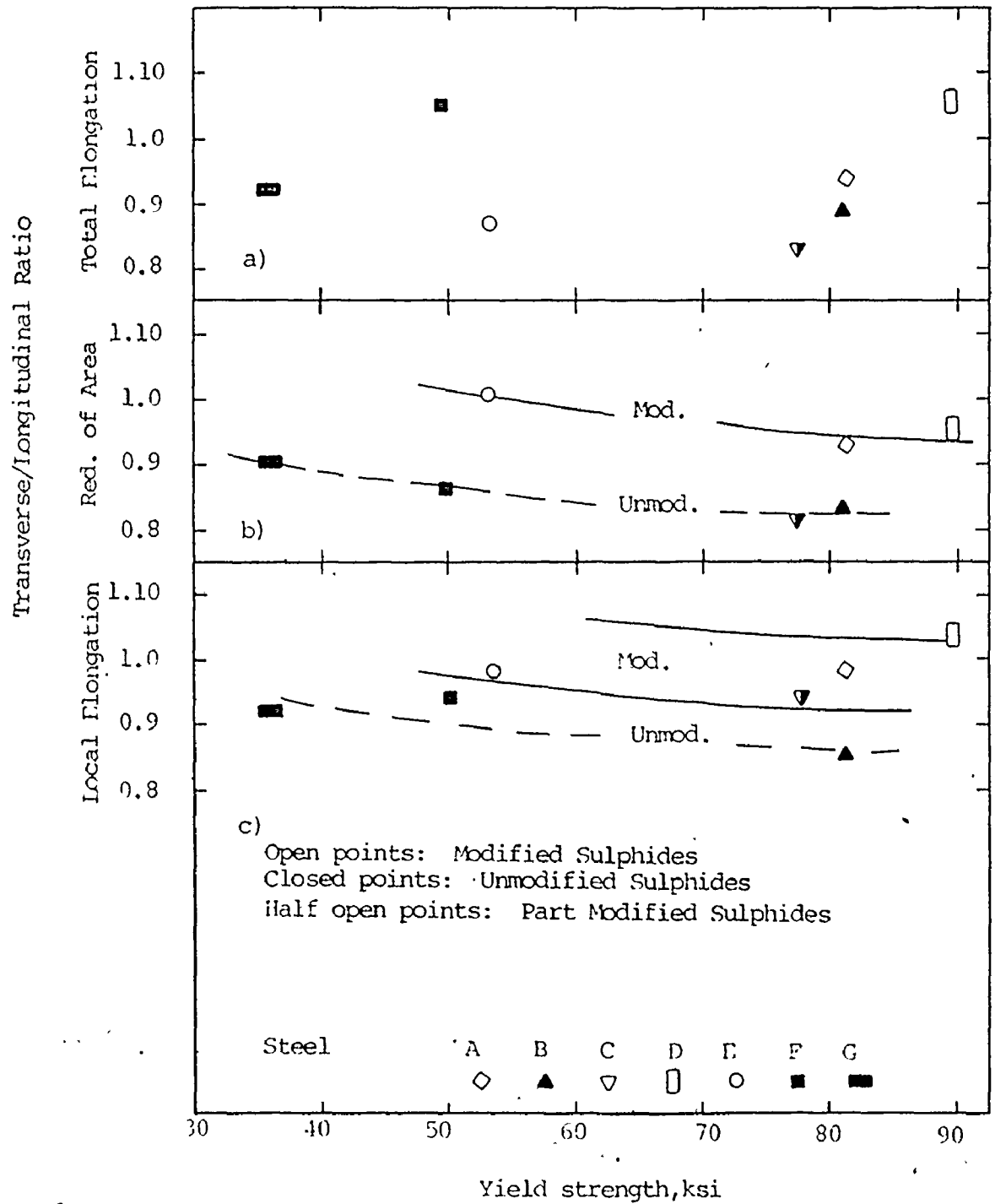


Fig. 23 The variation of the transverse/longitudinal ratio with yield strength and inclusion characteristics.

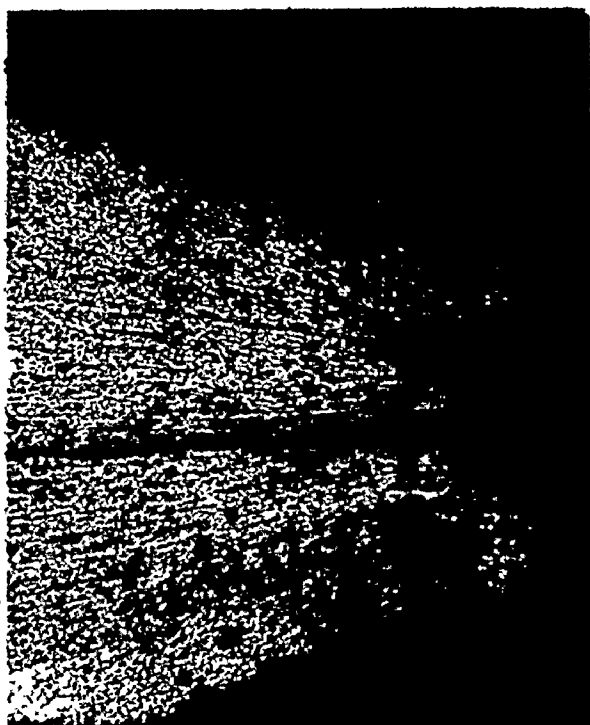
transverse specimens of the completely un-modified steels.

5.3.3 DEPENDENCE OF F_T AND E_L ON DRAWABILITY INDEX

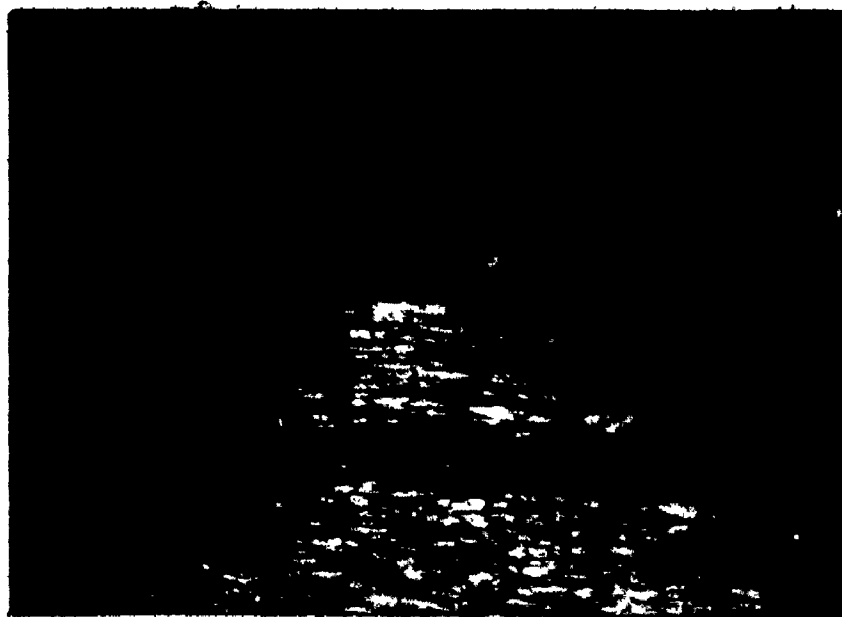
Both E_L and to a lesser extent, E_T increase with increasing drawability index, r value, as shown in Fig. 22. This behaviour would be consistent with a constant thickness strain criterion (or similar criterion) of fracture, which has been observed for HSLA sheet (46), and the expected change in strain path with increasing r value. In most hot rolled steels this effect is relatively unimportant since the range of r values is not large. However, in the higher alloyed steels C and D the r values obtained are much lower than in conventional hot rolled steels and some care must be exercised in comparing total and local elongations of the two types.

5.3.4 PLOT OF RATIO OF TRANSVERSE / LONGITUDINAL PROPERTIES WITH Y.S. AND INCLUSION CHARACTERISTICS

The influence of varying r value is the cause of some of the scatter in the results shown in Fig. 21 but the majority of this scatter can probably be accounted for in terms of variations in carbon and sulphur contents and steel microstructures. It can be an advantage in such circumstances, when trying to illustrate steel quality effects, to normalize for the variations in composition and microstructure between different steels by plotting the ratio of transverse/longitudinal properties. This has been done in Fig. 23 which more clearly illustrates the improvement in steel quality obtained through sulphide modification, at least in the case of R of A and E_L .



(a) Section perpendicular to the fracture surface.
Mag. 640X 2% Nital etchant.



(b) Association between carbide stringers and the
advancing crack tip. Mag. 640X, 2% Nital etchant.
Fig. 24 Optical micrograph showing the delamination
phenomenon encountered in steel D during
tensile testing.

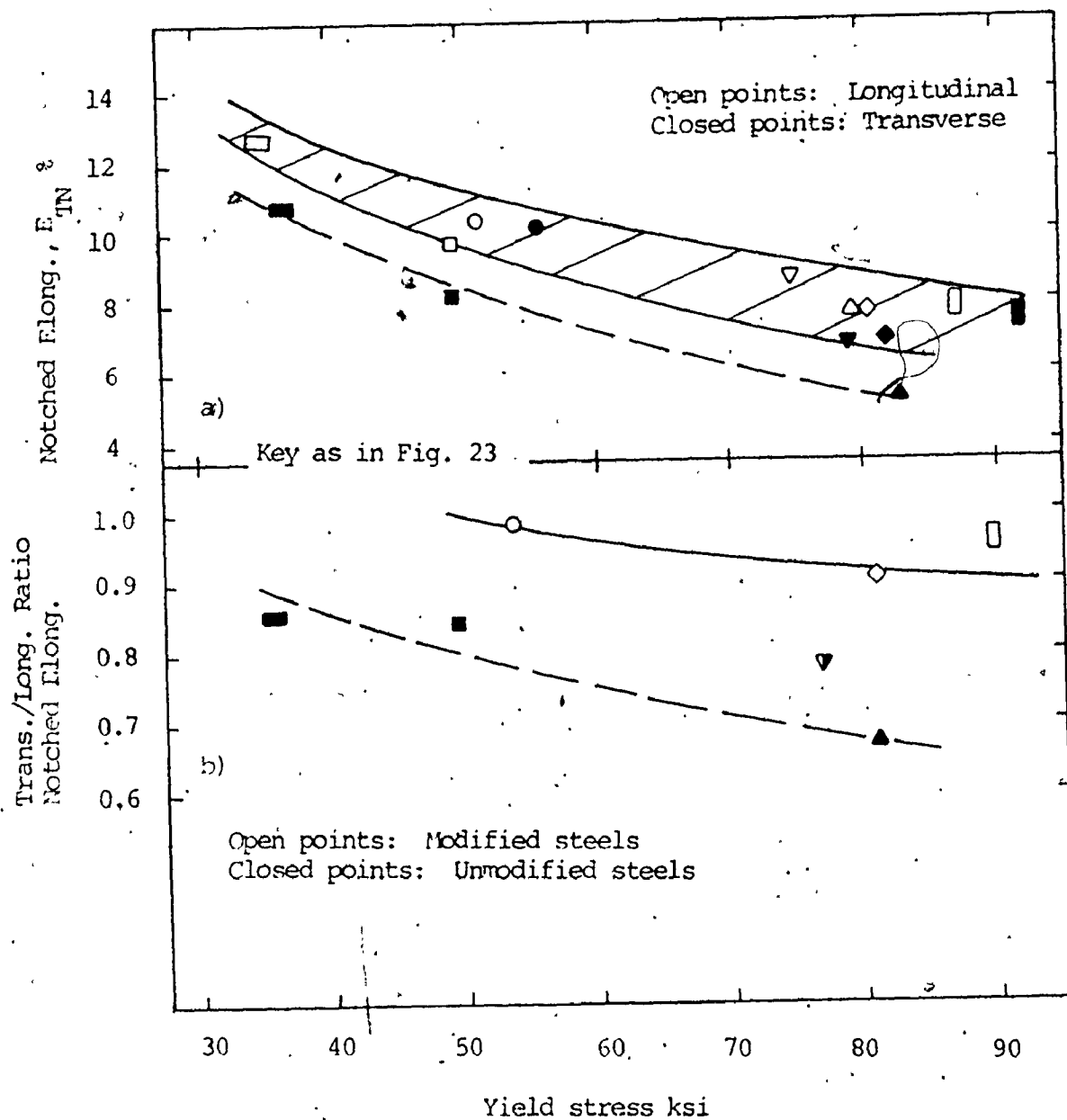


Fig. 25 The variation of the notched tensile elongation and the ratio of the transverse/longitudinal notched tensile elongation with yield stress and inclusion characteristics.

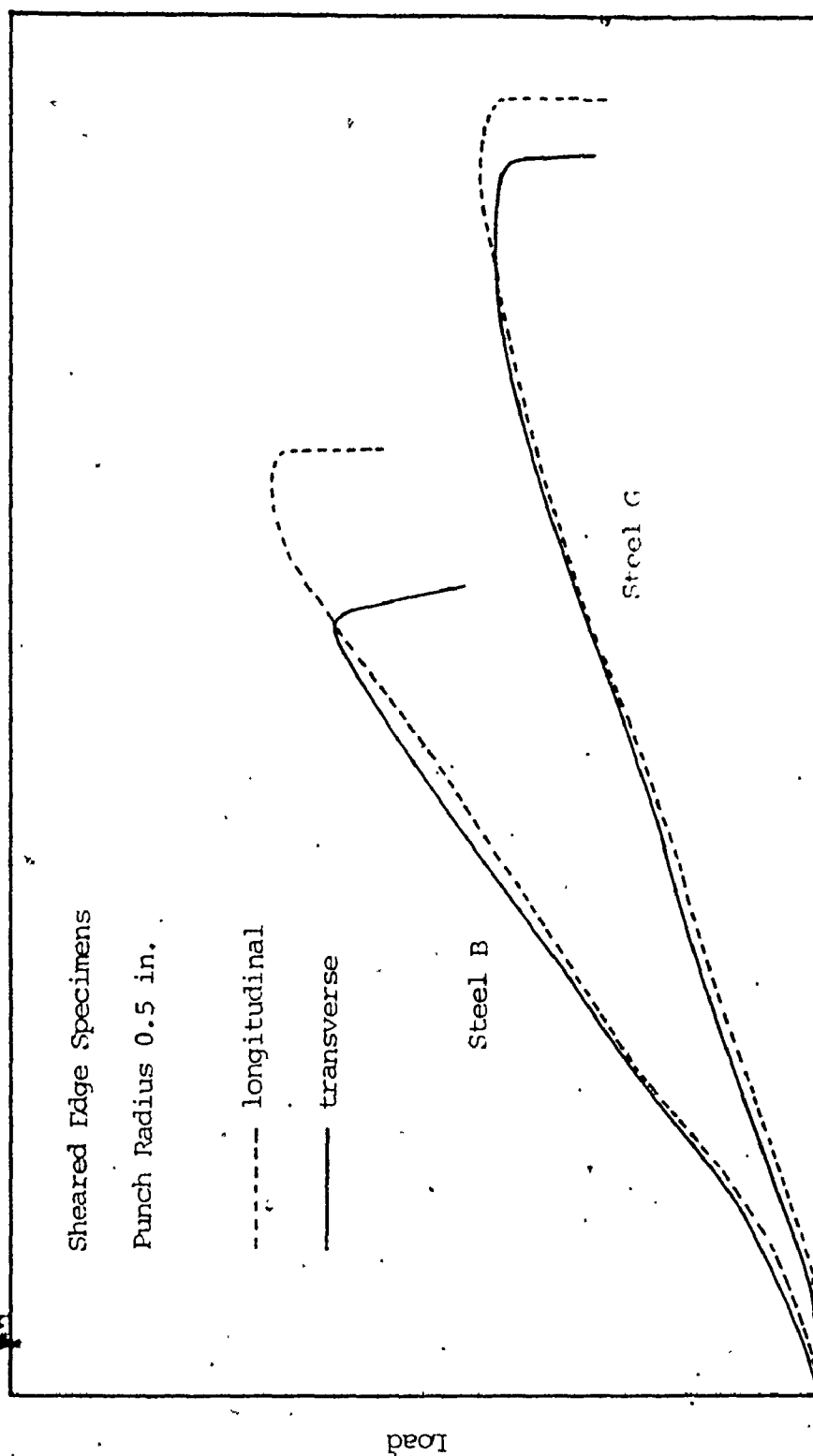


Fig. 26 Typical load vs punch travel curves for steels B and G in the stretch bend test.

TABLE 4
MAXIMUM PUNCH LOAD AND MAXIMUM PUNCH TRAVEL
ONLY TRANSVERSE SHEARED EDGE SPECIMENS

Steel	Maxm. Load (Tons)				Maxm. Punch Travel (in.m.)			
	Punch Radius (in.)				Punch Radius (in.)			
	.05	.125	.250	.500	.750	.05	.125	.250 .500 .750
A	NT	5.70	6.56	8.94	NT	NT	18.93	22.20 28.26 NT
B	4.44	5.38	5.12	7.40	9.16	14.32	16.00	16.95 23.84 25.34
C	3.74	NT	5.42	6.84	9.78	15.49	NT	20.27 24.83 32.35
D	3.48	4.22	4.92	7.98	9.44	13.00	11.69	15.90 25.00 29.63
E	NT	4.24	4.94	6.02	NT	NT	25.90	28.30 35.76 NT
F	2.82	3.56	4.50	5.9	6.36	16.73	20.80	27.60 33.89 36.16
G	3.16	3.64	4.50	5.2	6.38	21.99	27.93	33.70 37.40 44.84

NT -- NOT TESTED

5.3.5 FRACTURE CHARACTERISTICS OF STEEL D

An extensive investigation of the development of fracture in the tensile or bend specimens has not been undertaken. However, one feature of the tensile fracture characteristics of steel D is worth noting because it may have some bearing on the results reported later for the stretch bend tests. In all tensile specimens of steel D centre thickness delamination was evident running back into the tensile gauge length from the fracture surfaces. Otherwise the fracture characteristics of this steel showed high ductility as evidenced in Figs. 21, 22 and 23. The delamination in this steel was associated with carbide stringers which were a prominent feature.

5.4 NOTCHED TENSILE TEST

5.4.1 VARIATION OF E_{TN} AND THE RATIO OF THE TRANSVERSE / LONGITUDINAL

E_{TN} WITH Y.S. AND INCLUSION CHARACTERISTICS

The results, measured after specimen fracture from the 1 in. scribed gauge marks, are shown in Fig. 25 as plots of elongation and transverse/longitudinal elongation ratio vs yield stress. The results show similar trends to those obtained for normal tensile R of A and E_L value. (Figs. 20 and 22). However, the notched tensile results do appear to exhibit improved sensitivity as evidenced by the much lower elongation ratios obtained for the unmodified steels (Fig. 25b) as compared to those obtained for the same steels in normal tensile tests (Fig. 23).

5.5 STRETCH BEND TEST

5.5.1 PUNCH LOAD--PUNCH TRAVEL PLOTS

Typical load vs punch travel curves for stretch-bend tests are shown in Fig. 26. TABLE 4 shows how load and punch travel varies with

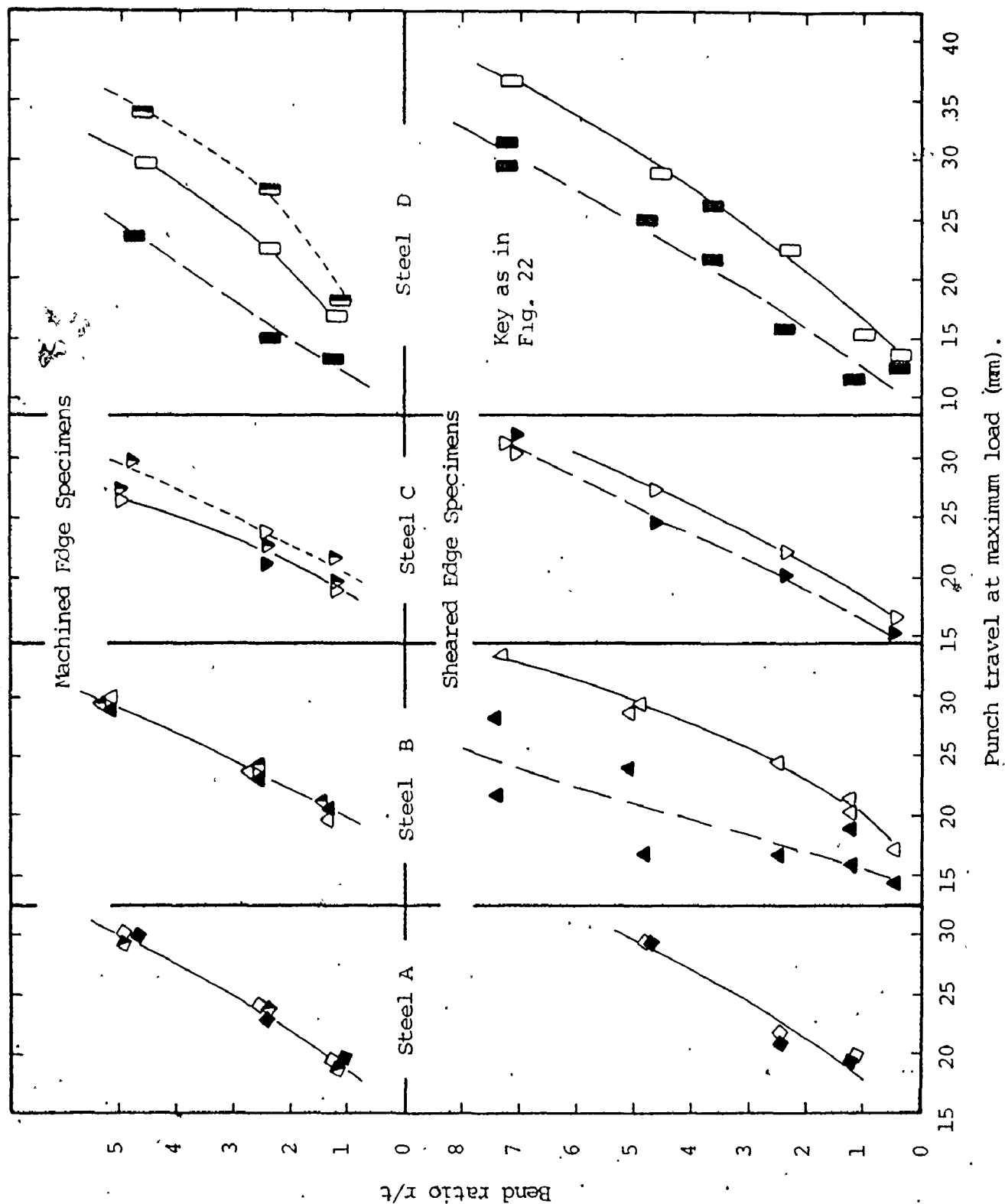


Fig. 27 The variation of Punch Travel at maxm. load with bend. ratio for the experimental steels

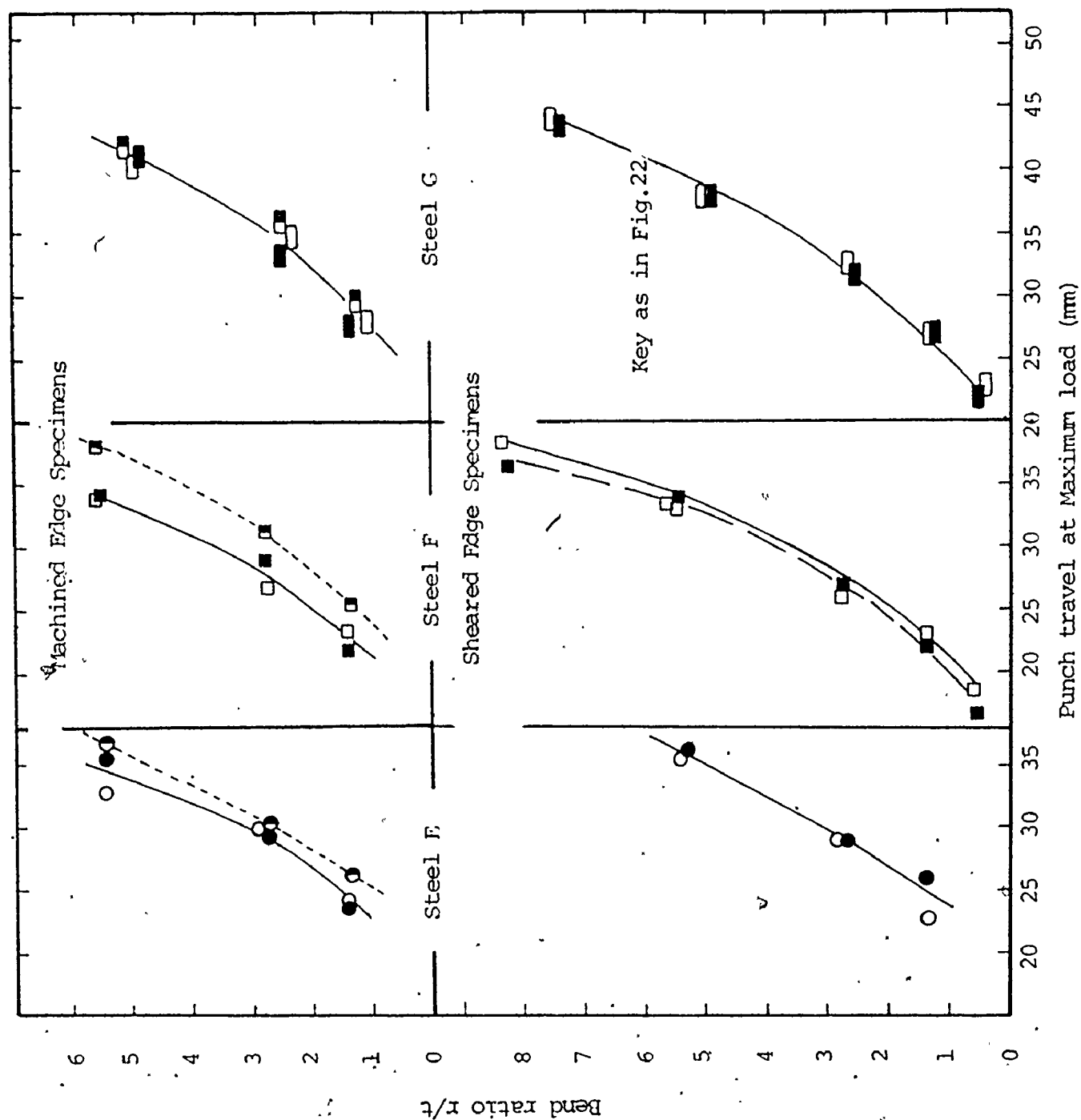


Fig. 27 (contd)

different punch radii. The load rises with deflection during the test until a maximum value is obtained which can be associated with crack nucleation and propagation or necking. Shortly afterwards failure ensues.

5.2.2 STRETCH BEND FORMABILITY OF THE HSLA SHEET STEELS

For the purpose of comparing the different steels the punch deflection at maximum load has been taken as an indication of stretch bendability. This is plotted against the bend ratio (punch radius/specimen thickness), r/t , for the different steels in Figs. 27. Longitudinal, transverse and diagonal specimens have been tested in the machined edge condition and longitudinal and transverse only in the sheared edge condition. For sheared edge samples there is no significant difference between the curves for longitudinal and transverse specimens for all the sulphide modified steels except for steel D where the difference is quite large. However, this steel has a noticeably banded microstructure and exhibits centre thickness delamination during tensile testing as noted previously.

In the 80 ksi yield strength unmodified steel B and partly modified steel C the curves for transverse specimens fall to lower values of punch travel than the curves for longitudinal specimens reflecting the influence of elongated inclusions. The difference between the two curves decreases at low r/t ratios consistent with the trend found in earlier work (36).

In the 50 ksi yield strength unmodified steel F there is a very small separation of the curves for longitudinal and transverse specimens and in the lowest strength steel G no separation is evident. Both steels have relatively low sulphur and carbon contents in addition to the lower

strength levels and the results obtained appear to indicate a relative insensitivity of the stretch-bend test to the presence of elongated inclusions under these conditions.

The curves for longitudinal and transverse machined edge samples of all steels except steel D are virtually co-incident with each other and with the longitudinal specimens of samples with sheared edges. This is the case even for steels B and F where in sheared specimens longitudinal and transverse deflections differ. This would appear to indicate that the stretch bend deflections in transverse specimens are decreased below those of the longitudinal specimens in the presence of elongated inclusions only if the specimen edges are sheared. A greater sensitivity to the presence of elongated inclusions may be expected in sheared specimens since the sheared edges contain microcracks which can initiate a crack if the conditions are favourable (32).

In the modified steel D, in which some microstructural and carbide banding is found, the deflections for transverse specimens are less than those for longitudinal specimens in both sheared and machined edge specimens. This result is difficult to reconcile with the results for the unmodified steels B, C and G where differences in deflection for longitudinal and transverse specimens occur only for sheared edge samples. As will be shown later differences in deflections for machined edge specimens can generally be associated with differences in r values but the difference in r values between longitudinal and transverse directions in steel D is small and does not appear to be capable of explaining the large effect on deflection found.

The explanation for the results found in steel D may be associated

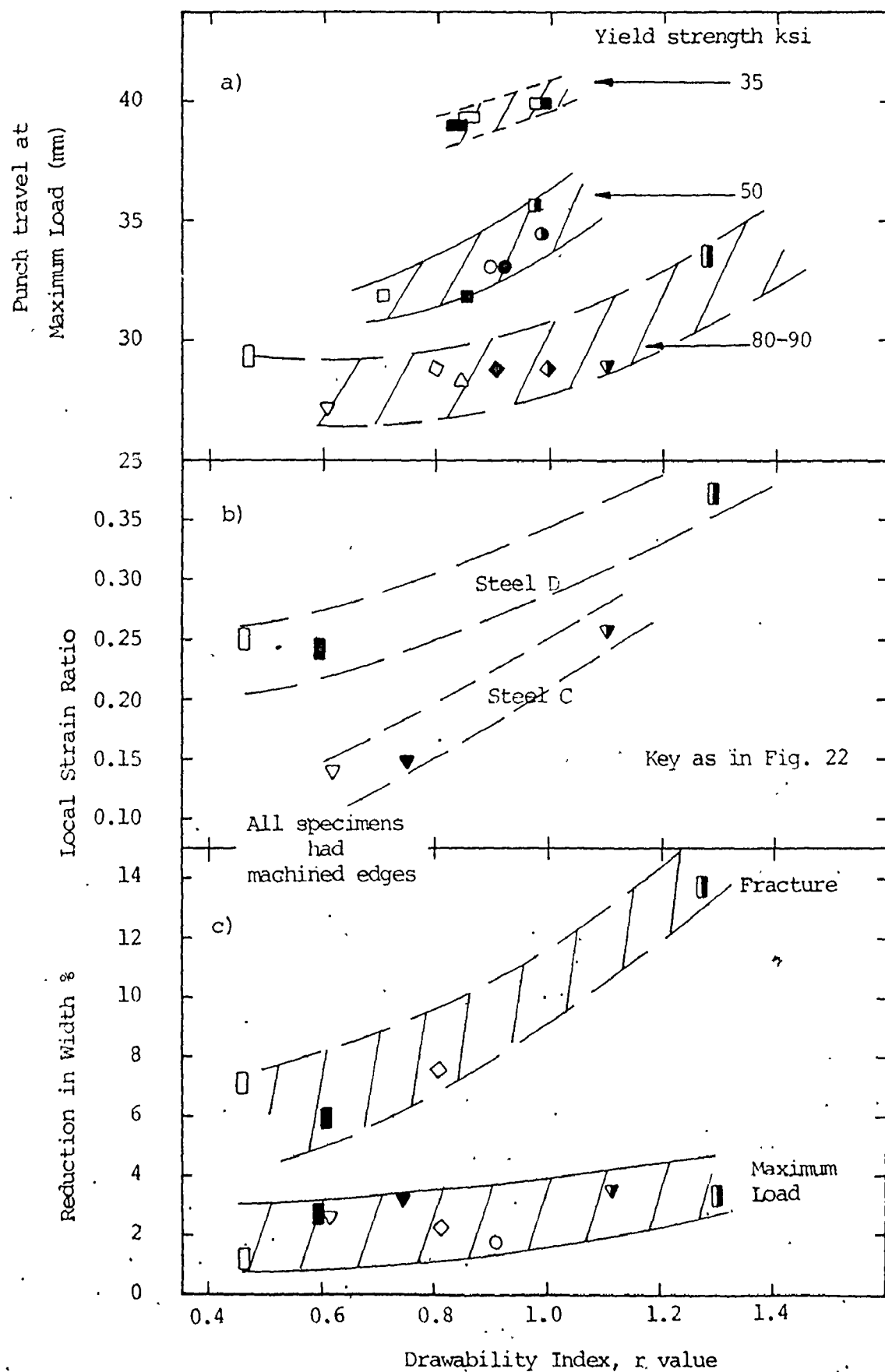


Fig. 28 The variation of drawability index of a, b, & c.

with the ease with which centre thickness delamination appears to occur during tensile testing. Little difference in longitudinal and transverse deflections for machined edge samples of steels B, C and G are found because of the absence of crack nucleating microcracks. However, in steel D, if delamination occurs readily during the stretch bending of machined samples it might be speculated that the delamination region could act as the necessary microcrack.

Steels A, B, E and G exhibit similar r values in all planar directions and in machined edge stretch bend tests similar deflections are obtained for specimens from the longitudinal, transverse and diagonal orientations. In steels C, D and F on the other hand the r values in the diagonal direction are significantly larger than in longitudinal and transverse directions and there is a corresponding difference in the stretch bend deflections with higher deflections being obtained for the diagonal specimens (Fig. 27).

5.5.3 CORRELATION OF PUNCH TRAVEL AT MAXM. LOAD, LOCAL STRAIN RATIO, % REDUCTION IN WIDTH WITH r VALUE

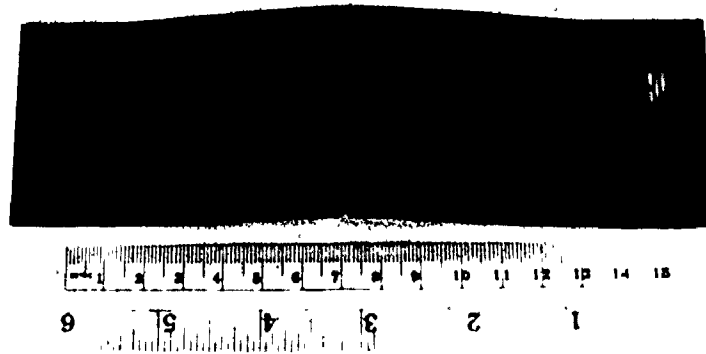
The correlation of Punch travel at maxm. load with r value for the different strength level ranges of the steels is shown in Fig. 28a. Results for transverse specimens of steels exhibiting mechanical fibering (e.g. elongated inclusions, banding) are not included in this plot. Although there is some scatter in the results due to variability of the matrix formability of these steels it is clear that deflections increase significantly with r values.

The higher deflections obtained at the higher r values can be attributed to a deviation of the straining path from plane strain towards

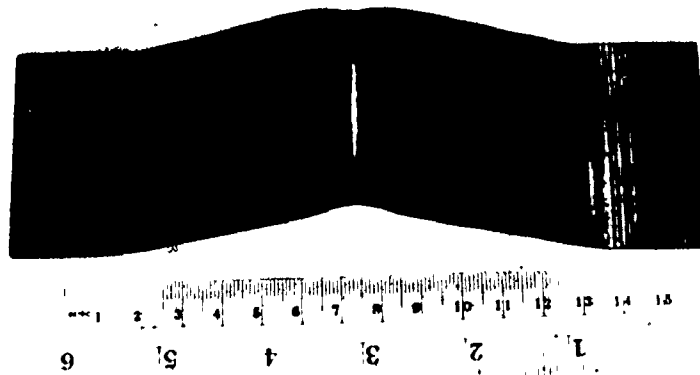
tensile strain as explained previously for the tensile results. To confirm this some measurements were made of strain ratios on grid circles adjacent to the fractured circle on fractured longitudinal, transverse and diagonal specimens of steels C and D. Since the grid circle diameters (.09 in.) are relatively large compared to the strain gradients in fractured bend specimens these values cannot be taken as a measure of the strain ratio operative in the test. However, it is considered that they are good for comparison. The results are shown in Fig. 28b from which it is clear that there is an effect of r value on strain ratio in the direction indicated above.

The influence of r value on strain ratio implies an influence on overall width strains in the stretch bend samples. Width strains have been measured in some samples at the apex of the bend. The results are shown in Fig. 28c. The lower curve represents samples bent to the same punch deflection but less than maximum load. The upper curve represents width strains for specimens of 80 ksi steels taken to fracture. Width strain increases with r value in both curves although the fracture curve shows the greater effect.

An important consequence of this dependence is that the correlation between laboratory stretch bend tests and commercial bending operations for materials with r values that differ significantly may be poor because in commercial operations the majority of the length of the bend will be forced to deform under plane strain conditions. In any case it is fortunate that most hot rolled steels exhibit r values that are approximately 1.0 and so do not vary greatly. It appears that it is only in the recently

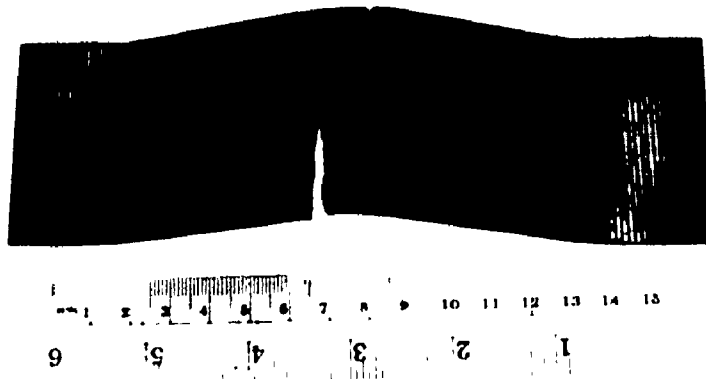


(a) Normal edge cracking at the bend apex

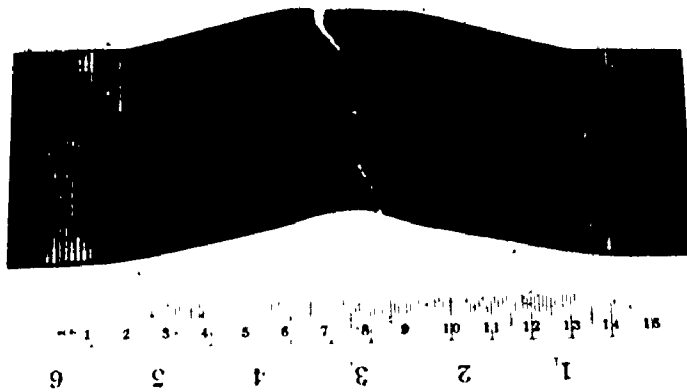


(b) Centre cracking at the bend apex

Fig, 29 Typical examples of fracture in the stretch bend test.



(c) Edge cracking at the specimen/punch junction for large bend radii.



(d) Centre cracking at the apex of the punch for large bend radii. Note the deviation of the crack from the bend apex along the lines of shear towards the specimen edges.

Fig. 29 (contd)

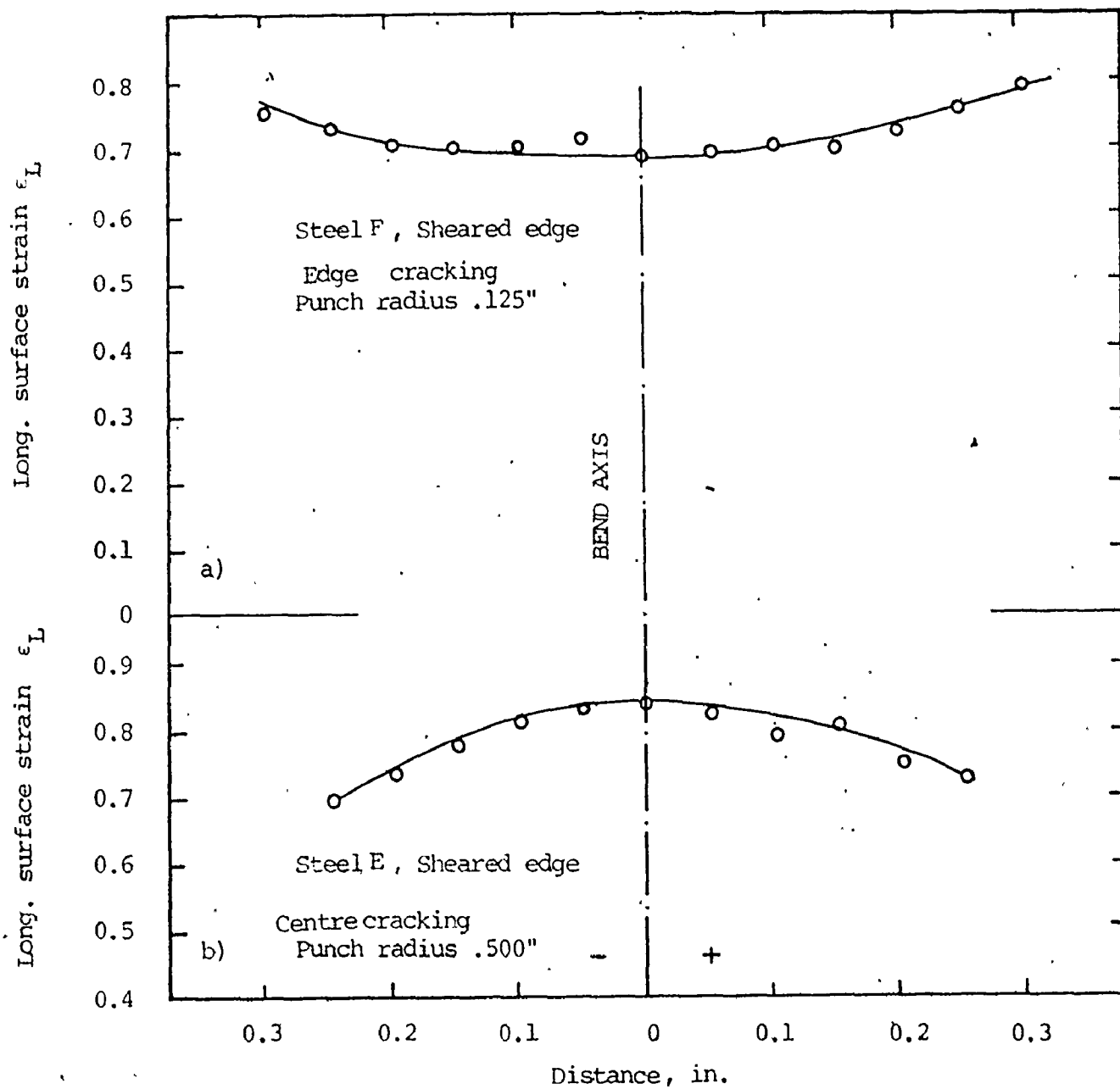


Fig. 30 Strain distribution along the axis of the bend.

TABLE 5POSITION OF CRACK INITIATION

Transverse sheared specimens only

Steel	Punch Radius in.			
	0.125	0.25	0.50	0.75
A	ND	C	C	NT
B	E	E	E	E
C	E	E	C	M
D	ND	C	C	C
E	ND	C	C	NT
F	E	E	M	E
G	E	E	C	E

IN ALL OTHER SPECIMENS FAILURE INITIATED AT THE CENTRE OF THE SPECIMEN

E = Crack initiation from the edge

C = Crack initiation from centre width

M = Mixed edge and centre

NT = Not tested

ND = Not clear from failed specimen

developed higher alloyed steels, where transformation of unrecrystallised austenite occurs at low temperatures, that low longitudinal and transverse r values are obtained. When comparing these steels with conventional steels some care must be exercised in the interpretation of the stretch bend test results.

These results indicate, therefore, that the punch deflections vary with r value. In transverse sheared specimens the deflections are also influenced by the presence of elongated inclusions but there is no significant effect of these inclusions in transverse machined specimens. Elongated inclusions only make their presence felt in specimens with sheared edges where crack initiating microcracks are present in the shear burr.

5.5.4 FRACTURE CHARACTERISTICS OF THE STRETCH BEND TEST

In support of the above it was generally observed that in the transverse sheared edge specimens of the unmodified steels containing elongated inclusions (i.e. steels B, C, and F) cracks initiated at the specimen edge and propagated towards the centre (Fig. 29a). In machined edge transverse specimens of these steels and in all other steels tested, sheared or machined; longitudinal, transverse or diagonal, cracks started at the centre of the specimen width (Fig. 29b). The strain distribution along the axis of bend in the two cases is as shown in Fig. 30.

These crack initiation characteristics of the specimens are detailed in TABLE 5. Results for .05 in. and some of the .125 in. radius tests are not included since it was not generally possible to identify the source of failure at these sharp punch radius.

Also at the two largest punch radii the cracking characteristics were sometimes more complex than described above due apparently to the increased importance of friction. For these punch radii, failure in the transverse specimens of the unmodified steels generally started from edge cracks which occurred close to the junction of contact between punch and specimens of the unmodified steels generally started from edge cracks which occurred close to the junction of contact between punch and specimen (Fig. 29c) and not at the apex of the bend as in all tests at the smaller punch radii (Fig. 29a). Two edge cracks frequently formed on opposite sides of the bend apex and propagated parallel to the bend axis until final failure occurred by shearing between them.

On the other hand cracking of the modified steels and of the longitudinal specimens of the unmodified steels occurred in the centre of the specimen width at the apex of the bend, as in the case of the smaller radii, although subsequent crack propagation was usually at an angle to the bend axis (Fig. 29d). This mode of cracking appears to indicate increasing importance of the tensile component in failure at the higher bend ratios with final crack propagation occurring along lines of shear at approximately 45° to the bend axis.

It was indicated earlier that steel D exhibits somewhat anomalous behaviour in the stretch bend test. It is possible that in this steel easy nucleation of cracks may occur through centre thickness delamination and it is perhaps significant that in this steel cracking does not start at the specimen edges even in the transverse sheared edge specimens.

Even in those sheared specimens of the unmodified steels where

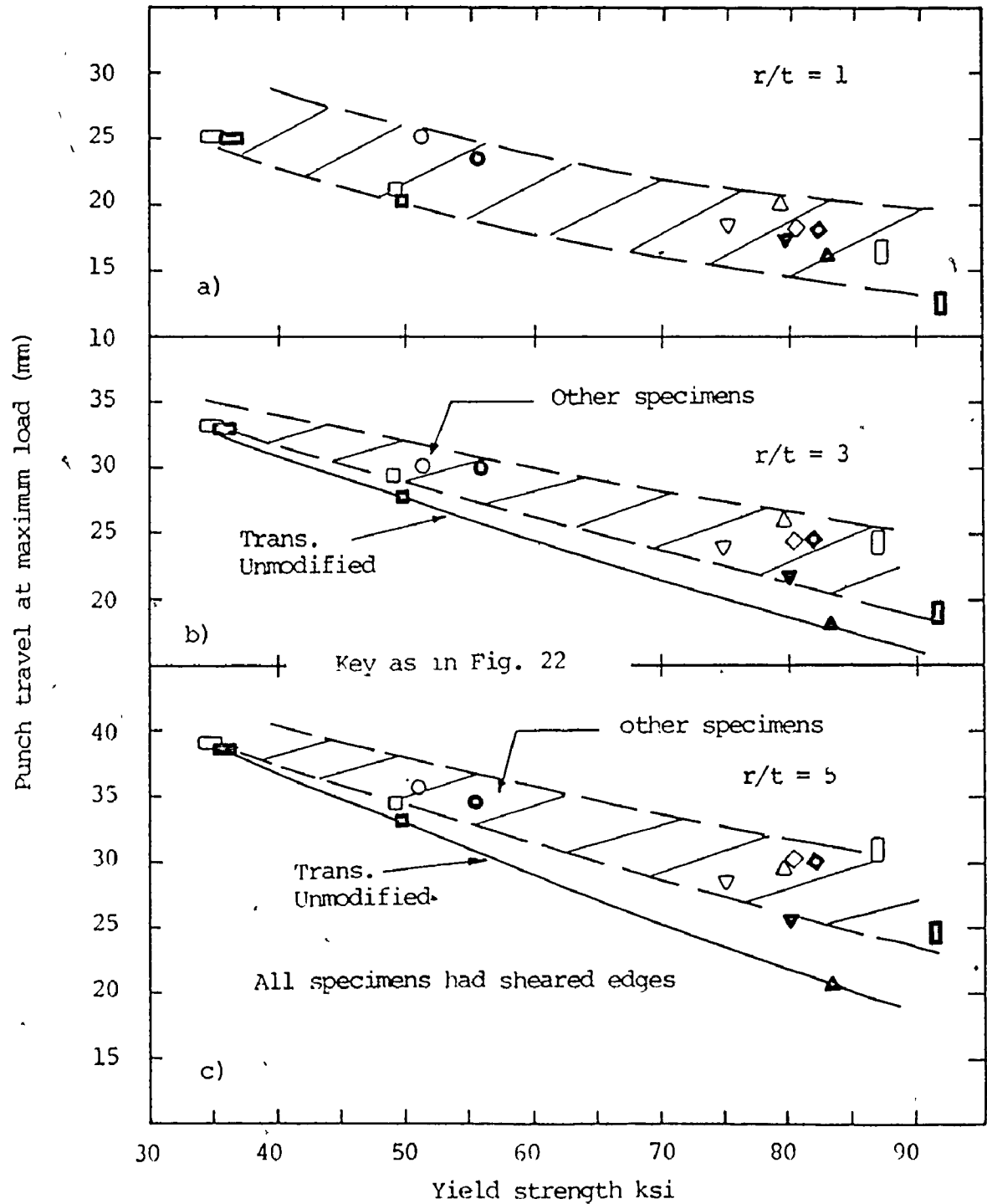


Fig. 31 The variation of punch travel in sheared edge specimens with yield strength and inclusion characteristics for bend ratios of a) 1, b) 3 and c) 5.

edge cracking initiates failure in transverse samples the differences in the punch travel for longitudinal and transverse specimens is not always very significant (as noted for steels F and G before). It is very large only in steel B at the higher yield strength (80 ksi) level and higher elongated inclusion content, TABLE 2.

5.5.5 DISCUSSION ON THE STRETCH BEND FORMABILITY OF THE HSLA SHEET STEELS

RESULTS

Punch deflections taken from the smoothed curves of Fig. 27 for the different steels at bend ratios of 1.0, 3.0 and 5.0 are shown as a function of yield strength level in Fig. 31. This plot summarises the results presented earlier. At the two larger punch radii a curve can be drawn through the points representing the transverse specimens of the unmodified steels. The other experimental points for the modified steels and longitudinal specimens of the unmodified steels fall in a broad band at higher deflections. The curve and the band come together at the lower yield strengths where the stretch-bend test shows limited sensitivity to elongated inclusions. The points representing transverse samples of the partly modified steel C and the modified steel D lie between the band and the curve.

In agreement with the present results Melbourne et al (36) found no significant difference between longitudinal and transverse deflections for unmodified aluminum killed mild steels of low strength levels. However, they found much larger effects in HSLA steels than in the present work although, the sulphur contents and the conditions of testing were similar.

However, the steels used by Melbourne et al were generally of much higher carbon content than the present steels (.13 - .22% compared to .08 - .09%) and consequently pearlite banding may have been an important factor in their results. In addition some of the lower strength steels used by them were silicon semi-killed steels and the silicate inclusions found in such steels are known to be generally far more deleterious to transverse formability than the manganese sulphide inclusions found in aluminum killed steels.

Other work (36) supports the finding of the present work that stretch bend deflections are not sensitive to inclusion content in machined edge samples (47), although in work on a thicker plate steel, Uko et al (39) found small differences in longitudinal and transverse deflections that could be attributed to elongated inclusions. It is reasonable to expect that some influence of elongated inclusions might be observed for machined edge specimens since the elongated inclusions will still be expected to influence void nucleation and growth when cracking starts from the centre width of the specimen. It is possible that with the present conditions and materials the difference in deflection between longitudinal and transverse machined edge specimens is so small as to be lost in the scatter of results. For instance, it is shown later that increasing the specimen span improves the sensitivity of the stretch bend test and it is possible that such improvements in sensitivity might reveal a separation between longitudinal and transverse curves for machined specimens. However, it is clear from the present results that sheared edge specimens are necessary for optimum sensitivity.

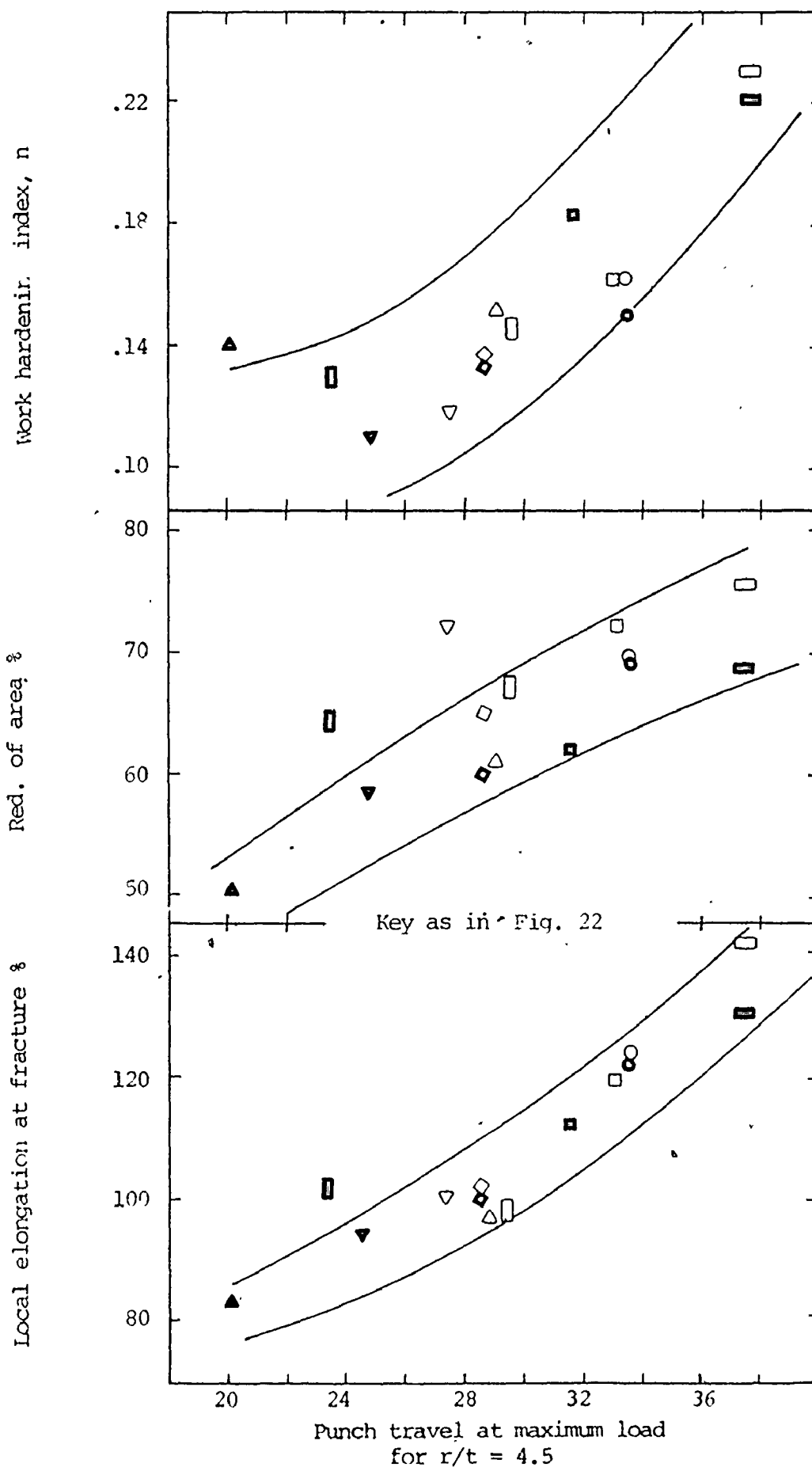


Fig. 32 The correlation between punch travel and the

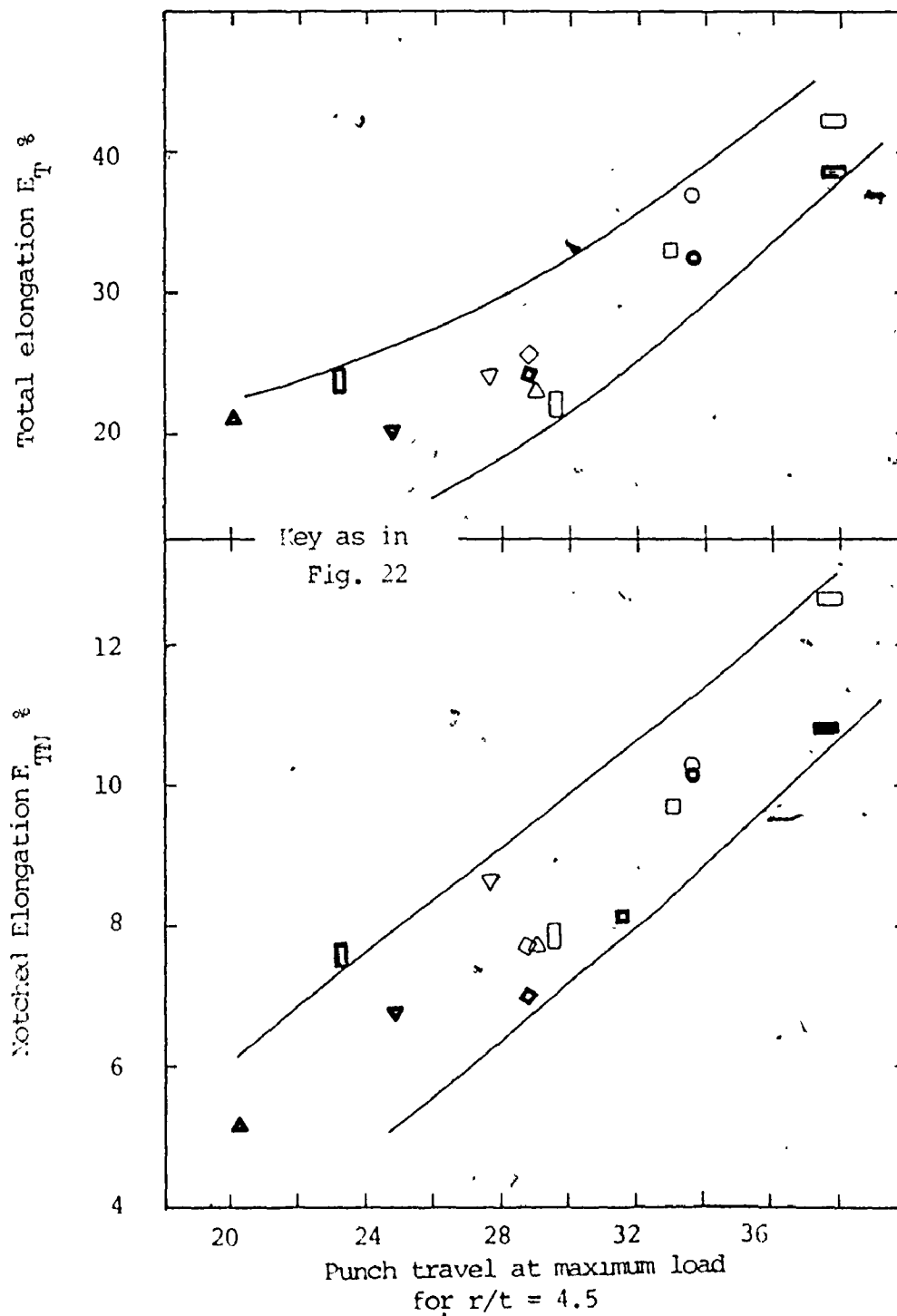


Fig. 32 The correlation between punch travel and the
the file

5.6 CORRELATION OF STRETCH BEND RESULTS WITH TENSILE FORMABILITY PARAMETERS

The punch deflection in the stretch bend test has been plotted against n value, E_T , E_L and R of A for the tensile test and E_{TN} from the notched tensile test in Fig. 32. The punch deflections used have been taken from the smoothed curves of Fig. 27 at a bend ratio of 4.5.

As expected the correlation with the work-hardening index, n value, is poor, particularly for the transverse specimens of the unmodified steels. The most sensitive correlations are found with E_{TN} , E_L and R of A , although the latter shows considerable scatter, no doubt associated with the difficulties of measuring this parameter accurately.

It is noticeable in the plots that steels D and G do not always show as good a correlation as do the other steels. Steel G shows quite large differences between the transverse and longitudinal local strain parameters, E_L and R of A , from the tensile test but no detectable difference in stretch bending deflections. Steel D exhibits the opposite effect, with very little difference in tensile parameters but quite large differences in stretch bend deflections for longitudinal and transverse directions.

The reason for this behaviour in steel D is not clear but it may be that the features of the microstructure causing delamination in tensile specimens may have a much greater effect on formability in bending than in tensile testing. It will be seen later that this steel exhibits excellent formability in the hole expansion test, a test which appears to be extremely sensitive to the presence of elongated inclusions or mechanical fibring. This and the correlations reported above suggests that there are anomalies in the stretch bending performance of this steel that require further investigation.

As has been indicated previously the sensitivity of the stretch bend deflection to elongated inclusions is poor at the lower yield strengths and inclusion contents of steel G. As will be seen below if local measurements of strain at fracture are made on the stretch bend samples these are as sensitive to elongated inclusion content as the essentially local measurements taken from the tensile test (i.e. E_L , R of A and E_N).

5.7 LOCAL STRAIN MEASUREMENTS AT FRACTURE IN STRETCH BEND TEST

The punch deflections from the stretch bend test have been shown to be relatively insensitive to the presence of elongated inclusions in the lower yield strength unmodified steels, at least where the sulphur contents are relatively low. Punch deflection is the most convenient measurement to take from the stretch bend test, however, there are other possible measurements that may be taken and may be more significant in assessing the quality of a steel.

5.7.1 VARIATION OF LOCAL FRACTURE STRAINS MEASUREMENT FROM STRETCH BEND TEST WITH Y.S. AND INCLUSION CHARACTERISTICS

In the present work three further formability parameters have been measured. These were:

- 1) the reduction in width at fracture, R of W, measured at the apex of the bend using vernier callipers.
- 2) the reduction in thickness at fracture, R of T measured in the centre of the width of broken specimens using a point micrometer.
- 3) the local surface elongation, E_B , at fracture measured in the centre of the specimen width at fracture from 0.09 in. electroetched circles spanning fracture.

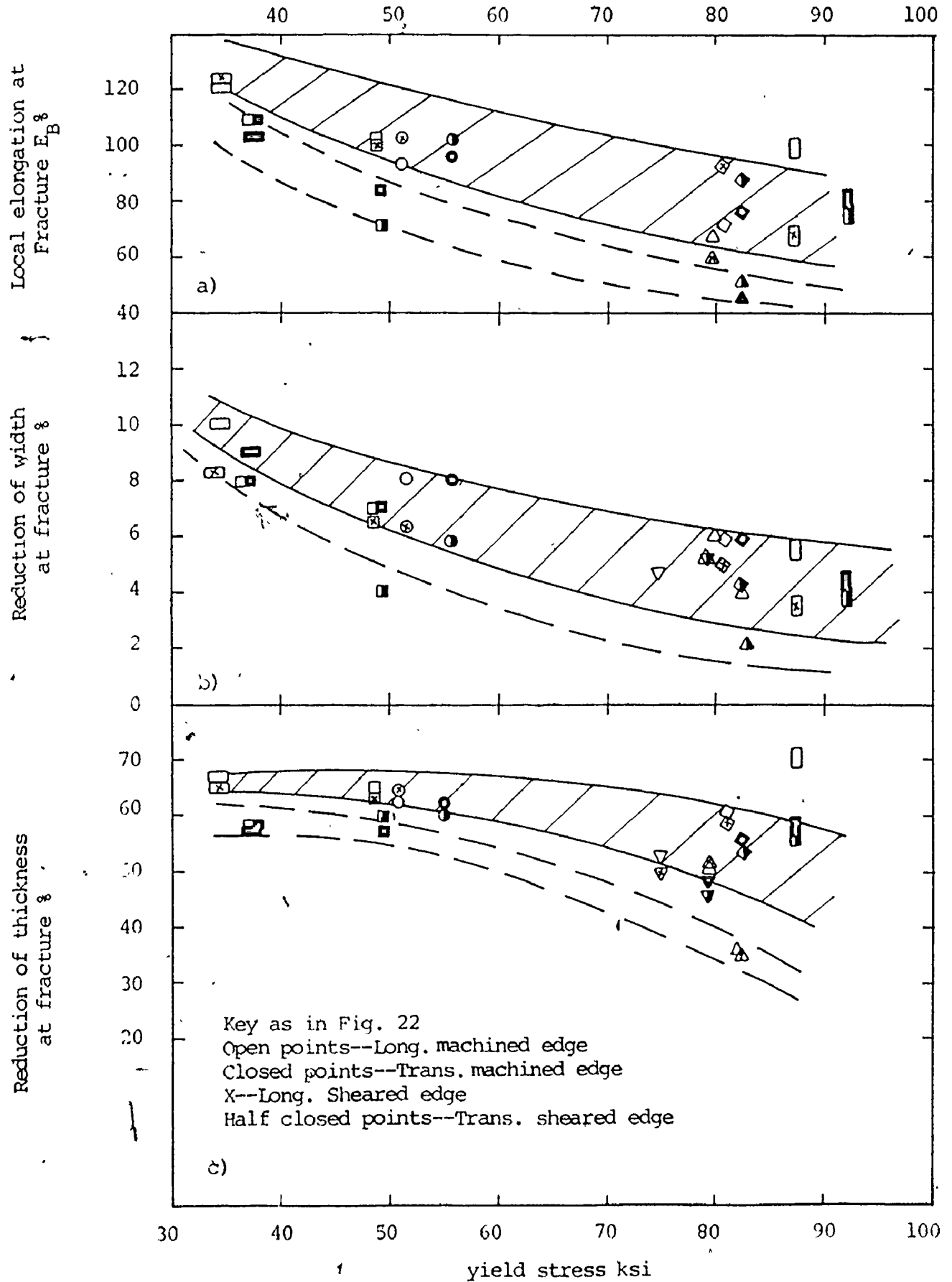


Fig. 33

PUNCH RADIUS .250"

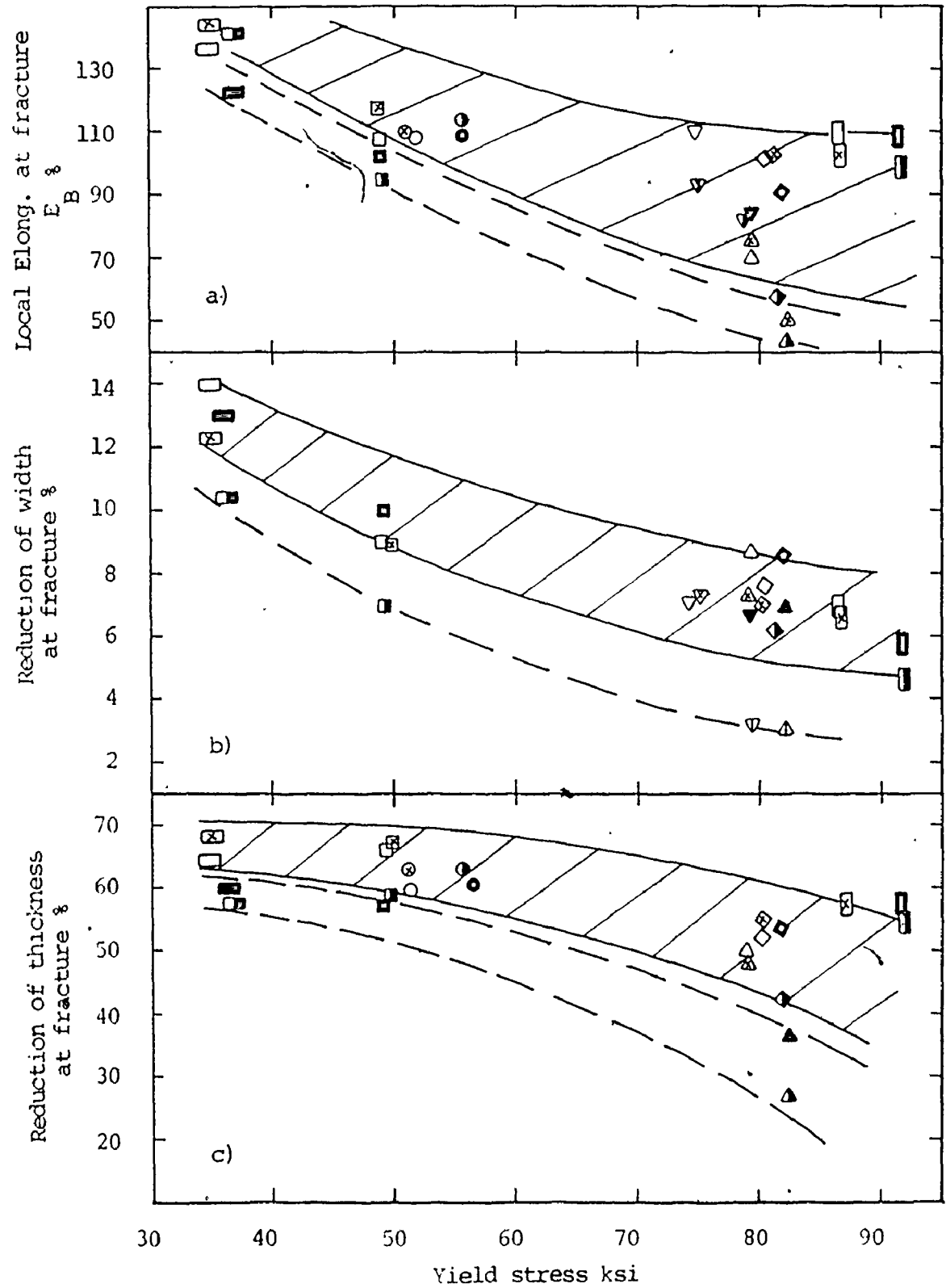


Fig. 33 (contd)

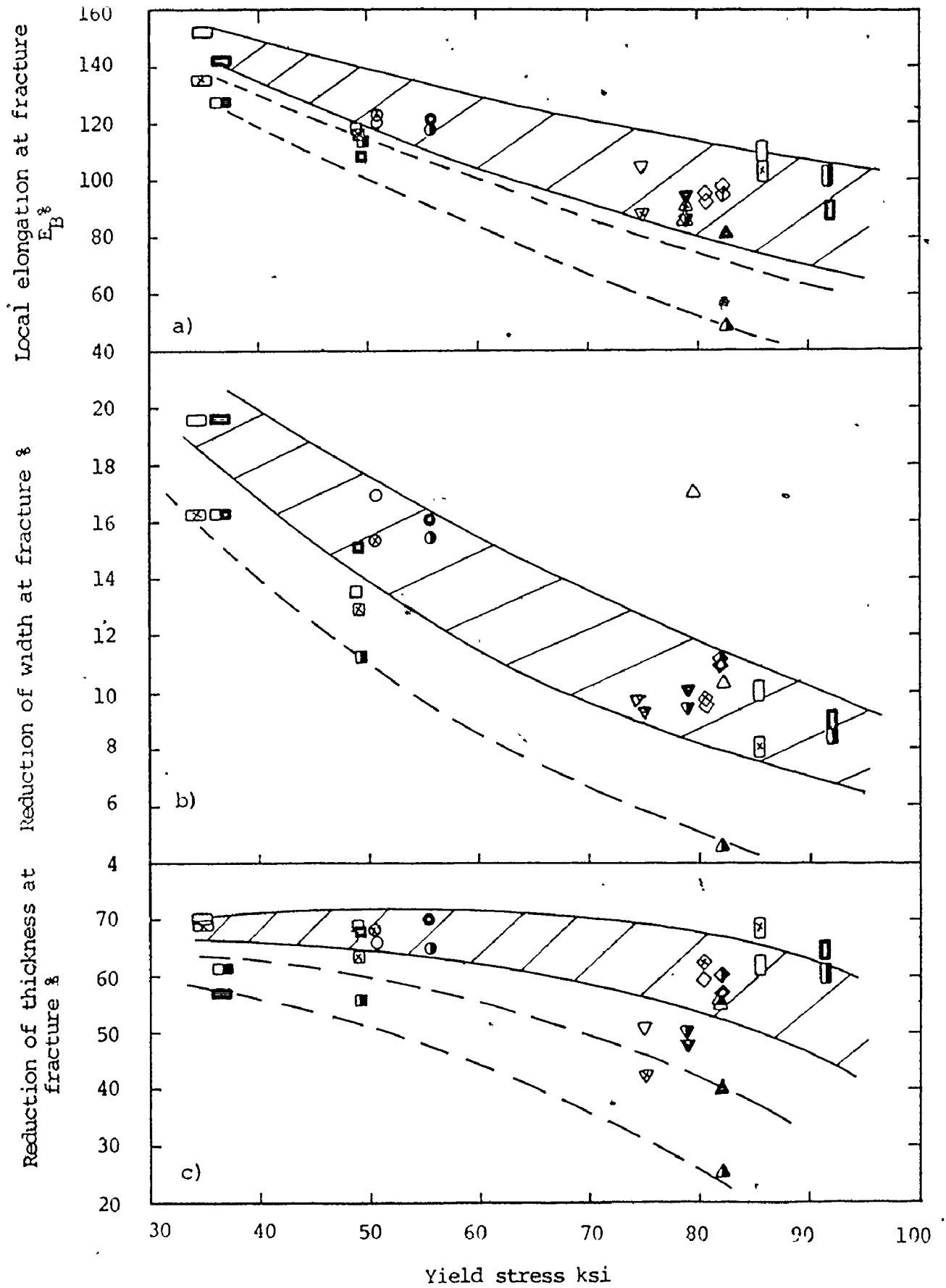


Fig. 33 (contd)

The results of these measurements for specimens bent over a .125 in., .250 in., .500 in. radius punch are shown in Figs. 33 as a function of yield strength level.

The variation of R of T and E_B with yield strength and edge preparation are similar. The measurements for both machined and sheared transverse specimens of the unmodified steels fall in a band at low values and within this band the measurements for machined specimens generally fall to higher levels than those for sheared specimens. The results for all other specimens fall in a higher band and the separation between the two bands is substantial even at the lowest strength levels where no effect is seen in punch deflection measurements (Fig. 31).

Similarly the R of W results for sheared edge transverse specimens of unmodified steels fall to lower levels than the other specimens (Fig. 33b). However, in this case, the results for machined transverse specimens of these unmodified steels do not show similar low width reductions but lie in the band of results for the other steels. The major fraction of width strain in stretch bend tests of machined specimens appears to occur between maximum load and failure as can be seen from Fig. 28c. It is clear that cracks initiating from the sheared edges in transverse specimens with elongated inclusions prevent significant width strain after maximum load whereas when failure is initiated in the centre of the specimen width, as in all machined specimens, large width strains can develop. This behaviour is consistent with the difference in punch deflections obtained between transverse specimens of the unmodified steels with machined and sheared edges if increased width strain is associated with increased punch deflection.

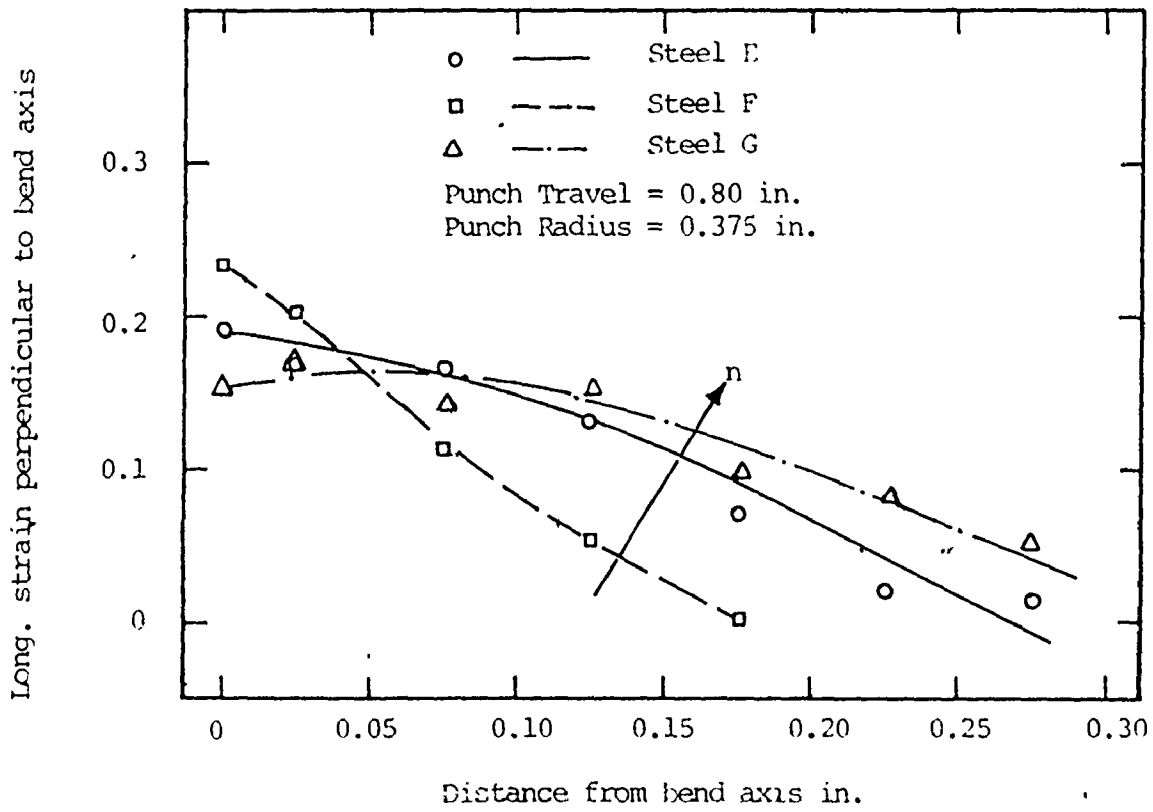


Fig. 34 Effect of yield strength on strain distribution

In sheared edge specimens crack nuclei are present at the edge and propagation will occur when the stresses at the edge reach a sufficient level. In machined specimens on the other hand, voids must develop, grow and coalesce to form a crack nucleus before crack propagation can take place across the specimen width. The greater local strains required to achieve this are reflected in the higher values of R of T and E_B for machined as compared with sheared samples of the transverse unmodified steels, although results for both sheared and machined specimens of these steels fall below those of the modified steels.

These local measurements of strain at fracture in the stretch bend test are essentially similar to the local measurements at fracture from the tensile test (R of A and E_L) and have similar sensitivity to the presence of elongated inclusions.

5.7.2 CHANGE IN STRAIN DISTRIBUTION WITH YIELD STRENGTH FOR THE SPECIMENS DEFORMED TO 0.80 IN. PUNCH TRAVEL

Longitudinal strains perpendicular to bend axis are plotted against the distance from the bend axis for different yield strength, Steel E, F, G sheared edge specimens. The specimens were deformed to .80 in. punch travel by .375 in. radiused punch. The distribution of strains are as shown in Fig. 34. As it is obvious, the maximum strain increases with yield strength with the characteristic steep strain gradients. The uniformity in strain distribution increases as the work hardening exponent 'n' increases. The results are only qualitative since 0.80 in. punch travel is close to the maximum in Steel F only.

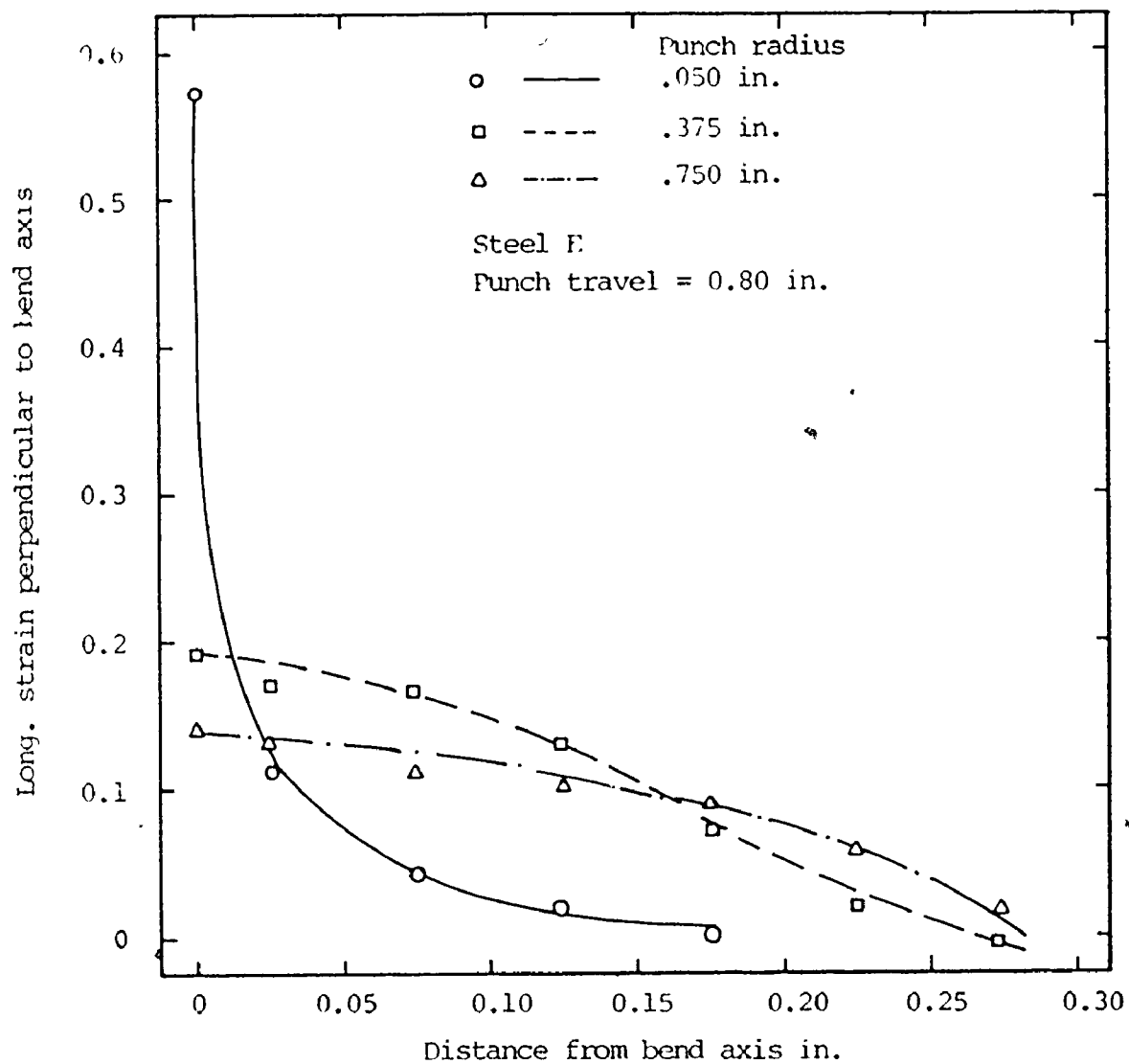


Fig. 35 Effect of Punch radii on strain distribution

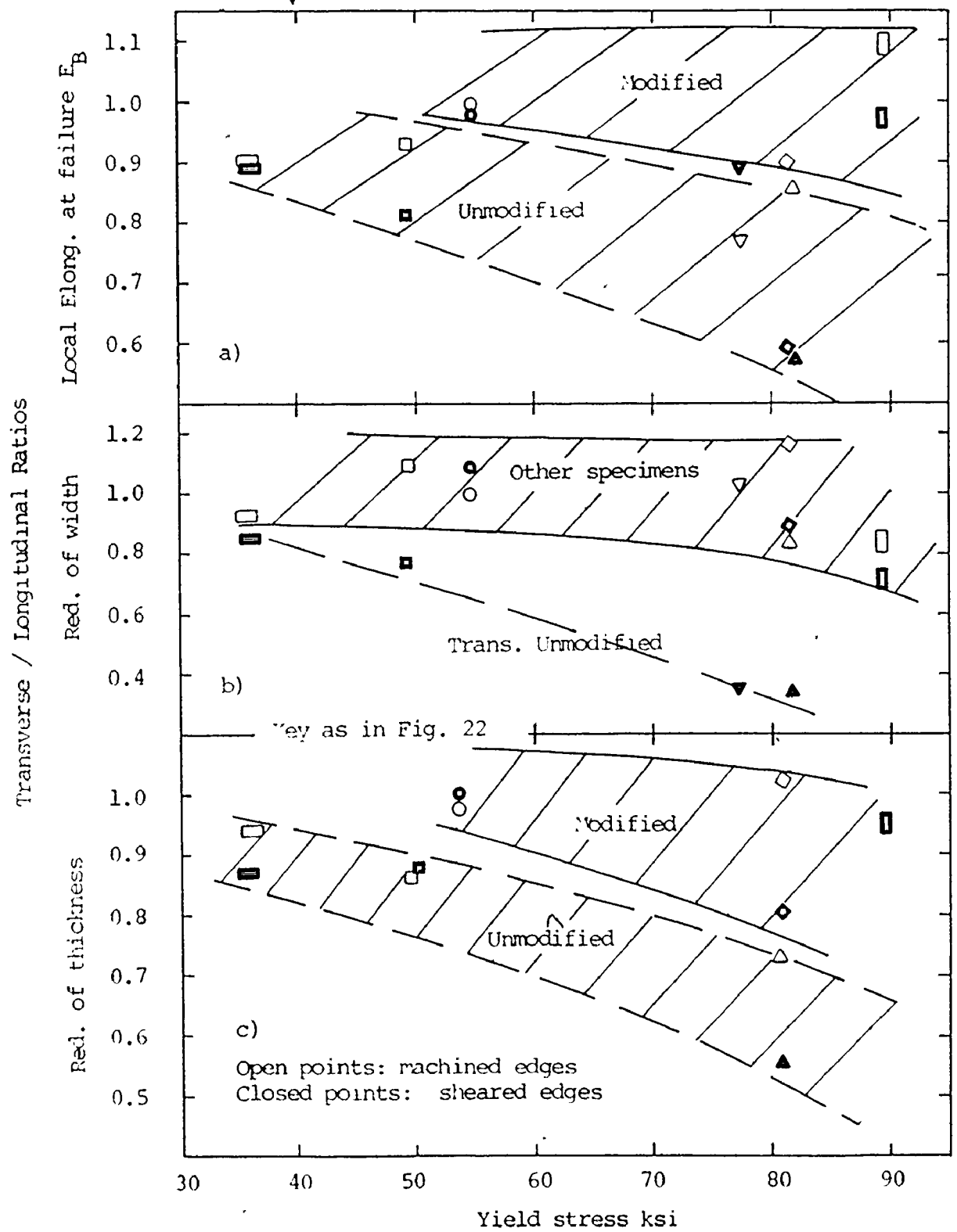


Fig. 36 The variation with yield strength and inclusion characteristics of a, b, and c.

5.7.3 CHANGE IN STRAIN DISTRIBUTION WITH PUNCH RADII FOR STEEL E DEFORMED TO 0.80 IN. PUNCH TRAVEL

The longitudinal strain perpendicular to the bend axis are plotted against the distance from bend axis for steel E, sheared edge specimen deformed to 0.80 in. punch travel by 0.05 in., .375 in., .750 in. radiused punch. The results are only qualitative since 0.80 in punch travel is close to maximum for 0.05 in. radiused punch only. The plot Fig. 35 clearly indicates a sharp strain gradients and higher value of maximum strain for the sharper bend radii. The uniformity in strain distribution increases but the maximum strain level decreases as bend radius increases because of the larger contact area between punch and specimen.

5.7.4 DISCUSSION ON THE LOCAL FRACTURE STRAINS RESULT IN STRETCH BEND TEST AS FORMABILITY PARAMETERS

The scatter in results in Fig. 33 is largely due to variations in steel compositions, microstructure and r values. The difference between the results in modified and unmodified steels can be shown more clearly by plotting the ratio of the transverse to longitudinal stretch bend R of T , E_B , and R of W values as was done for the tensile test parameters in Fig. 23. The results for these stretch bend parameters are shown in Fig. 36. In each plot the results for unmodified sheared specimens lie in bands below the values for the modified steels. Values for machined samples of the unmodified steels generally lie between those for the modified steels and those for the sheared unmodified steels. That the machined and sheared specimens do not generally exhibit similar values in these steels can be associated with the different mode of failure in the two conditions, i.e.

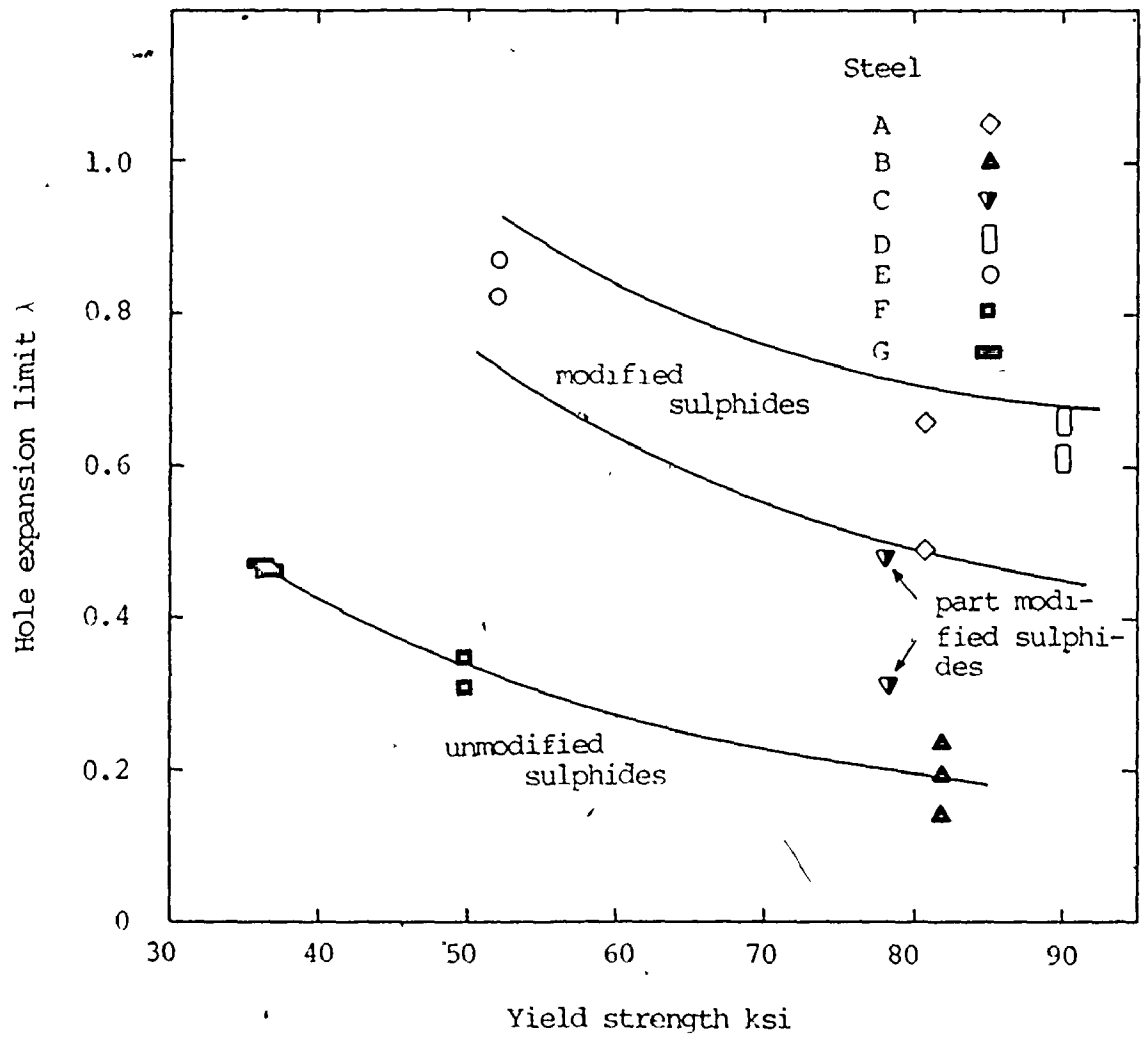


Fig. 37 The variation of the hole expansion limit, λ , with yield strength and inclusion characteristics.

edge cracking in the sheared unmodified steels and centre cracking in the machined unmodified steels as explained above.

These results show that measurements of local strain at fracture give a sensitive indication of material quality, in fact much more sensitive than punch deflections. Although the latter appears to give an excellent indication of quality in steels of high strength level and relatively high inclusion content (such as steel B in Fig. 20) at low strength levels and in the steels of lower inclusion content it is less reliable. For instance the punch deflection for steel F and G give little and no indication respectively that these steels contain elongated inclusions (see Fig. 31). However, the local strain measurements in Figs. 33 and 36 clearly show that transverse properties differ from longitudinal ones in these steels whereas these differences in modified steels are small.

Unfortunately, width and thickness reductions and local elongations at failure are far more tedious to measure and subject to greater measurement errors than punch deflections and the value of the stretch bend test as a quality control test is greatly reduced if such measurements are required.

5.8 HOLE EXPANSION TESTS

5.8.1 HOLE EXPANSION LIMIT VS YIELD STRENGTH

The average value of the hole expansion limits for the experimental steels are shown as a function of yield strength in Fig. 37. These results exhibit excellent conformity with what one would expect from their inclusion shapes and contents, TABLE 5. The results for the unmodified steels (B, F and G) fall on a curve at relatively low ratios while those for the completely modified steels (A, D and E) fall on a curve at much higher values.

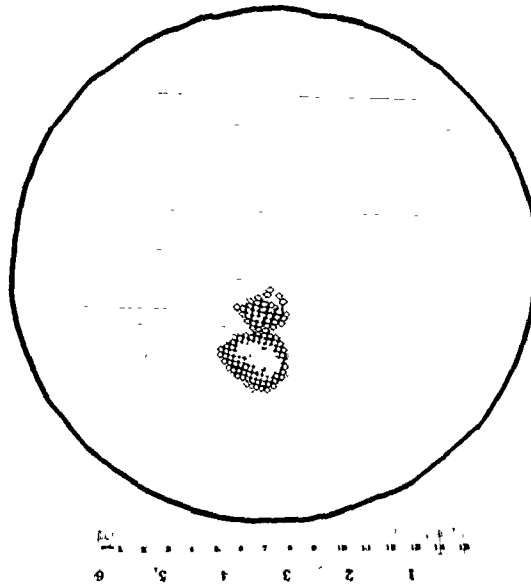


Fig. 38 A hole expansion test piece illustrating the mode of failure. Steel F.

The results for the partially modified steel C falls at intermediate levels. In addition although the major cracking from the sheared centre hole occurred in the rolling direction in all steels (Fig. 38) in the modified steels A, D and E additional incipient cracks were found in other orientations to the rolling direction suggesting less directionality in the case of crack growth. These additional cracks were not found in the unmodified steels.

5.8.2 DISCUSSION ON HOLE EXPANSION TEST AND STRETCH BEND TEST AS QUALITY CONTROL TEST

The results in Fig. 37 are essentially similar to those for the stretch bend tests portrayed in Fig. 31 and rate the steels in the same order of quality. However, the distinction between the modified and unmodified steels is far more clear cut in Fig. 37 than in Fig. 31, especially at the lower strength levels. For instance, the stretch bend deflection of the unmodified mild steel G is greater than the deflections of all other steels, even those with completely modified inclusions (Fig. 31). However, the hole expansion limit of this steel is much less than the limits for any of the completely modified steels including those of the highest yield strength level tested, A and D. The content of elongated inclusions in steel G is highest of all the steels tested TABLE 5 and it is clear that this is the major factor in the low limit for this steel. These results indicate that the hole expansion test would be a much superior test for monitoring quality control.

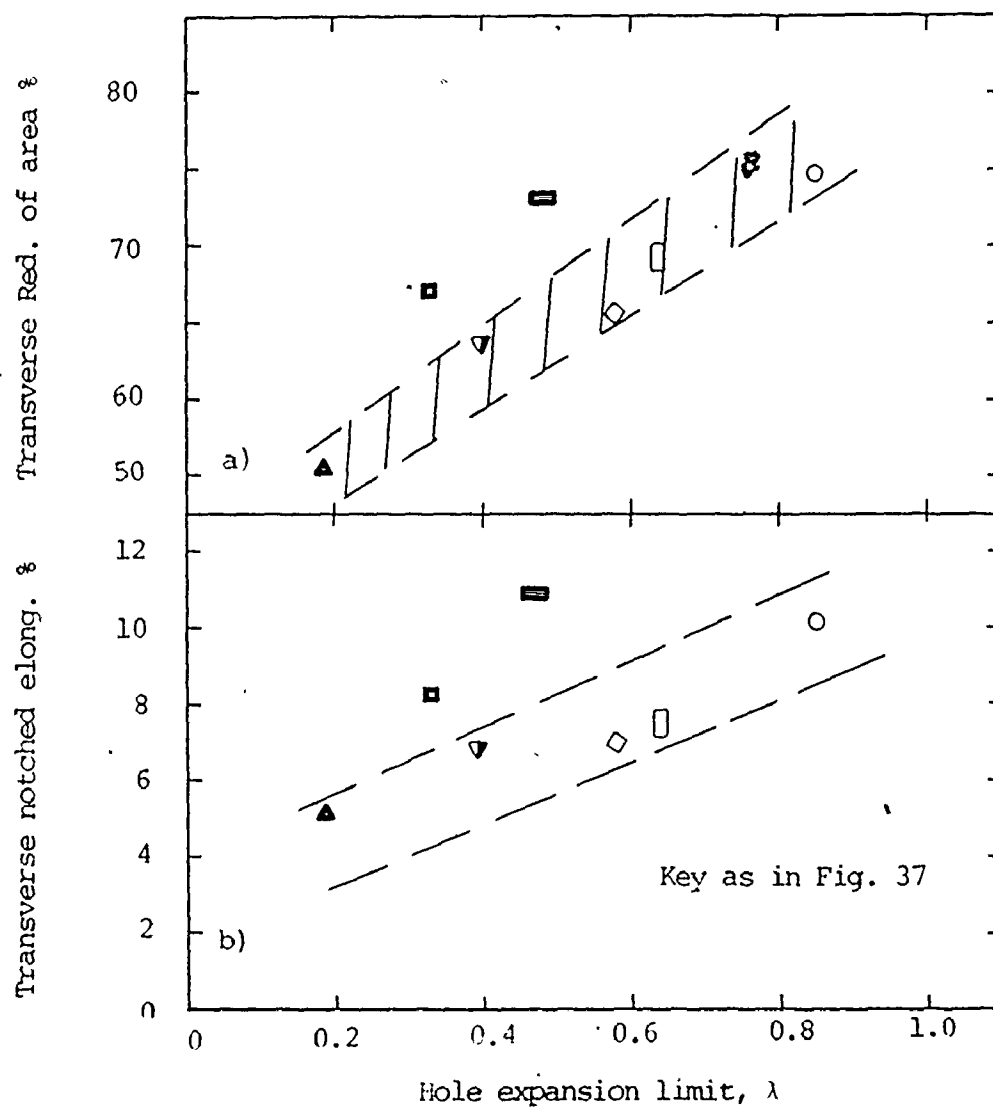
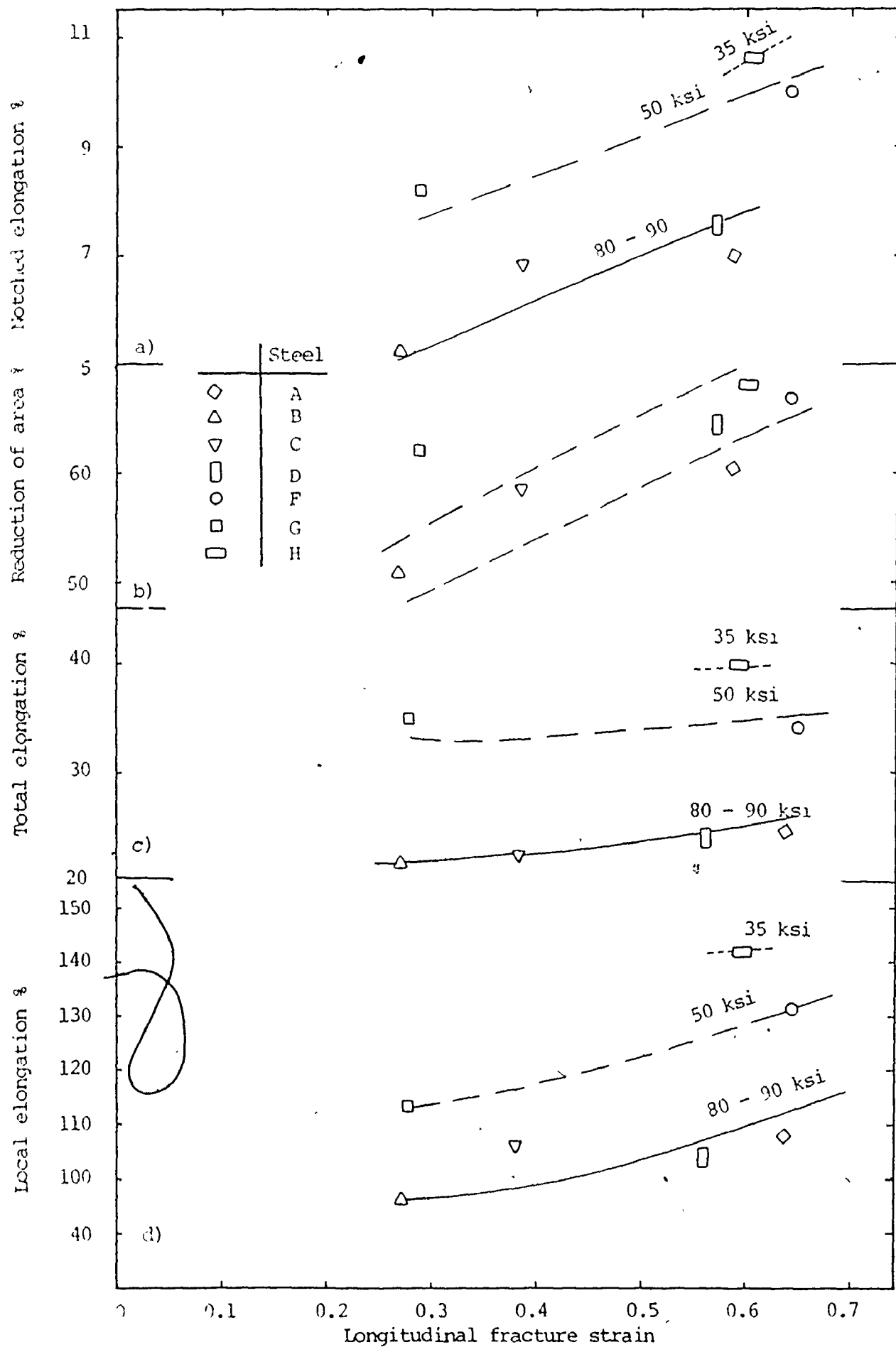


Fig. 39 The correlation between the hole expansion limit and a) the tensile reduction of area, R of A b) the elongation of notched tensile specimens, E_{TN}



5.8.3 CORRELATION BETWEEN HOLE EXPANSION TEST FORMABILITY PARAMETERS AND TENSILE TEST PARAMETERS

The hole expansion limit and fracture strain results do not correlate well with tensile formability parameters. Correlations with the transverse notched tensile elongation E_{TN} and the transverse tensile reduction of area, R of A , with hole expansion limit are shown in Fig. 39. The correlations with other tensile parameters are poorer still and these cases are not shown. Correlation with fracture strains is shown in Fig. 40... It appears from these correlations that the hole expansion limit and fracture strain is far more sensitive to elongated inclusions than any of the tensile parameters. This is particularly so at the lower strength levels as evidenced by the separation of the results for steels F and G from the general curve for the other results.

5.8.4 CORRELATION BETWEEN HOLE EXPANSION LIMIT AND E_{TN}

In the case of the notched tensile test this is rather surprising since it might be expected that the notch acts in the same way as the sheared edge as a crack initiator. It is possible that the rather large radius at the notch may have limited its efficacy in this respect.

5.9 PUNCH STRETCHING TEST

5.9.1 PLOT OF CUP HEIGHT AND YIELD STRENGTH

Values of the cup heights at failure for the punch stretching tests are shown as a function of yield strength in Fig. 41. Two tests were done for each steel and the reproducibility of cup heights was good in all steels except steel B.

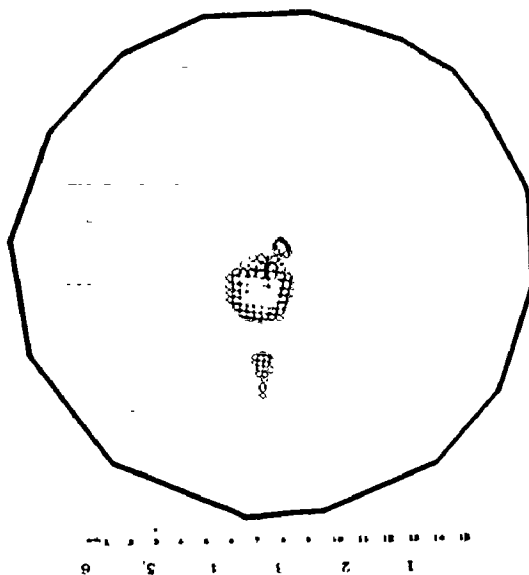


Fig. 42 An example of failure in hemispherical punch stretching.

5.9.2 DISCUSSION BETWEEN PUNCH STRETCHING AND STRETCH BEND TEST

These results are similar to those shown in Fig. 31 b and c for the stretch bend tests. The results show a fairly clear separation into two bands, the upper band containing the modified steels and the lower the unmodified steels with the partly modified steel C falling between the two bands. In comparison with the stretch bend test results the punch stretching results distinguish more clearly between modified and unmodified steels. However, it is shown later that the sensitivity of the stretch bend test increases with the span between the clamping jaws and it appears probable that with a larger span the stretch bend test would predict punch stretching performance with good accuracy.

5.9.3 DISCUSSION ON THE RELATIVE ASSESSMENT OF HOLE EXPANSION, PUNCH STRETCHING AND STRETCH BEND TEST

It is clear from a comparison of Figs. 37 and 41 that the hole expansion limit is not the best parameter to use as a guide to punch stretchability. The latter is clearly reduced by the presence of elongated inclusions and cracking always occurs in the rolling direction (Fig. 42) but is certainly not as sensitive as indicated by the difference in the hole expansion limits for modified and unmodified steels. Similar conclusions can be drawn from the recent results of Hilsen et al (25) on HSLA sheet steels in punch stretching and hole expansion test.

This is not to say, of course, that the hole expansion limit is not a good quality control parameter. In fact it would appear to be an excellent parameter if testing for the absence of elongated inclusions is

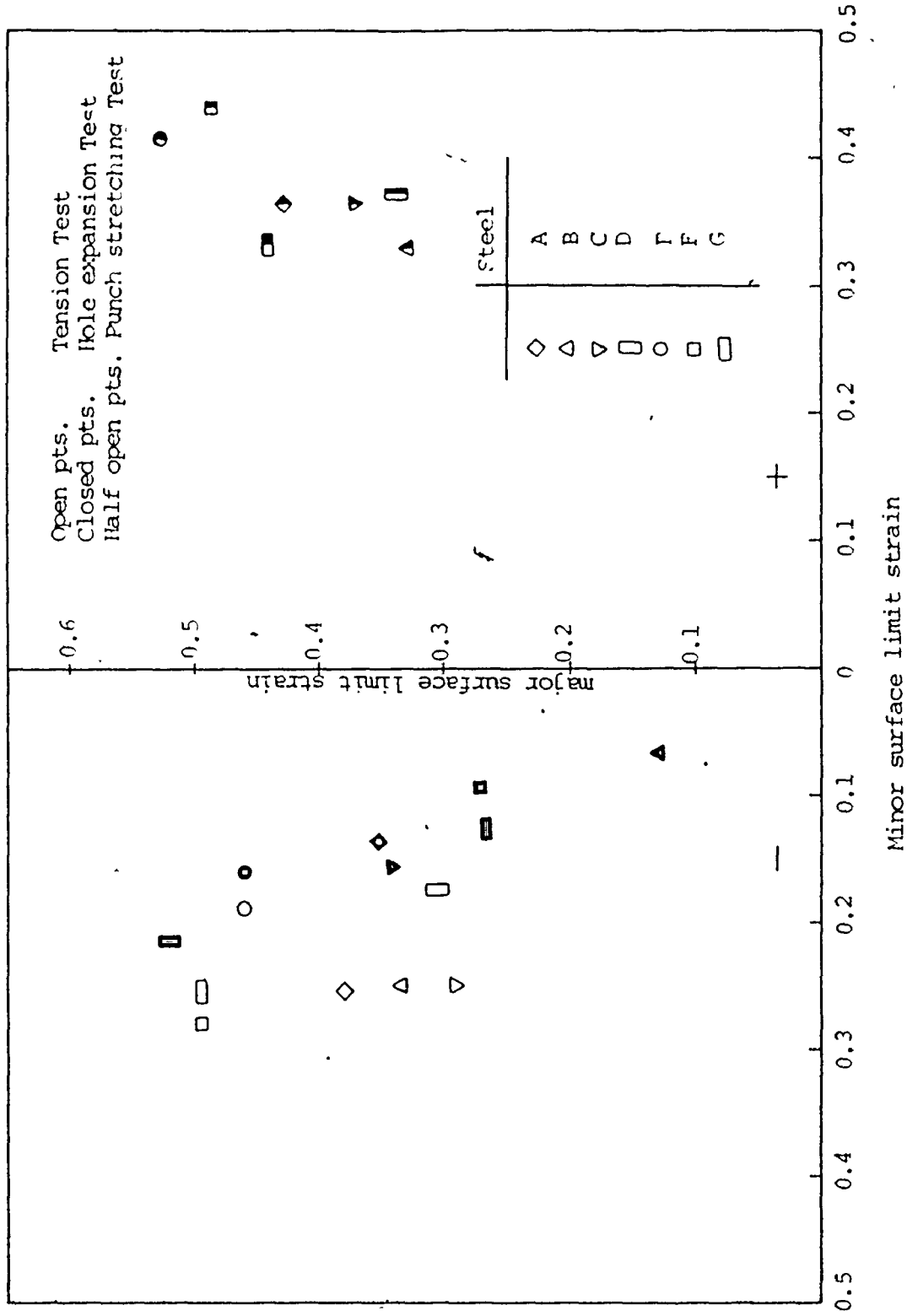


Fig. 43 FLD for the experimental steels

the aim. In addition, as emphasised by Melbourne et al (36), cracking from sheared edge is perhaps the major cause of failure in HSLA sheet steel forming operations and the hole expansion limit should be excellent in the monitoring of steel quality in such cases.

One difficulty with the hole expansion test, as mentioned previously is that no comparison of longitudinal and transverse values can be made to specify the directionality of formability in the material. The expected level of the hole expansion limit for fully modified material must be known so that comparison can be made with the values obtained in the test material. This is no problem in routine testing since this expected value will soon be established. However, in limited testing or in the testing of new steel types etc., it could pose problems.

In this respect the stretch bend test has the advantage since the test result is based on a comparison of longitudinal and transverse deflections. Certainly from the present work it is not nearly as sensitive to elongated inclusions as the hole expansion test, at least for lower strength levels and lower inclusion contents, but the sensitivity does increase with span. It appears that using the longer span the test would be adequate for routine quality control in HSLA sheet steels although more work is required to ascertain this.

Though no attempt has been made to draw FLD for the materials but the results of the limit strains in Tension Test, Hole Expansion Test, Punch Stretching Test are plotted in Fig. 43 to give an idea of the strain levels in the three different straining conditions.

CHAPTER VI

INFLUENCE OF TESTING CONDITIONS IN STRETCH BENDING

The majority of stretch bend tests in the present work were carried out using 2 in. wide specimens with oiled polythene lubrication between punch and specimen - the test conditions used by Hero et al (39) using the same apparatus. Little work has been done on the effect of test conditions in the stretch bend test. Since, for the purposes of correlation with commercial operations, it is quite important to understand how deformation conditions in the stretch bend test change with test conditions. A small additional program of work was carried out to investigate this.

6.1 EFFECT OF LUBRICATION:-

Since the deformation mode in commercial bending of sheet metal is restricted to plane strain it would be ideal to obtain this mode in the stretch bend test. However, substantial width strain does occur in the stretch bend test and it is reasonable to assume that this is assisted by lubrication. Consequently, a brief investigation of stretch bend tests with no lubrication was carried out using sheared edge samples of steel F to determine the effects on deflection and width strain. Longitudinal and transverse specimens of steel F were tested in the dry condition using the same punch radii as previously used for the lubricated specimens.

6.1.1 PUNCH DEFLECTION FOR DIFFERENT BEND RATIOS

The stretch bend deflections for the dry conditions are compared

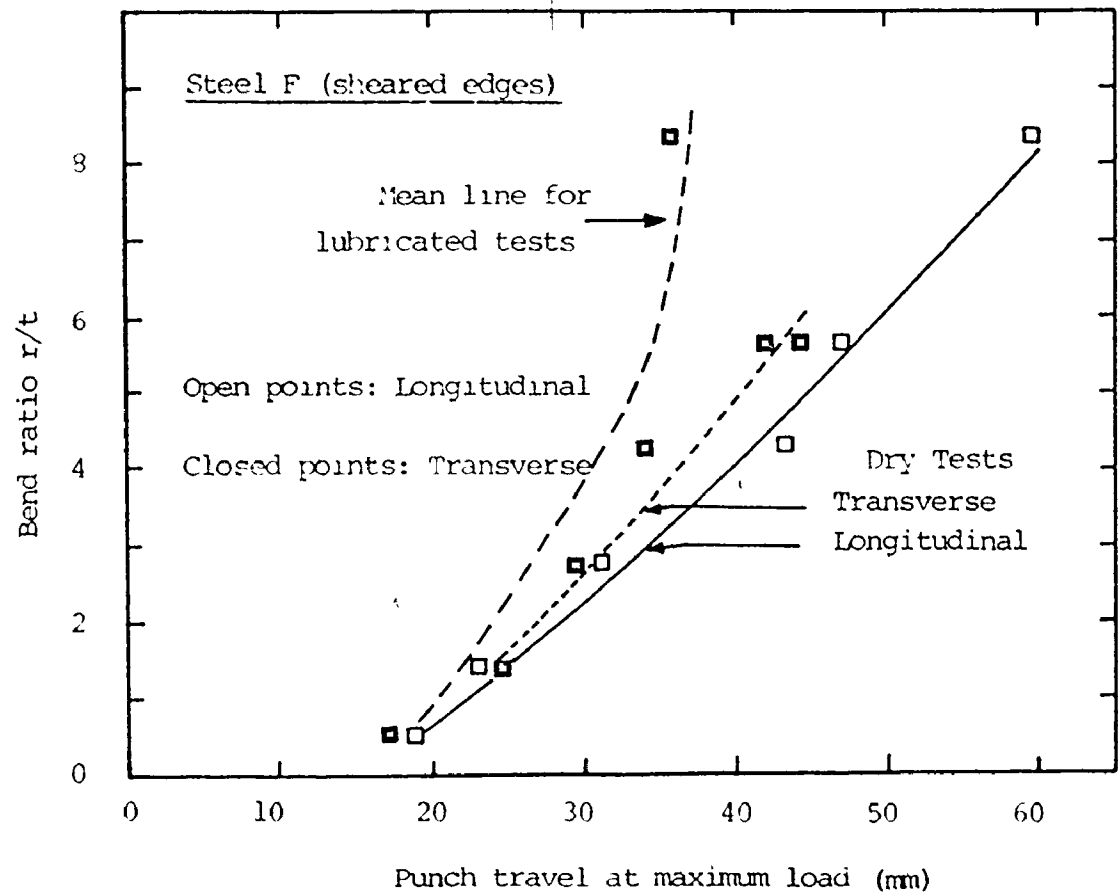


Fig. 44 A comparison of the punch travel-bend ratio relationship for normally lubricated specimen of Steel F and specimens tested without any lubrication.

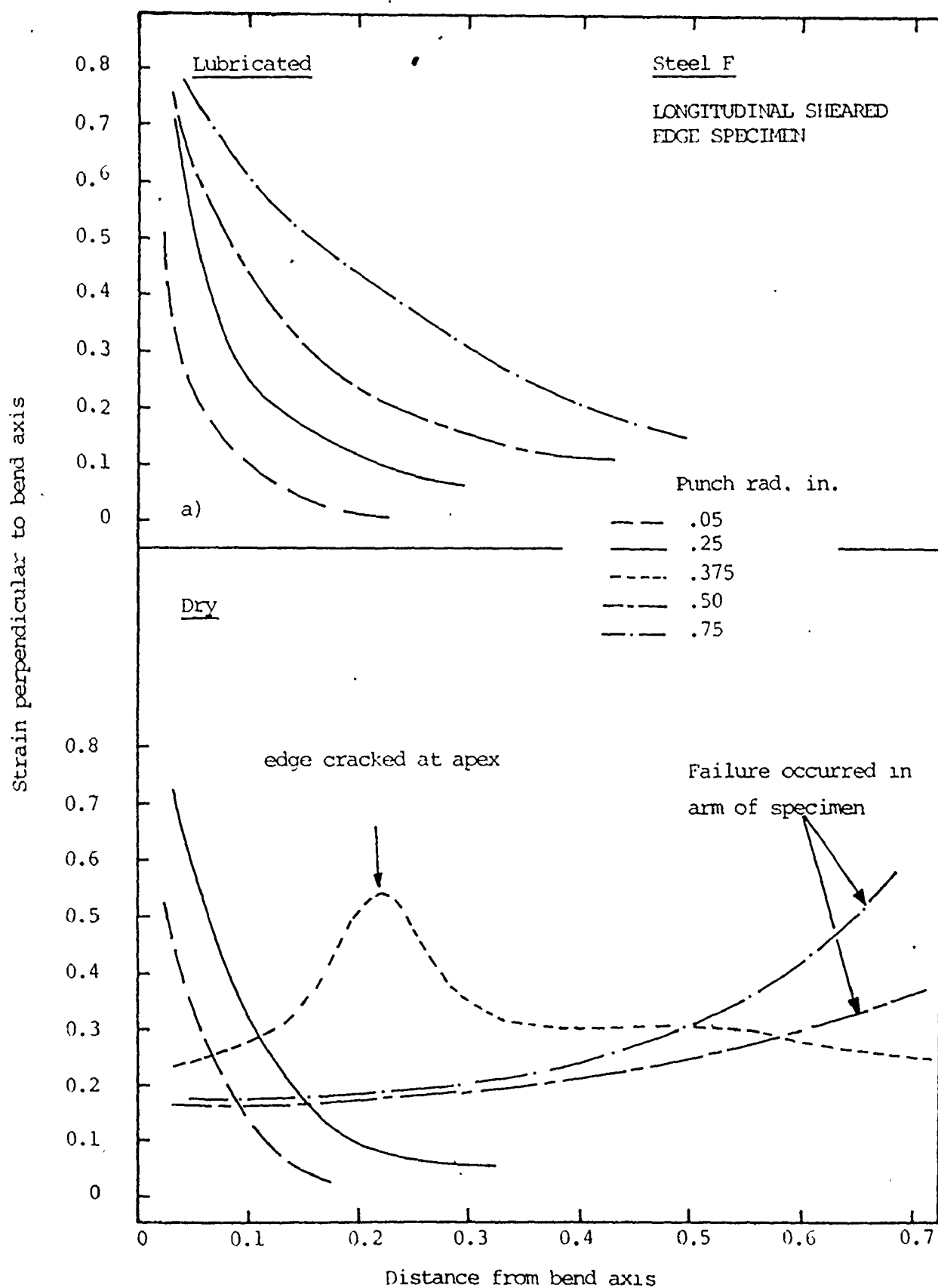


Fig. 45 A comparison of the strain distributions obtained perpendicular to the axis of the bend for a) normal lubricated tests
b) dry for Steel F.

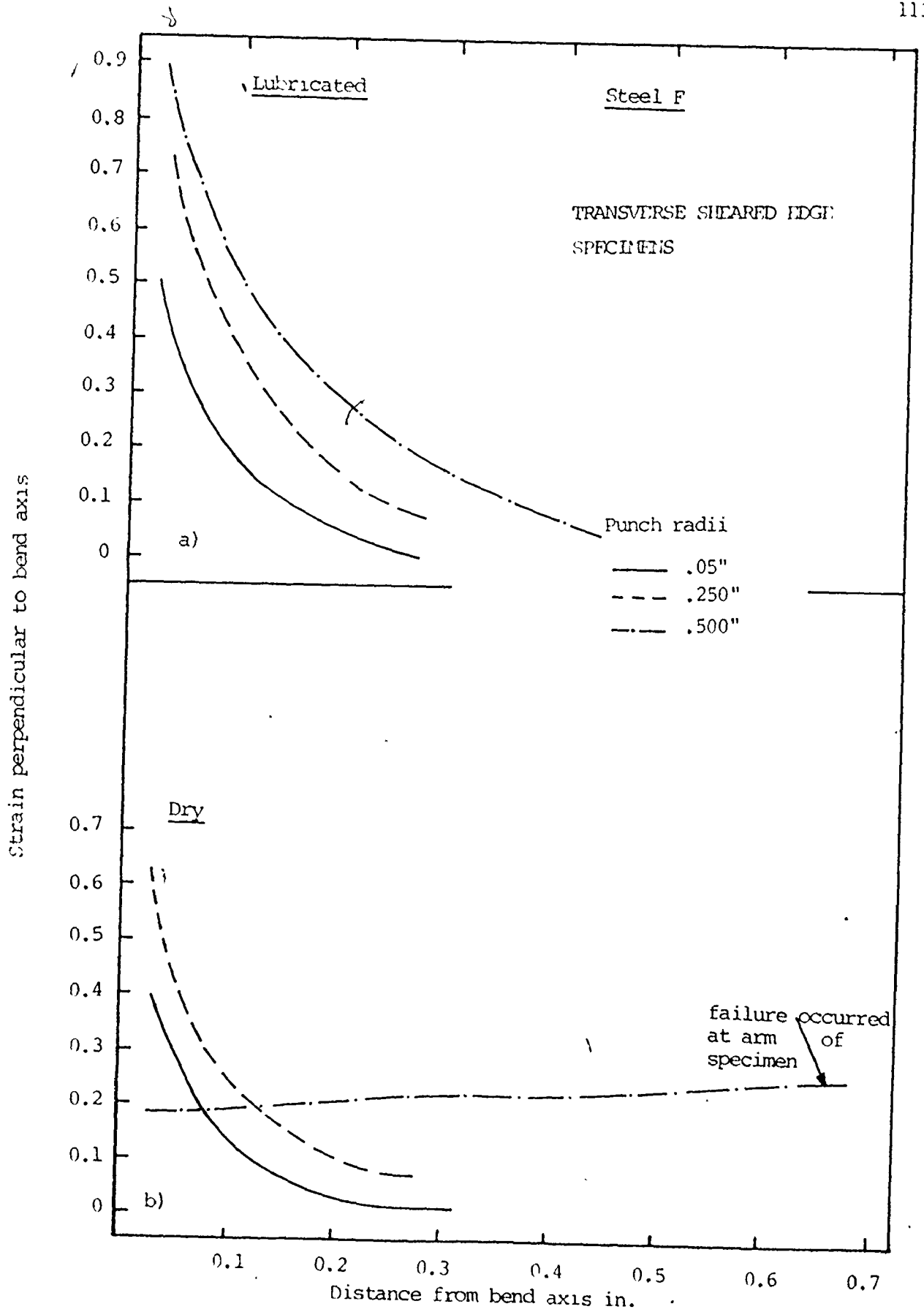
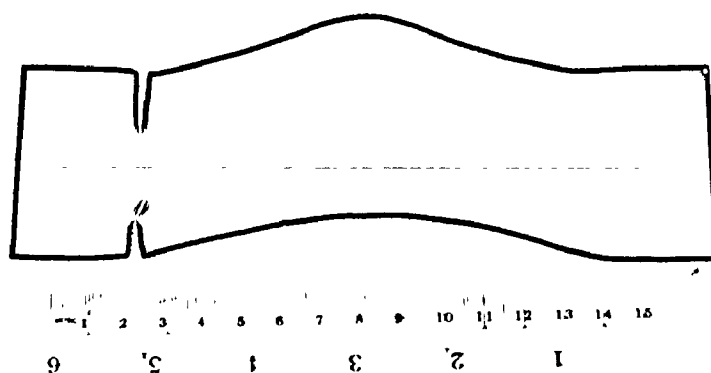
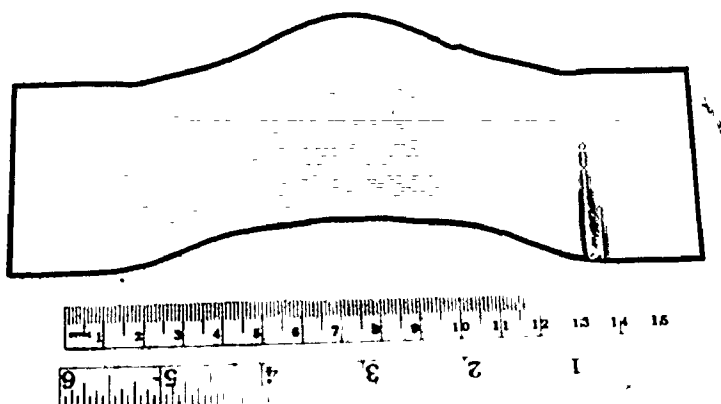


Fig. 45 (continued)



(a) Failure at the clamping jaws



(b) Failure in a tensile mode half way between bend apex and the clamping jaws.

Fig. 46 Typical failures for specimens tested without lubrication.

7
to those previously obtained for lubricated conditions in Fig. 44. Steel F is an unmodified 50 ksi yield strength steel and in both, dry and lubricated tests the results for transverse specimens fall to lower values than those for longitudinal specimens, although this difference is slightly greater for the unlubricated specimens. However, both longitudinal and transverse deflections for the dry tests are larger than those for lubricated tests and the difference between the two increases with increasing bend ratio at the larger bend ratios. This effect is due to a difference in the distribution of strain for the two lubrication conditions as shown in Fig. 45 where strains perpendicular to the axis of the bend, as measured from electro etched 0.09 in. grid circles, are plotted against distance from the apex of the bend.

For the smaller bend ratios the strain distribution in lubricated and dry specimens are similar and failure occurs at the apex of the bend for both conditions. However, for bend ratios greater than about 4.0 (i.e. .375 in. punch radius for this steel) the failure site moves from the apex of the punch and occurs under tensile conditions in the sides of the bent specimen and in some cases at the junction with the clamping jaws (Fig. 46). This type of failure is different from the edge cracking at the punch-specimen junction sometimes encountered in lubricated specimens at large punch radii. In these unlubricated cases failure occurs in a tensile mode, with considerable width strain, roughly half way between punch and clamping jaws.

This can be attributed to the increased frictional resistance to straining over the punch radii in the dry specimens at the larger bend ratios. Under these conditions straining is restricted over the punch radius as can be seen from Fig. 45 and the major portion of straining and failure occurs in the side arms of the bend under friction free plane tensile conditions.

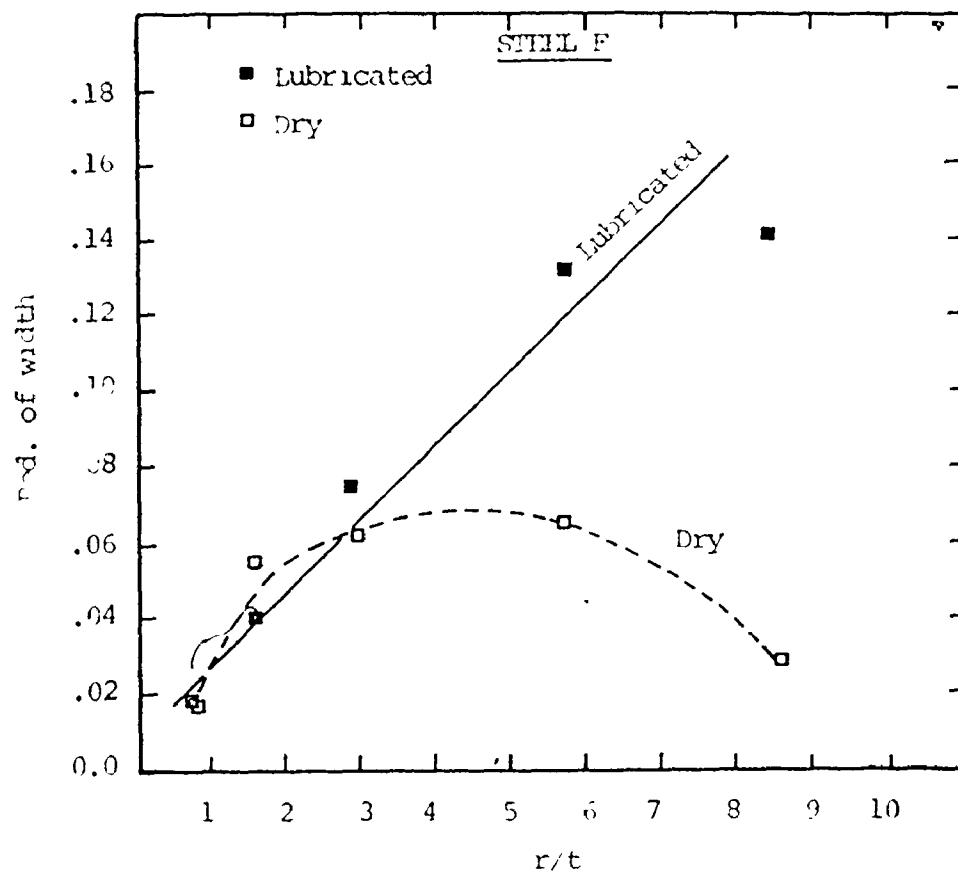


Fig. 47 The variation of width strain in the stretch bend test with punch radius for dry & lubricated conditions.

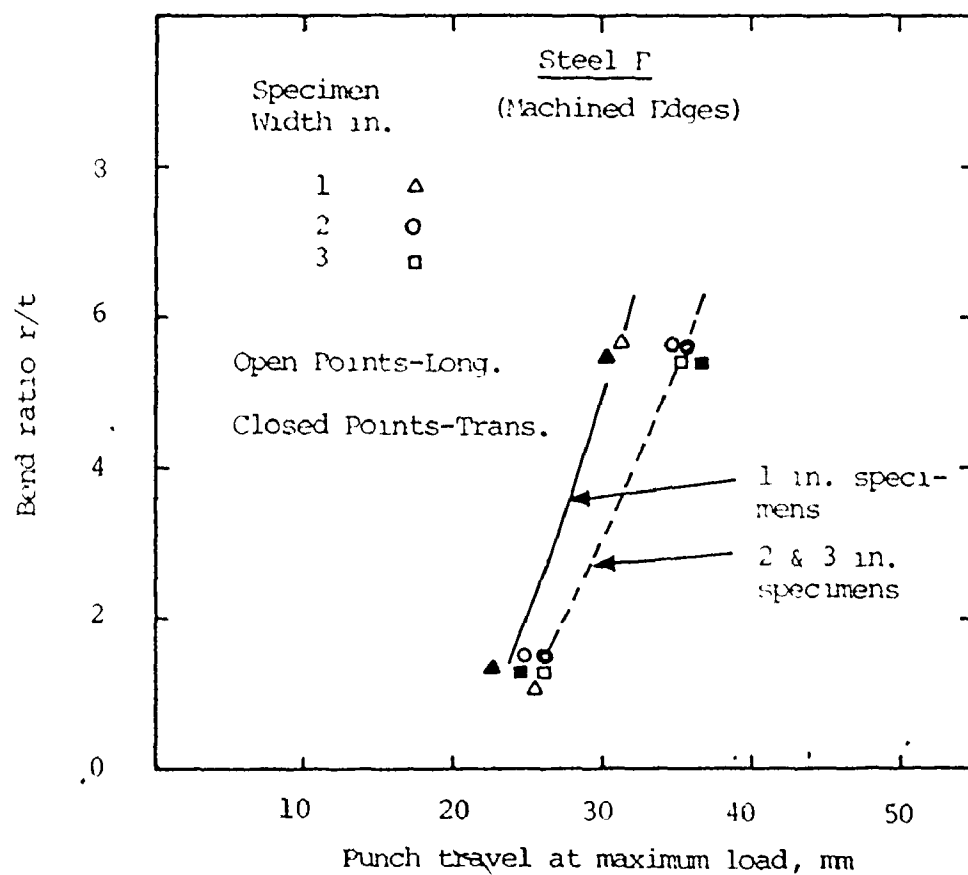


Fig. 48 The influence of specimen width on the punch travel-bend ratio relationship.

In Fig. 47 the R of W for dry and lubricated specimens are compared. As expected, R of W at the apex of the bend at fracture in dry specimens deviate to lower values than in lubricated specimens (i.e. the strain path is closer to plane strain) at low r/t values. At larger punch radii than about 0.375 in. (i.e. about $r/t = 3.0$) in Fig. 47 the results for the two conditions are not comparable because of the change in failure site in the dry specimens.

Since the stretch bend test is of little value, if failure occurs well away from the punch radius in a tensile mode with considerable width strain, the use of unlubricated tests is restricted to the smaller punch radii where, unfortunately, the test appears to be less sensitive to steel quality, as measured from the differences between longitudinal and transverse defections. In general, therefore, it appears that some lubrication is necessary to obtain best results from the test.

6.2 EFFECT OF SPECIMEN WIDTH

6.2.1 PUNCH DEFLECTION FOR DIFFERENT BEND RATIOS

An alternative possibility for reducing width strains in the stretch bend test is the use of wider specimens. To investigate this, number of tests were carried out with steel E using 1 in., 2 in. and 3 in. wide specimens and punch radii of 0.125 and 0.50 in. The results are shown for machined edge specimens in Fig. 48. Punch deflections were similar in the 2 in. and 3 in. specimens but were slightly lower in 1 in. specimens.

6.2.2 EFFECT OF SPECIMEN WIDTH ON WIDTH STRAIN

The overall reductions in width obtained and the local width strains

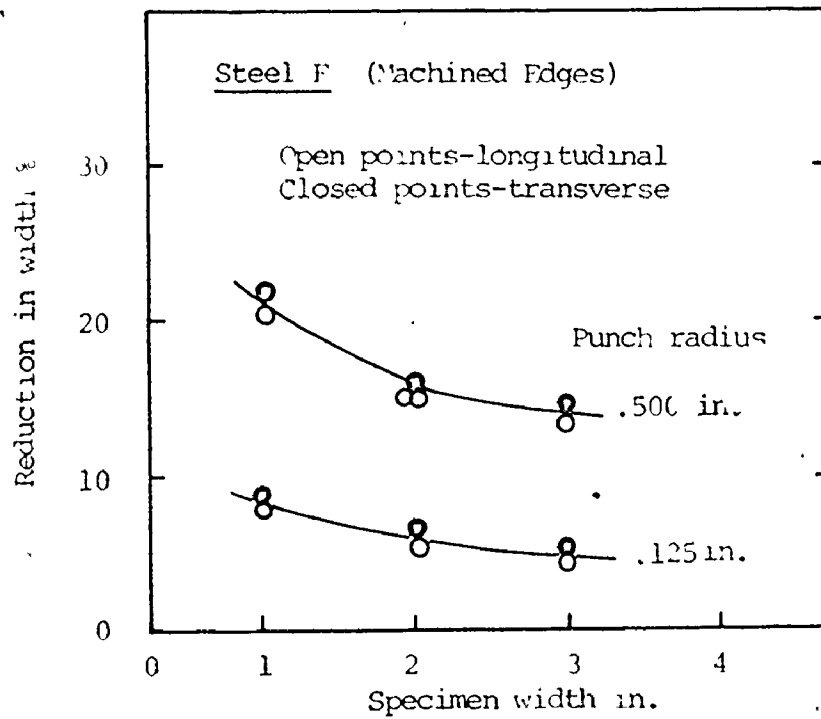


Fig. 49 The influence of specimen width on the width reduction at fracture at the apex of the bend for tests with 0.5 in. and 0.125 in. punch radii.

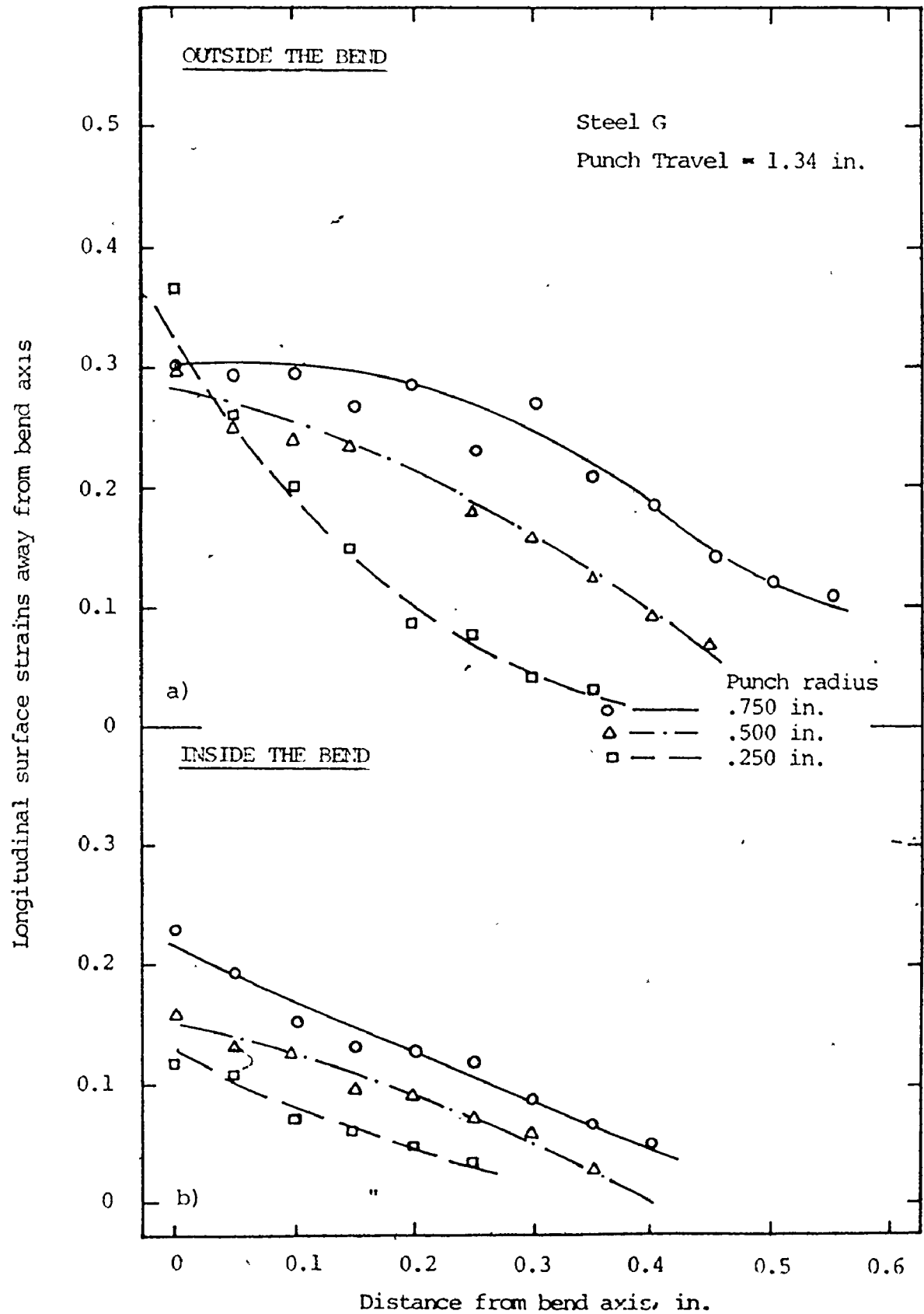


Fig. 50 Strain development during stretch bending a) outside the bend b) Inside the bend.

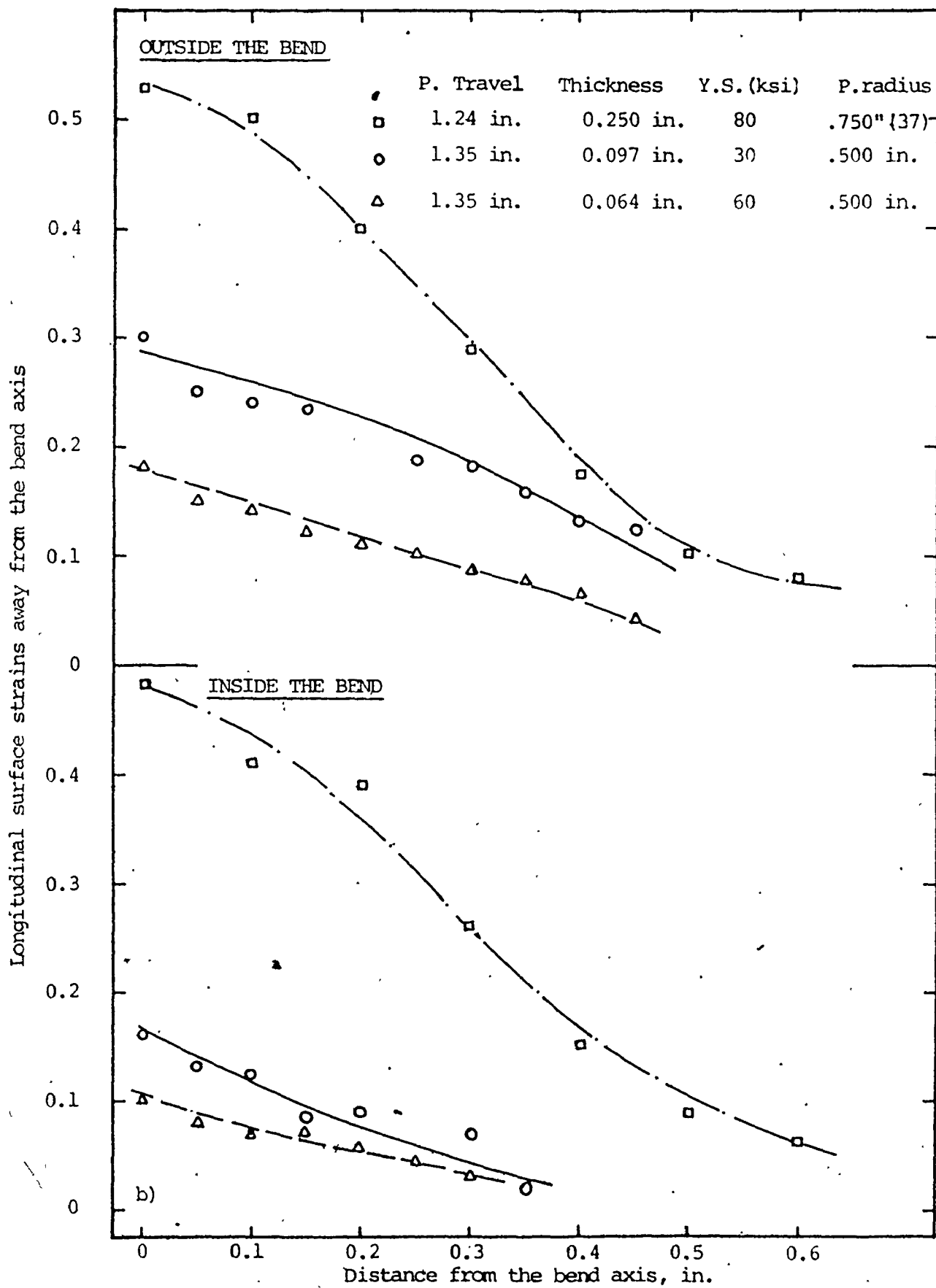


Fig. 51 Effect of specimen thickness on the strain distribution during stretch bending.

TABLE 6
EFFECT OF SPECIMEN WIDTH ON WIDTH
STRAIN--MACHINED EDGE SPECIMENS

STEEL E

SPECIMEN WIDTH		REDUCTION OF WIDTH %	
		PUNCH RADIUS	
		.125"	.500"
L	1"	8.00	20.5
T		8.30	22.5
L	2"	6.20	15.7
T		5.80	15.3
L	3"	4.20	13.5
T		5.40	14.4

L -- LONGITUDINAL SPECIMEN
T -- TRANSVERSE SPECIMEN

measured on .09 in. grid circles at fracture showed only a small increase with decreasing specimen width at the .125" punch radius, but at the .50 in. radius although there was little difference between 2 and 3 in. specimens the values in the 1" specimens were much higher (Fig. 49). At these larger punch radii width strains are significant (e.g. 15% reduction of width in Fig. 49) and the test does not approximate to plane strain conditions. However, although 2 in. specimens are significantly better than 1 in. specimens, there appears to be little justification for using 3 in. specimens under these conditions. TABLE 6 gives the value of the Width Strains.

6.3 DEVELOPMENT OF STRAINS DURING THE STRETCH BEND PROCESS

Long strains inside and outside the bend were measured along the longitudinal axis of the sheared edge specimens of steel G deformed to 1.34 in. by .250 in., .500 in., .750 in. radius punch and the results are plotted in Fig. 50.

An attempt is also made to see the effect of specimen thickness on the distribution of strain in Stretch Bend processes. The results are plotted in Fig. 51. These results cannot be compared with any degree of accuracy because of the large variations in yield strength level of the steels. More work is needed before any conclusion can be framed.

But the results of Fig. 50 and Fig. 51 confirms the earlier work of Uko (37) that stretching is the main deformation process during Stretch Bending even well before the crack starts initiating when deformed by larger punch radii.

6.4 EFFECT OF SPECIMEN SPAN

The stretch bend testing apparatus used was designed to allow the

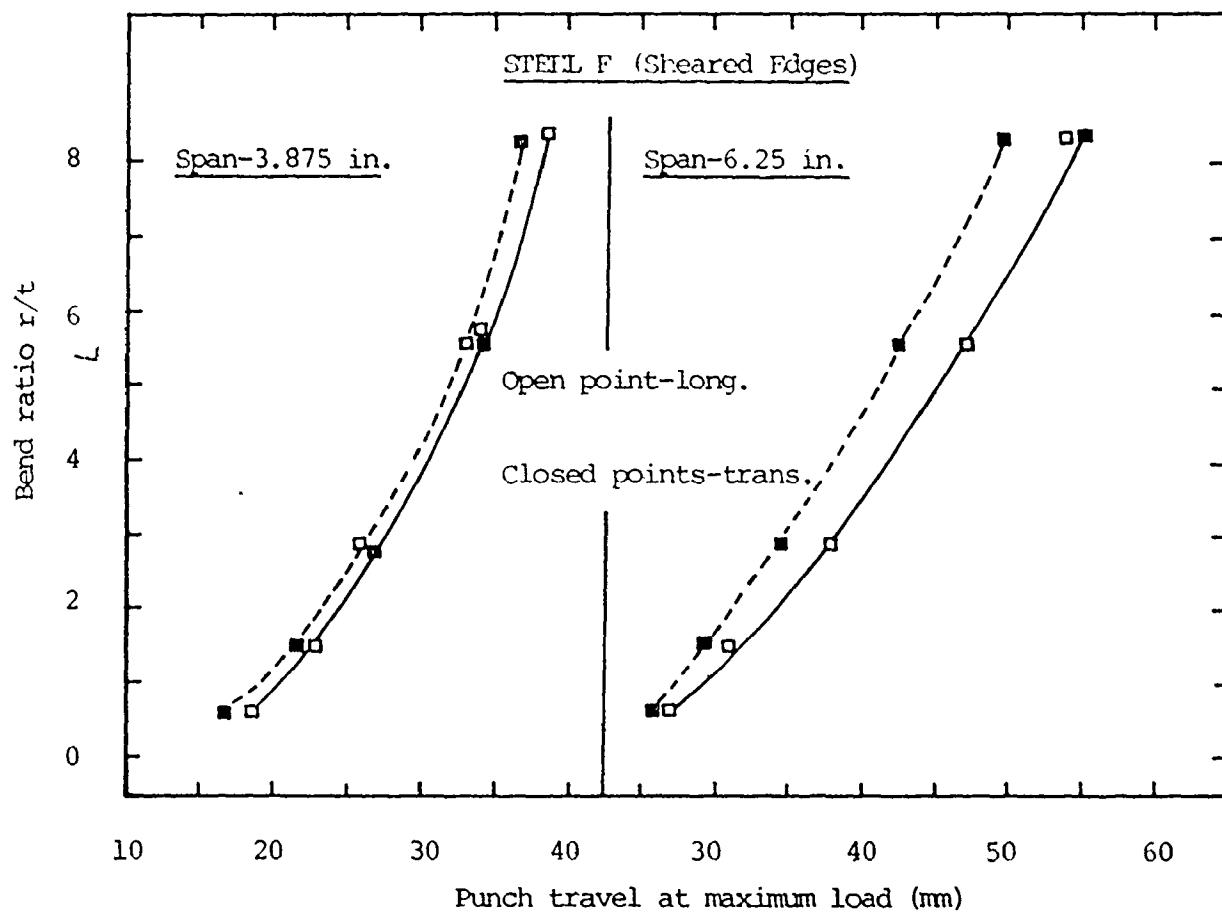


Fig. 52 The influence of specimen span on the punch travel-bend ratio relationship for steel F. Note the increased separation of the curves for longitudinal and transverse specimens in the tests at the larger span.

use of two spans between the clamping jaws (dimension A in Fig. 14). These spans were 3.875 in. and 6.25 in. In all the work reported in the body of this thesis, a span of 3.875 in. was used since this was the value used by Uko (37) and Melbourne (36) and it was thought that comparison with their results might be invalidated by using the larger span. However, workers at United States Steel have recently been making use of the stretch bend test using an apparatus with a very large span and reporting good sensitivity to elongated inclusions even at relatively low sulphur and strength levels (38).

As a consequence of this, some stretch bend tests were carried out in the present work using the larger 6.25 in. span. These were carried out on steel F, the unmodified 50 ksi yield strength steel. Tests with the smaller span on this steel exhibited small differences only between longitudinal and transverse samples (Fig. 27).

The results are shown in Fig. 52. They lie to larger deflections than those at the smaller span as expected but more importantly, with one anomalous result, the difference between the curves for longitudinal and transverse specimens is much more definite than for the shorter span, particularly at the larger punch radii.

The reason for the improved sensitivity for the larger span may be simply related to the overall larger deflections obtained which reduce the influence of errors in the deflections obtained which reduce the influence of errors in the deflection measurements (e.g. errors in the zero position).

At the larger punch radii the ratio of specimen deflection to

span is lower for the larger span. In addition in transverse specimen edge cracking does not occur at the apex of the bend in these cases but in the regions away from the apex at the boundary of punch contact. This suggests that, at least at the larger radii where the largest difference between longitudinal and transverse deflections is found, the bending deformation in the stretch bend test is of limited importance in distinguishing between steels of different quality. At the smaller punch radii, failure occurs at the apex of the bend and the bending mode is clearly influential. However, under these conditions the difference between longitudinal and transverse specimens is small.

Taken to its logical conclusion this would indicate that the tensile part of the deformation is of most importance in optimising the sensitivity to elongated inclusions and the punch bending serves only to assist in obtaining approximately plane strain conditions and in locating the position of fracture. A plane strain tensile test on a sheared edge specimen would probably be equally useful in distinguishing steel quality provided the position of crack initiation could be fixed so that useful strain measurements could be made (the notched tensile test would come into this category if the notch acts as a crack initiator).

CHAPTER VII

CONCLUSIONS

1. From the literature available, it can be said that in the presence of significant amount of elongated inclusions, geometric instability is not a major factor limiting the formability of HSLA sheet steels.
2. During shearing, elongated inclusions has significant influence on blade penetration. The blade penetration could be related to material ductility in a general way.
3. The punch deflection at maximum load in Stretch Bend Test can be used to distinguish between steels with and without elongated inclusions although the sensitivity of the test is poor for steel of lower strength levels and inclusion content and at lower bend ratio.
4. Elongated inclusions only make their presence felt in specimens with sheared edges where crack initiating microcracks are present in the shear burr. The specimen span of 3.875 in. is inadequate to detect the influence of elongated inclusion in machined edge specimen. However sheared edges are necessary for optimum sensitivity.
5. Local strains at fracture in both tensile (E_L , R of A) notched tensile (E_{TN}) and the stretch bend test (eg. R of W, R of T or E_B) give a reliable indication of the presence of elongated inclusions. However, the difficulties involved in taking these measurements limit their usefulness for quality control work.

6. Edge cracking is associated with Transverse sheared edge specimens of unmodified steels while centre cracking is characteristic of all the other cases studied. At large punch radii the fracture behaviour becomes more complex because of the increasing importance of friction.
7. The punch deflection in the stretch bend test increases with increasing drawability index (r value) and care should be exercised in interpreting test results for steels having unusual r values.
8. The hole expansion limit in the hole expansion test is very sensitive to the presence of elongated inclusions even in steels of low yield strength. It is an excellent parameter if the absence of elongated inclusion is the aim.
9. It can be an advantage to normalize for variation in composition and microstructure between different steels by plotting the ratio of Trans./Long. properties when trying to illustrate the steel quality effect.
10. Considerable width strain is observed in the stretch bend tests and there is a little justification in using large width specimen.
11. Some lubrication between punch and specimen appears to be essential in the stretch bend test particularly at the larger punch radii. In unlubricated tests failure tends to occur in a tensile mode in the friction free arms of the bent specimen.
12. Limited results in the present work indicate that the difference between longitudinal and transverse punch deflection (ie. the sensitivity

of the test) for steels containing elongated inclusions increased with increasing span between the clamping jaws.

13. Stretch bend behaviour of Steel D is not very clear.

The author strongly feels the necessity of further work before Stretch Bend Test can be established as a Standard Quality Control Test for predicting the formability of HSLA sheet steels, especially in the following areas:

1. Stretch Bend Testing of Machined edge and sheared edge specimens of HSLA sheet steels with and without sulphide control, using larger test span (6.25 in.).
2. Stretch Bend Testing of HSLA sheet steels with unusual drawability index (r value) and the detailed study of the fracture behaviour. Steel D falls into this category.
3. Establishing a standard method for the measurement of local strains at fracture.
4. Optimum dimensions of specimen span, width and thickness and bend radii with respect to the actual press forming of the components.
5. An analytical model relating local strain at fracture (R of A , E_L) in Tension test, punch travel at maximum load (stretch bend test) and yield strength would also be invaluable.

REFERENCES

1. F.B. Pickering, "The effect of Composition and Microstructure on Ductility and Toughness", ISIJ, 1971, 9.
2. R. Pearce and A.A. Mazhar, "High strength Low alloy steels research at Cranfield", Conf. of Inst. of Sheet Metal Engg., 1975, Brighton.
3. A.P. Lee and J.R. Hiam, "Factors affecting the forming limit curve of sheet steel used for Press Forming", CIM Conf. of Metallurgists, Quebec, 1973, 1.
4. R. Sowerby and J.L. Duncan, "Failure in Sheet Metal in Biaxial Tension", Int. Journal of Mech. Sciences, vol 13, 1971, 217.
5. R. Sowerby and J.L. Duncan, "Tearing in Sheet Metal Forming Processes" Technical Paper, MF 71-134, Society of Manufacturing Engineers, 1971.
6. Z. Marcinik and K. Kuczynski, "Int. Journal of Mech. Sciences", vol 9, 1967, 609.
7. H.V. Minh, R. Sowerby and J.L. Duncan, "Variability of Forming limit curves", Int. Journal of Mech. Sciences, vol 16, 1974, 31.
8. B.N. Ferry and E.J. Paliwoda, "Formability and high strength low alloy steels", Canadian Met. Quart., vol 13, No. 2, 1974, 415.
9. M.G. Cockcroft, "Ductility", ASM, 1968, 33.
10. F.A. McClintock, "Ductility", ASM, Metal Parks, 1968, 255.
11. T. Gladman, B. Holmes and I.D. McIvor, "The Effects of Second Phase Particles on the Mechanical Properties of Steel", London Iron and Steel Inst., 1971, 68.

12. T. Gladman, D. Duleien, I.D. McIvor, "Structure Property Relationships in High Strength Microalloyed steels", Microalloying 75, Session 1, 25.
13. F.A. McLintock, "Int. Journal of Fracture Mechanics," 1968, vol 4, p. 101.
14. B.I. Edelson and W.M. Baldwin, "Transactions, American Society for Metals", 1962, vol 55, p. 230.
15. M. Korchynsky and H. Stuart, "Low alloy High Strength Steels", London Scandinavian Conf., 1970, 17.
16. T. Gladman et al, "Effect of Second phase particles on the Mech. Props. of Steels", Iron and Steel Institute, 1971, 68.
17. E. Smith, "International Journal of Fracture Mechanics," 1968 vol 4, p. 131.
18. F.B. Pickering, "High strength low alloy steels--A Decade of Progress", Micro alloying 75, Session 1, 3.
19. L. Luyckx, J.R. Bell, A. McLean and M. Korchynsky, "Sulfide Shape Control in High strength low alloy steels", Metallurgical Transactions vol 1, 1970., 3341.
20. B. Polland, "Effect of Manganese content on sulfide shape control by Zirconium in steel", Metals Technology, July 1974 , 343.
21. J.L. Mihellich, J.R. Bill, and M. Korchynsky, "Effect of Inclusion shape on the Ductility of Ferrite Steels", Journal of the Iron and Steel Inst., 1971, 469.
22. I.L. Dillamore et al, "The effect of second phase particles on mech. props. of steel", The Iron and Steel Inst., 1971, 190.

23. T. Matsuoka, T. Kawai, S. Ueda and Y. Hobo, "Improvement in Formability of Hot Rolled High Tensile strength Steel Sheet by Cerium addition", Trans. ISI Japan, 15, 3, 1975, 137.
24. G. Glover and J. Havramak, "Mechanical Properties of Niobium and Titanium steels for High strength sheet," Jnl. Aust. Met, 18, 1973, 85.
25. R.R. Hilsen and T.E. Fine, "Stamping Potential of Hot Rolled Columbium bearing High Strength steels", Micro alloying 75, Session 4, 5.
26. R.A. Grange, "Effect of Microstructural Banding in Steel", Met. Trans., 2, Feb. 1971, 417.
27. K. Matsudo, T. Shimomura, K. Osawa, M. Yoshida and Y. Uchida, "Relation between Press formability and Notched elongation of Steel Sheets, "Nip. Kokan Tech. Rpt., overseas, June 1974.
28. T. Yamaguchi and H. Taniguchi, "Study of Formability of Hot Rolled Steel Sheet", Nippon Kokan Tech. Rpt., 45, 1969.
29. G. Glover, "The influence of Sulphur content on the formability of HSLA sheet steels", Proc. 8th Biennial Congress of IDDRG, Gothenburg, Sept. 1974, 147.
30. J.M. Gray, "Strength-Toughness relations for precipitation strengthened low alloy steels containing Niobium", Met. Trans., 3, 1972, 1495.
31. I. Kozasu, T. Shimizu and M. Kubota, "The effect of Nonmetallic Inclusions on Ductility and Toughness of structural steels", Trans. ISI Jap., 13, 1973, 20.
32. R. Pearce and A.A. Mazhar, "Formability of HSLA steel sheet shearing", Met. Tech. July 1976, 338.
33. J.D. Grozier, "The Hutchinson Bend Test", Jnl. of Mats., 1972, 3.

34. T. Nakagawa and K. Yoshida, "Improvement in the Deformability of Sheared Edge of Steel Sheets", Proc. ICSITS, Suppl. Trans., ISIJ, vol. II, 1971, 813.
35. Y. Ito, K. Masigiuchi and N. Onasmi, "Effect of Plastic anisotropy on the Bore Expanding behaviours of cold rolled steel sheets", Proc. ICSITS, Suppl. Trans., ISIJ, vol II, 1971, 958.
36. S. Melbourne, R. Pietrowski and G.M. Marsh, "Testing HSLA steels sensitivity to sheared Edge Cracking", Dofasco Research Report, 1.
37. D.K. Uko, M. Eng. Thesis, 1975, McMaster University, Hamilton.
38. P. Maild, United States Steel Research Centre, Private Communication.
39. H. Hero, D.K. Uko, A. Filipovic, R. Sowerby, J.L. Duncan, D.J. Embury, "Formability and Fracture of some HSLA Steels". Part I and II, Metal Working Research Group Rpt. No. 84, McMaster University, Aug. 1976.
40. T.J. Baker, K.B. Gove, J.A. Charles, "Inclusion deformation and toughness anisotropy in hot rolled steels", Metals Society 1976, 183.
41. A.R. Rosenfield, "Criteria for Ductile Fracture of two phase alloys", Metallurgical Reviews, 1968, 29.
42. L.M. Brown and J.D. Embury, "The Initiation and Growth of voids at second phase particles", Proc. Third Int. Conf. on strength of Metals and alloys, Cambridge, 1973, 164.
43. S.R. Paul Chowdhry, "Stretch forming of Sheet Metal, A Review of some instability theories and the Design and Construction of a Testing Rig for Formability studies of Thicker Gauge Materials", M. Eng. Thesis, McMaster University, Hamilton, Nov. 1974.

44. T.R. Thompson, "Strech Forming of Killed Drawing Quality steels",
B.H.P. Melb. Res. Lab. Rep. MRL 62/2, July 1974.
45. R.H. Davison and D.R. Dendel, "The Formability of Mn-Mo-Cb High
Strength Steel Sheets", Annual Conf. of Metallurgists, Quebec, 1973, 1.
46. M.J. Painter and R. Pearce, "Formability of HSLA Sheet Steels",
Met. Tech., 2, 2, 1975, 62
47. J. Hain, Dofasco Research Laboratory, Private Communication
48. B.K. Sareen, "Study of Formability and Fracture characteristics of
Aluminum Alloys", M. Engg. Thesis, McMaster University, 1976.